# A STUDY OF THE ICE MAKING OPERATION IN THE DESALINATION FREEZING PROCESS BASED ON THE INVERSION OF MELTING POINTS DUE TO APPLIED PRESSURE

by 544

SHEN-YANN CHIU

B.S., National Taiwan University, 1962

---

A MASTER'S THESIS

submitted in partial fulfillment of the

requirements for the degree

MASTER OF SCIENCE

Department of Chemical Engineering

KANSAS STATE UNIVERSITY
Manhattan, Kansas

1968

Approved by:

Liang-Tseng Fan

Major Professor

# TABLE OF CONTENTS

# LIST OF FIGURES

PAGE

# LISTS OF TABLES

# INTRODUCTION

Due to the difference in the effect of applied pressure on melting points, a substance which melts at a temperature lower than the freezing point of an aqueous solution may be made to melt at a temperature higher than the melting point of water by a sufficiently high applied pressure. Therefore, a working medium can be selected to form a cyclic auxiliary system for removing the heat from the salt water to produce ice and concentrated brine and for supplying heat to melt the ice so formed at a higher pressure. At the end of a cycle the auxiliary system is returned to its original state. This is the basic underlying theory of the desalination freezing process (hereafter, it will be called the Inversion Freezing Process) investigated here.

The specific objectives of this research were:

1. To design and build experimental equipment which could be used to produce ice continuously under atmospheric pressure.
2. To determine the ice production rate under various operating conditions.
3. To determine the ice crystal sizes produced from this process.

# REVIEW OF LITERATURE

The oceans represent the largest water reservoir of the earth. Only 29% of the global surface is covered with land; the remaining 71% is ocean. Ocean water, however, contains on the average 3½ per cent (by weight) of dissolved salts mainly NaCl, a concentration that makes the water unsuitable for many household and industrial uses and for the irrigation of conventional land-grown crops.

There is at all times an exchange of water between oceans and seas, on the one hand; and rivers and lakes on the other hand, the emptying of a river into the sea is an illustration of the flow of fresh water into salt water. Flow in the opposite direction also takes place; moisture evaporates as a result of solar heating from the surface of the sea and is carried upward to the cooler regions of the atmosphere, where it is condensed and returned to earth again as rain to fill the streams, rivers, and lakes with fresh water.

The natural evaporation-condensation action is, by far, the most important of nature's desalination processes. Alternate natural desalination processes such as freezing and biological processes, exist.

Unfortunately, fresh water produced from the sea by natural methods is not always available at the locations and in the quantities required by man. In the past, decisions on where and how to live have, to a large extent, been dependent upon the availability of a natural supply of fresh water.

In recent decades, as the result of the large increase in world population and various military and political factors, there has been a tremendous drive to open arid areas for large-scale settlement. Moreover, water shortages appear occasionally in highly industrialized areas in zones of moderate climate with abundant rainfall. When there is no fresh water within a reasonable distance and ocean water or brackish ground water is available, salt removal from water becomes necessary. This process is called "salt water conversion" or "water desalination".

Salt water conversion can be accomplished in many ways. Some methods of producing fresh water from salt water have been known in concept for centuries; other methods have been uncovered only in the past few years. Some methods are now utilized commercially, some have progressed to the pilot plant stage of development, and others are still under study in laboratories.

The principal desalination processes can be summarized as follows (1).

A. Distillation:
   a. Long-tube vertical
   b. Flash distillation
   c. Vapor compression
   d. Multieffect multistage

B. Membranes:
   a. Reverse osmosis
   b. Electrodialysis
   c. Transport depletion

C. Freezing:

a. Direct freezing

b. Indirect freezing

D. Humidification:

a. Solar

b. Diffusion

E. Chemical:

a. Hydrates

b. Ion exchange

## THE CONVENTIONAL FREEZING PROCESSES.

Separation of fresh water from salt water by freezing is based on the fact that when salt water freezes, fresh water ice crystals form, and the salt remains in solution in the unfrozen water. A freezing process is generally a two step operation requiring both cooling and heating. In any freezing process, the salt water is cooled until ice is formed. The ice is separated from the brine and then melted to produce the product water of the process.

Freezing processes have been studied for over 20 years and are still in a period of rapid development. Generally, they can be divided into two categories, namely, direct freezing and indirect freezing. In the former, water acts as its own refrigerant, that is, the evaporation of water vapor removes the heat necessary for the formation of ice. In the latter, a liquid more volatile than and immiscible with water, such as butane, is used as a refrigerant.

In both direct freezing and indirect freezing, ice crystals are formed in a freezing vessel (or crystallizer) in which the pressure is maintained at about 0.005 atm. As rapid evaporation of the refrigerant takes place in it, the sea water cools and eventually freezes (The freezing temperature is -2.05°C for pure sea water and -3.8°C for doubly concentrated sea water, which is the liquid phase in the crystallizer). In other words, the inlet stream(s) splits into vapor and ice, and the heat needed for the evaporation is supplied by conversion of water to ice.

The ice produced from the crystallizer must be washed because it is in the form of a fine slush still holding up to 50 weight per cent brine in the space between the crystals. Countercurrent washing procedures have been developed in which the ice crystals rise against a stream of wash water flowing downward. This method is so efficient that only a few percent of the fresh water has to be used for this purpose (2).

The pressure in the crystallizer is maintained by the continuous pumping of vapor by a compressor. For the purpose of saving energy and equipment, the vapor is pumped into a vessel, called a melter, in which the pressure is maintained at 4.6 mm mercury in the direct freezing process and a little bit over atmospheric pressure in the indirect freezing process. The washed ice is also continuously fed. Into the melter within the vessel, the refrigerant vapor condenses to liquid; at the same time, the ice crystals melt and turn into water. In the direct freezing process, liquid water is obtained from the condensation of vapor and becomes a part of the fresh water product. In the indirect freez-

ing process, vaporous refrigerant is condensed and returned to the crystallizer.

Freezing processes have the following characteristics.

1. They operate at low temperatures thus minimizing scale and corrosion problems. Low temperature plants may be expected to last longer than those operating at high temperatures.
2. In the freezing and melting steps heat transfer is accomplished without passing through metal surfaces. The great advantages of transferring the latent heat of phase change by direct contact between phases are that scale formation is unimportant and that temperature differences required for heat transfer are small.
3. Freezing processes can be designed for practically any feed from dilute brackish water to sea water.
4. Freezing processes operating on brackish water can convert economically a larger fraction to fresh water product than other processes, such as electrodialysis and reverse osmosis.
5. Freezing is the only developed process which can use electrical power directly to desalt sea water. This allows plants to be built where cheap steam is not available. Electrical power may be transported hundreds of miles, but steam must be used near its source.
6. Due to the nature of the equipment used in freezing, the most suitable size of a freezing process appears to be between 50,000 and 5 million gallons of fresh water per

day (That of a distillation process appears to be on the order of 100 million gallons per day).

The conventional freezing processes have the following disadvantages.

1. High equipment cost due to the large volume of vapor involved.
2. High energy cost because of the low energy efficiency of the compressor in compressing the vapor.
3. Poor control of crystal formation because of the vigorous agitation and the local subcooling due to the rapid vaporization of liquid.

THE INVERSION FREEZING PROCESS.

This process, which was proposed by the Chengs (3), appears to possess the same advantages as the conventional freezing processes but not their disadvantages. The process is based on a distinctly different way of upgrading heat. Due to the difference in the effect of applied pressure on melting points, a substance which melts at a temperature lower than the freezing point of an aqueous solution may melt at a temperature higher than the melting point of water at a sufficiently high applied pressure. Therefore, a working medium (or refrigerant) can be selected to form a cyclic auxiliary system to remove the heat of crystallization in the partial freezing operation and to supply the heat required to melt the ice so formed. The process is distinct from the conventional freezing processes in that it handles only the condensed (liquid and solid) phases. This has a considerable effect on the

energy requirments of the process and favors the control of ice crystallization.

Theory. The shape and direction of a univariant pressure vs. temperature curves for the melting point of a pure substance and the eutectic temperature of a binary mixture are given by the Clausius-Clapeyron equation (4). The melting point is seen to be raised (positive slope) as pressure increases if the solid is denser than the liquid; a negative slope is found in a few cases, such as water, bismuth and gallium, where the liquid is denser than the solid. According to P. W. Bridgman (5), the melting point of water decreases one degree centigrade with an increase in the applied pressure of about 100 atmospheres, and the general tendency of most systems is to have a positive slope of the fusion curve, the average value being 50-60 atm./deg. C.

The Inversion Freezing Process employs a substance or a mixture of substances as a working medium. It is so selected that its melting point is lower than the freezing point of the aqueous solution from which fresh water is to be separated under low pressure. However, when the applied pressure exceeds a certain value, the melting point is raised to exceed the melting point of water under the same applied pressure. Figure 1 compares the melting point change of water with pressure with that of an ideal working medium. It also shows schematically the conditions of the low pressure ice-making operation, the inversion point, and high pressure ice-melting operation. It reveals that if the melting point of substance A is lower than the melting point of substance B and if solid A is contacted with liquid B, directly or indirectly,

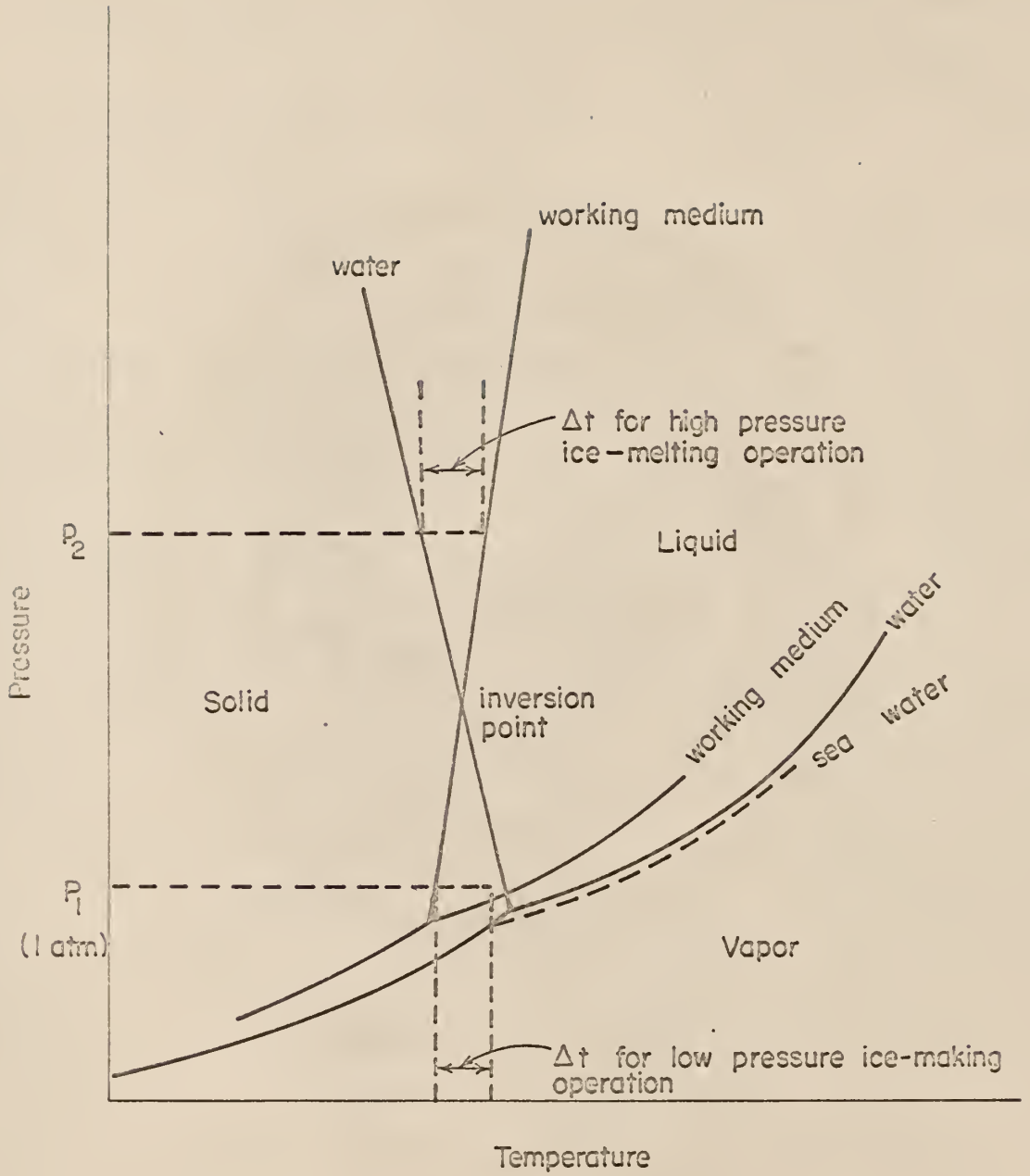


Fig. 1. Phase equilibrium diagram for an aqueous system and an ideal working medium ( schematic) .

solid A will melt and liquid B will be solidified by the heat exchanged between them. Therefore, a substance or mixture of substances which forms a working medium to absorb the heat of crystallization at a low pressure by melting can remove the heat of fusion of ice at a sufficiently high pressure by solidifying itself.

Figure 2 illustrates the general process and shows that partial freezing of an aqueous solution can be coupled with melting of the working medium by the following procedure:

$$\begin{matrix}\text{Aqueous Solution} \\ + \\ \text{Working Medium} \\ \text{(solid)}\end{matrix} \xrightarrow{\text{(at low pressure)}} \begin{matrix}\text{Ice} \\ + \text{ Conc. Aqueous Solution} \\ + \text{ Working Medium} \\ \text{(liquid)}\end{matrix} \qquad \text{.....} \qquad (1)$$

The melting of ice is coupled with the solidification of the working medium through the following procedure:

$$\begin{matrix}\text{Ice} \\ + \\ \text{Working Medium} \\ \text{(liquid)}\end{matrix} \xrightarrow{\text{(at high pressure)}} \begin{matrix}\text{Fresh Water} \\ + \\ \text{Working Medium} \\ \text{(solid)}\end{matrix} \qquad (2)$$

Considering the overall effect, the working medium operates in a cycle to reuse heat by drawing the heat of crystallization and transferring it to the melting of ice. Some work has to be supplied to the system in order to conform to thermodynamic requirements.

Selection of a working medium. The working medium may be either a pure substance or a mixture of substances. It may have a sharp melting point, such as a eutectic point, or it may have a melting point range. It is desirable to select a mixture whose

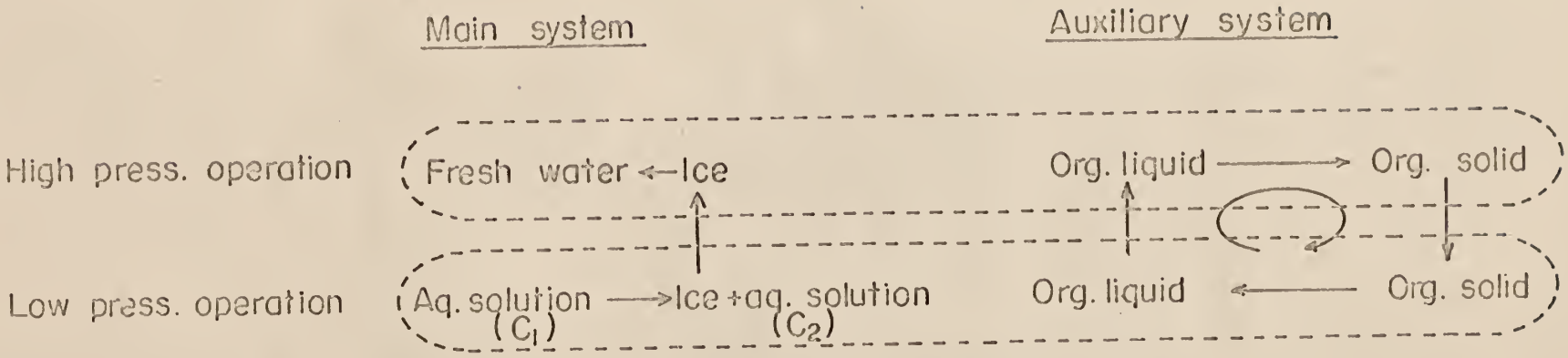


Fig. 2. Coupling between a main system (aq. solution system) and an auxiliary system (working medium system)

melting-point range approximates closely the range of the freezing point of the aqueous solution during the freezing operation.

An ideal working medium should have the following qualities: a proper melting range, a very low solubility in water, a large value for the latent heat of fusion, and a low value of $(\frac{dP}{dT})$ for melting. It should also be non-toxic, cheap, and readily available. Theoretically, any substance which has a proper melting point (or melting range) and has low solubility in water can be used. But the problem of economy will probably limit the practical working medium to a hydrocarbon or mixture of hydrocarbons.

Phase diagrams (solid-liquid equilibrium) for binary systems of saturated hycrocarbons have been reported by R. Salzgeber (6) and by S. S. Kaa (7). Figures A-1, A-2 and A-3 in Appendix A show the phase diagrams, obtained under atmospheric pressure and high pressures, of n-tridecane (pure grade)—n-tetradecane (pure grade), n-tridecane (technical grade)—n-tetradecane (technical grade), and n-tridecane (technical grade)—n-pentadecane (technical grade) binary systems, respectively (7). It can be seen that any one of those systems with proper composition meets the required melting range both at atmospheric pressure and high pressures. The latent heat of fusion of high n-paraffin hydrocarbons is particularly high, around 50-60 cal/gr for even C-number hydrocarbons and around 40 cal/gr for odd C-number hydrocarbons (8). Those hydrocarbons have also been reported to be insoluble in water (9). The manufacturers have estimated the long range price of n-paraffin hydrocarbons for quantities of several million pounds per year to be within 4.5-5 ¢/lb (10,11).

Benzene forms eutectic mixtures with many substances (12), and the eutectic temperatures are in the range suitable for the desalination of sea water. A mixture of benzene and naphthalene is a desirable system because it has a low value of $(\frac{dP}{dT})$ for melting and is readily available. There are objections to its use as a working medium, however. They are that it has a slight but signigicant solubility in water, it is toxic, and it has rather high volatility. Using this mixture as a working medium would require post treatments to remove it both from the product fresh water and from the reject salt water.

A working medium may be found among alkylnaphthalenes, for example, 2-n-propylnaphthalene (melting point: $-3^{\circ}$ C, density: 0.9770 gr/ml, very slight solubility in water). Since the density of an alkylnaphthalene is so close to that of an aqueous solution, elaborate equipment may be required for their separation.

Process description. Figures 3 and 4 are the block diagram and flow-sheet respectively of the proposed process. The process is divided into a low pressure part and a high pressure part. An outline of the operation is as follows: The aqueous feed solution, say sea water, is cooled by heat exchange with out-going fluid streams, viz. product fresh water and reject concentrated brine. In order to balance all the inefficiencies of the process plus the reversible work for separation, a refrigeration step would, by necessity, have to remove a certain amount of heat from the process. Some of the heat should be removed from the lowest temperature level in the whole process. In Fig. 4, it is shown that refri-

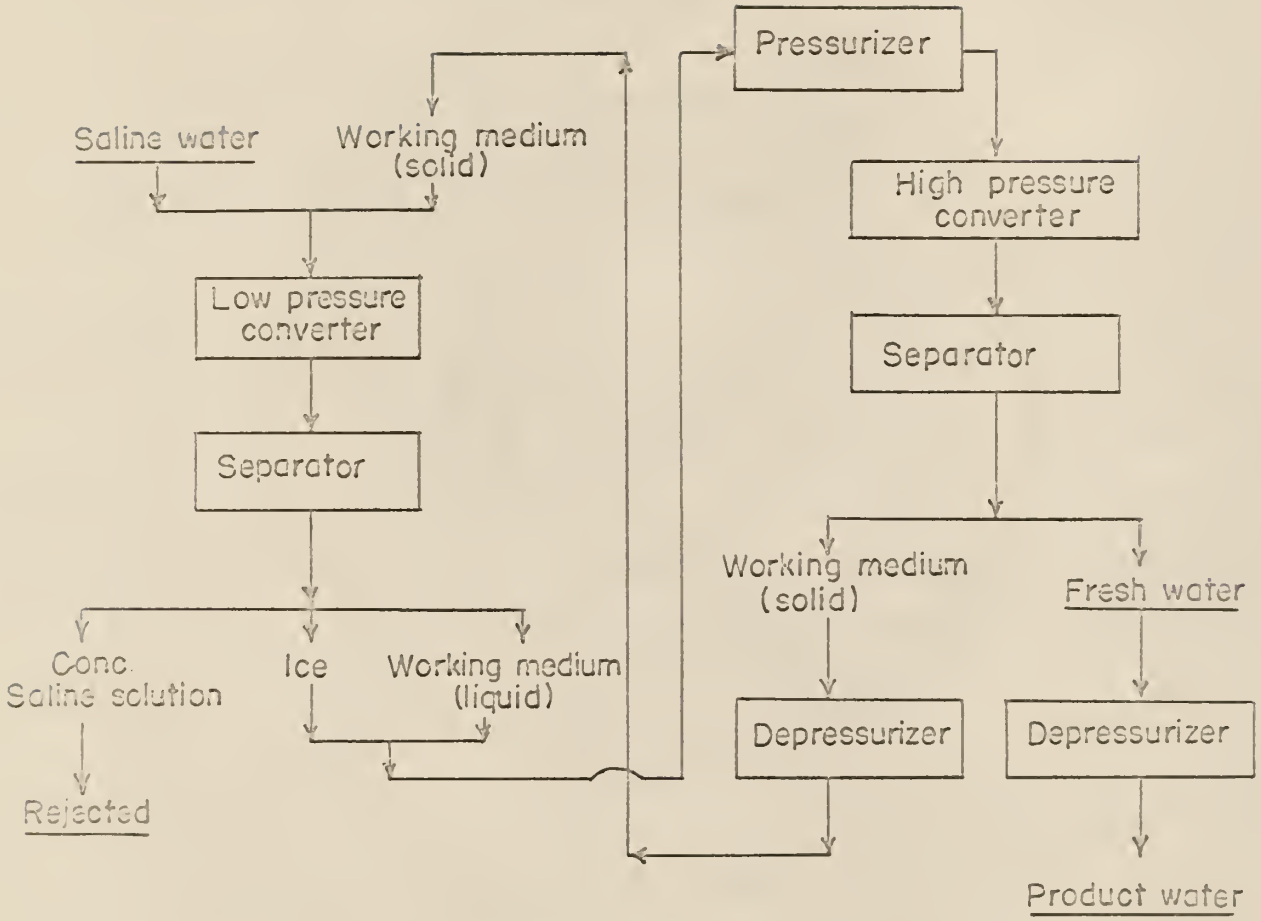


Fig. 3. Flow diagram for desalination of saline water by high pressure inversion of melting points.

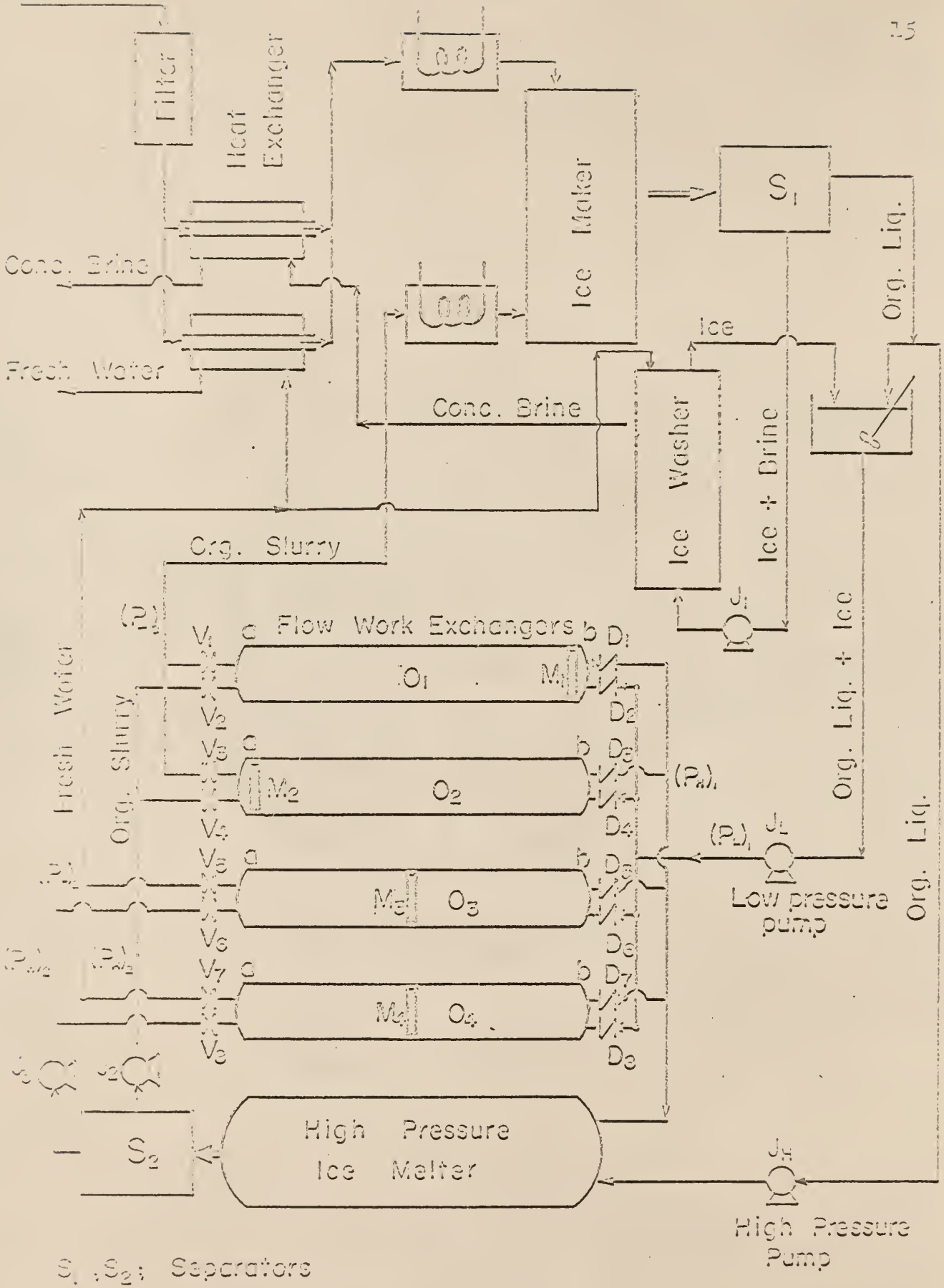


$S_1$ , $S_2$ ; Separators

$J_1$ , $J_2$ , $J_3$ ; Circulation pumps

Fig. 4. Flow sheet for desalination of sea water by high pressure inversion of melting points.

geration is used to remove heat from the recycle organic slurry and the aqueous feed solution before they go into the low pressure converter or ice-maker. The mixture discharged from the ice-maker is separated into an organic liquid and an ice-brine slurry in separator $S_1$. Ice-brine slurry is separated into ice and concentrated brine, and the resulting ice is washed free of mother liquor in an ice washer. The ice washing operation has already been well developed by those working with conventional freezing operations (2). The separated concentrated brine is heat exchanged with feed solution before being discharged. The washed ice is reslurried with organic liquid to form an ice organic liquid slurry and the mixture is pressurized either by a conventional high pressure pump, or by a flow-work exchanger (13). When the slurry of ice in the organic liquid is pressurized to a sufficiently high pressure, ice begins to melt and the organic liquid begins to solidify. The mixture is then discharged from the high pressure ice melter and is separated into organic slurry and fresh water. They are either depressurized through conventional turbines or by flow-work exchangers. The depressurized slurry is further cooled by refrigeration, as has been previously described, and is sent to the ice-maker. The depressurized fresh water is heat exchanged with the aqueous feed before being discharged as product water.

The advantages of this process. In addition to those common to all freezing processes, the Inversion Freezing Process has the following advantages:

1. An efficient low-cost crystallizer can be constructed due to the condensed phase operation.

2. Ice crystal formation can be easily controlled because the subcooling can be kept low due to the involvement of only condensed phases. This advantage leads to the possibility of large granular ice crystal formation and thus a reduction of ice crystal washing cost.
3. Energy requirement can be reduced because of the condensed phase operation and the adoption of flow-work exchangers.

# EXPERIMENTAL

One of the objectives of this work was to set up a continuous experimental system for ice-making at atmospheric pressure. The ice crystals are formed according to the following equation:

$$\text{Aqueous Solution } (C_1) + \text{Working Medium (solid)} \longrightarrow \text{Ice} + \text{Aqueous Solution } (C_2) + \text{Working Medium (liquid)} \quad \ldots\ldots\ldots\ldots\ldots\ldots \quad (3)$$

A mixture of n-tridecane and n-tetradecane was chosen as the working medium in this work because it has the following qualities: non-toxicity, a very low solubility in water, a proper melting range, a large value of the latent heat of fusion, a high value of $(\frac{dT}{dP})$ for melting, no hydrate formation, low cost, and ready availability.

## SELECTION OF ICE MAKER.

Three different types of ice maker were considered and tested, they were: (1) a counter-current continuous-contact vertical column with slow agitation, (2) a co-current continuous-contact horizontal column with slow agitation, and (3) a back-mixed contacter.

The back-mixed type contacter was finally selected for use in this work for the following reasons:

1. Suspended solids can be handled easily.
2. The degree of dispersion may be established at any level through mechanical agitation without causing "flooding".

3. Any proportion of the inlet streams aqueous and organic may be handled easily, with either phase dispersed, and the ratio of the two flow streams may be controlled at will.
4. Reasonably reliable scale-up from small to industrial size is possible.

EQUIPMENT SET-UP.

The overall experimental set-up which was used for obtaining the data is shown schematically in Fig. 5. The principal piece of equipment used was the ice-maker. Other items of the equipment and instruments served to make organic slurry, to keep the salt water at its freezing temperature, to move the fluid, to measure the flow rate and to achieve the recycling. Figure 6 shows the overall view of the equipment used in the closed cycle operation. A description of the individual equipment pieces associated with the fluid flow is presented below:

Organic slurry maker. The equipment was modified from a soft ice-cream machine made by the Sweden Electrical Company. Figure 7 shows the schematic diagram of this slurry-making system. The exit slurry temperature (and, therefore, the solid content) was controlled by a precision temperature controller made by the Yellow Spring Instrumment Company, Inc. It was an "on-off" type, Model 71, direct dialing. It had a temperature range of control from $-6^{\circ}$ C to $+124^{\circ}$ C with a sensitivity better than $\pm 0.05^{\circ}$ C below $60^{\circ}$ C. The temperature probe was installed at the center of the cooling cylinder.

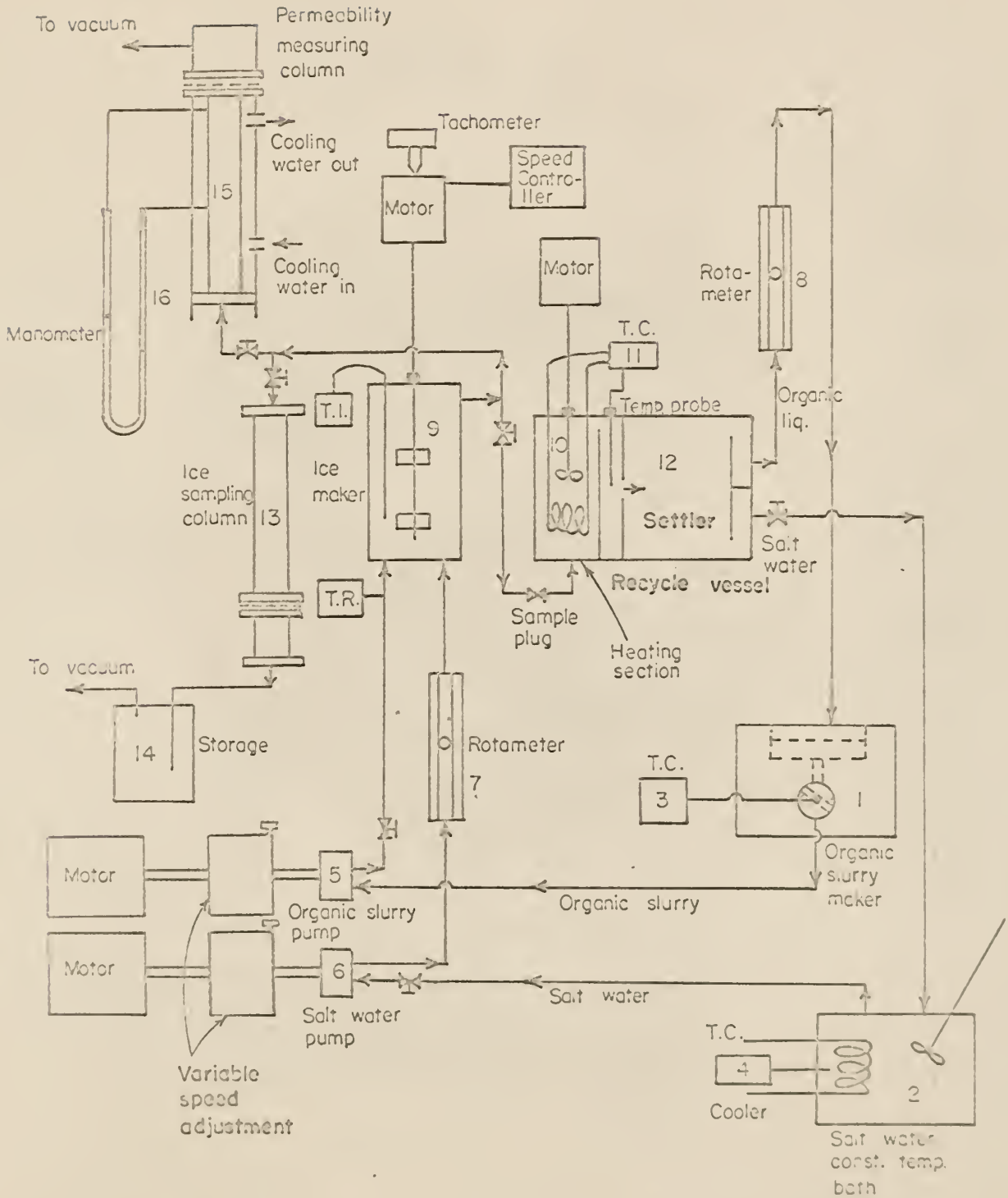


Fig. 5. Schematic flow diagram of a closed cycle ice-making system.

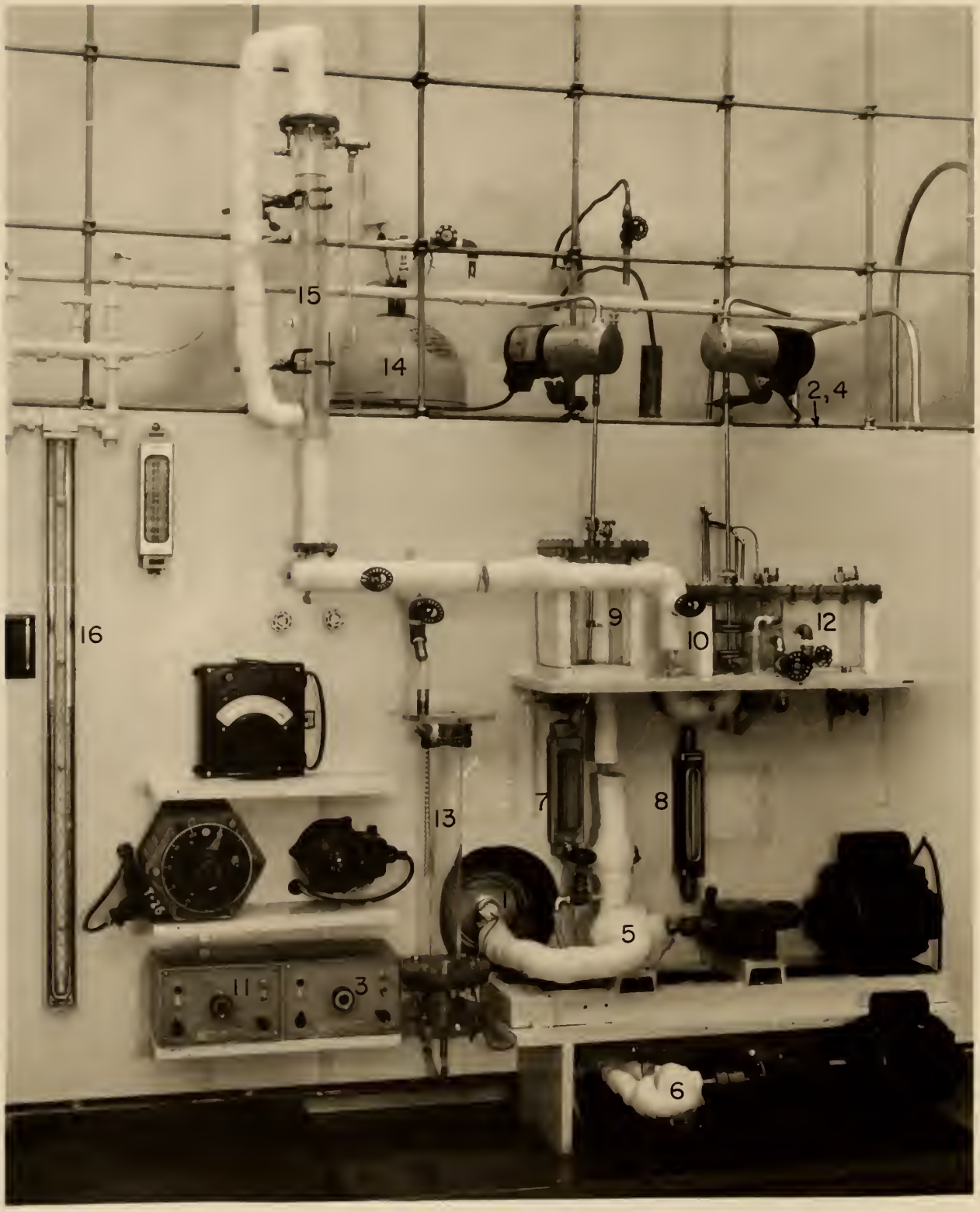


Fig. 6. Over all view of bench scale apparatus.

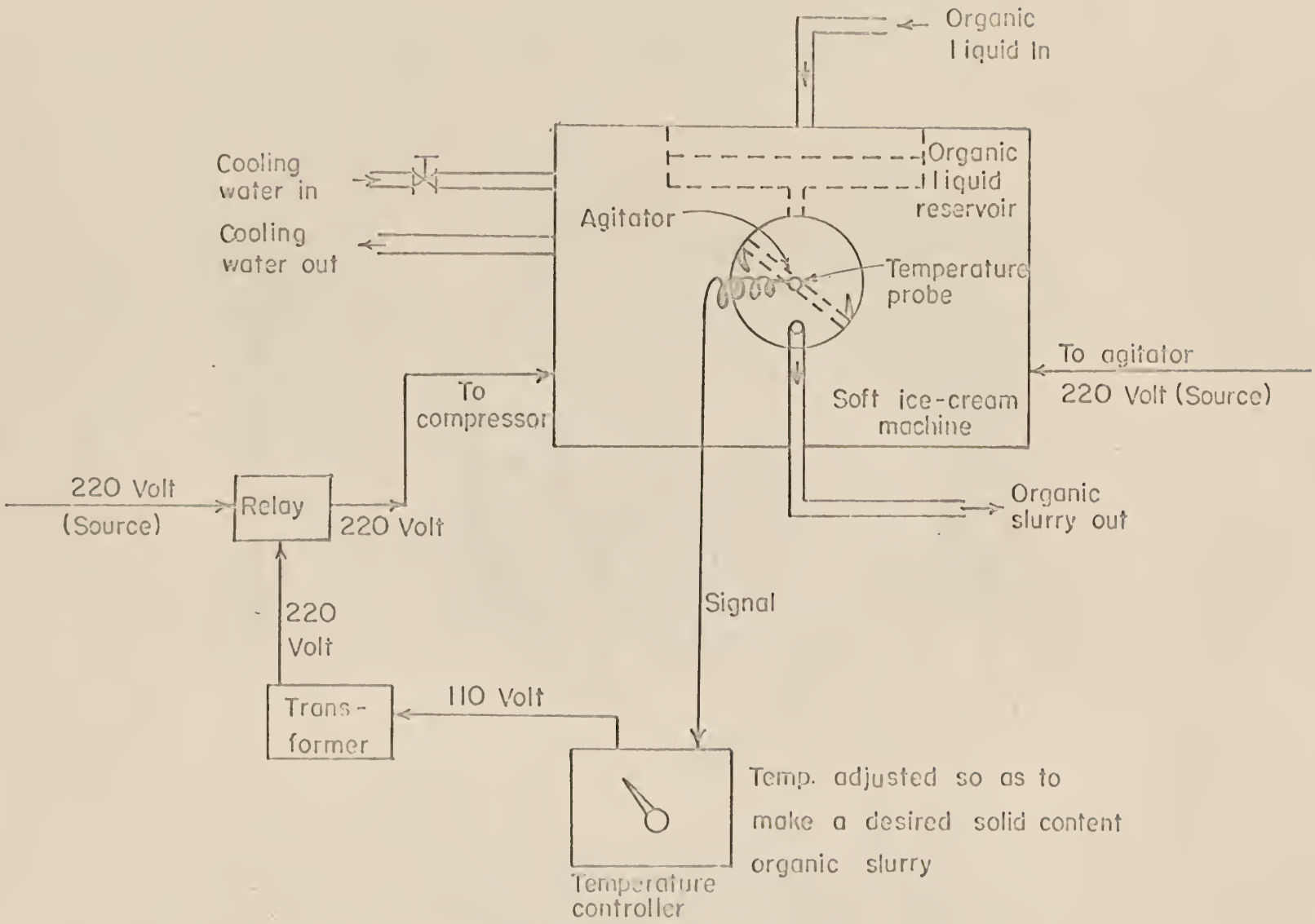


Fig. 7. Schematic diagram of organic-slurry making system.

The volume of the cooling cylinder was 4 liters. The cooling rate of this machine was about 200 cal/sec.

Salt water constant temperature bath. This bath was used to supply the salt water to the Ice Maker at a temperature close to its freezing temperature. It was made by the Blue M Electrical Co., Model No. PCC-A. Temperature was maintained by a cooling coil. The cooling elements were controlled by a "Blue M Microcontroller". The capacity of the bath was about 14 liters.

Organic slurry pump. A gear pump driven by a G.E. 1725 rpm, one horse power motor was used. The pump was made by Eastern Industries, Model No. 104-A21. The speed of the pump was adjusted by using a Zero-Max torque convertor, Model JKI, speed range 0 to 400rpm. The maximum capacity of this pump was about 50 ml/sec.

Salt water pump. A brass gear pump, made by the Price Pump Co., Model No. 2, driven by a one horse power motor (Westinghouse, style 309P916A, 1725 rpm) was used. The speed of this pump was regulated by using a Zero-Max torque convertor, Model 142X, speed range 0-400 rpm. The maximum capacity of this pump was about 30 ml/ sec.

Salt water flow meter. The volumetric flow rate of the salt water from the Salt Water Pump was measured by a "Brook" rotameter, Type 5-1110-5. The rotameter was calibrated by measuring the time required to fill a 250 ml. graduate cylinder. Calibrations for the temperature of 3° C were run and are given in Fig. B-1 in Appendix B.

Organic slurry temperature recorder. A " Honeywell Two-Pen Electronic 19* Lab Recorder" was used to indicate and to record

the organic slurry inlet temperature of the Ice Maker. It provided high speed responses, quick selection of multiple span (from 100 microvolts to 100 volts), positive and negative zero range ability, and selection of multiple chart speeds (10 fixed speeds). A span of 0.5 millivolts was used throughout the experiment. The accuracy was within $\pm 0.03^{\circ}$ C.

Ice Maker. (See Fig. 8) The salt water from the rotameter and the organic slurry from the pump entered the Ice Maker from the bottom. The vessel was constructed of $\frac{1}{2}$-in. thick plexi-glas. It was rectangular, flat-bottomed with inside dimensions 8.7 X 8.7 X 16.5 cm. The agitator impellers were attached to a shaft located at the center of the vessel. The drive motor was a 1/20 HP D. C. motor, maximum speed 1500 rpm. The agitator speed was regulated by an electronic speed controller supplied by Cole-Parmer Instrument And Equipment Co., Catalog No. 7025. The rotary speed was measured by a calibrated tachometer, obtained from Stewart-Warner Corporation, Model 757-W. To minimize the heat losses, the outside of the vessel was insulated with 1" thick styrofoam.

From the Ice Maker, the stream was directed into the Recycle Vessel to achieve the recycling or into the Ice- Sampling Column to obtain samples for the study of ice-crystal size.

Recycle Vessel. (See Fig. 9) This vessel, consisting of a heating section and a settler, was designed to make possible the recycling of the effluent from the Ice Maker. The ice crystals and the organic solids contained in the effluent from the Ice Maker were first melted in the heating section, then the aqueous and organic phases were separated in the settler, and finally each

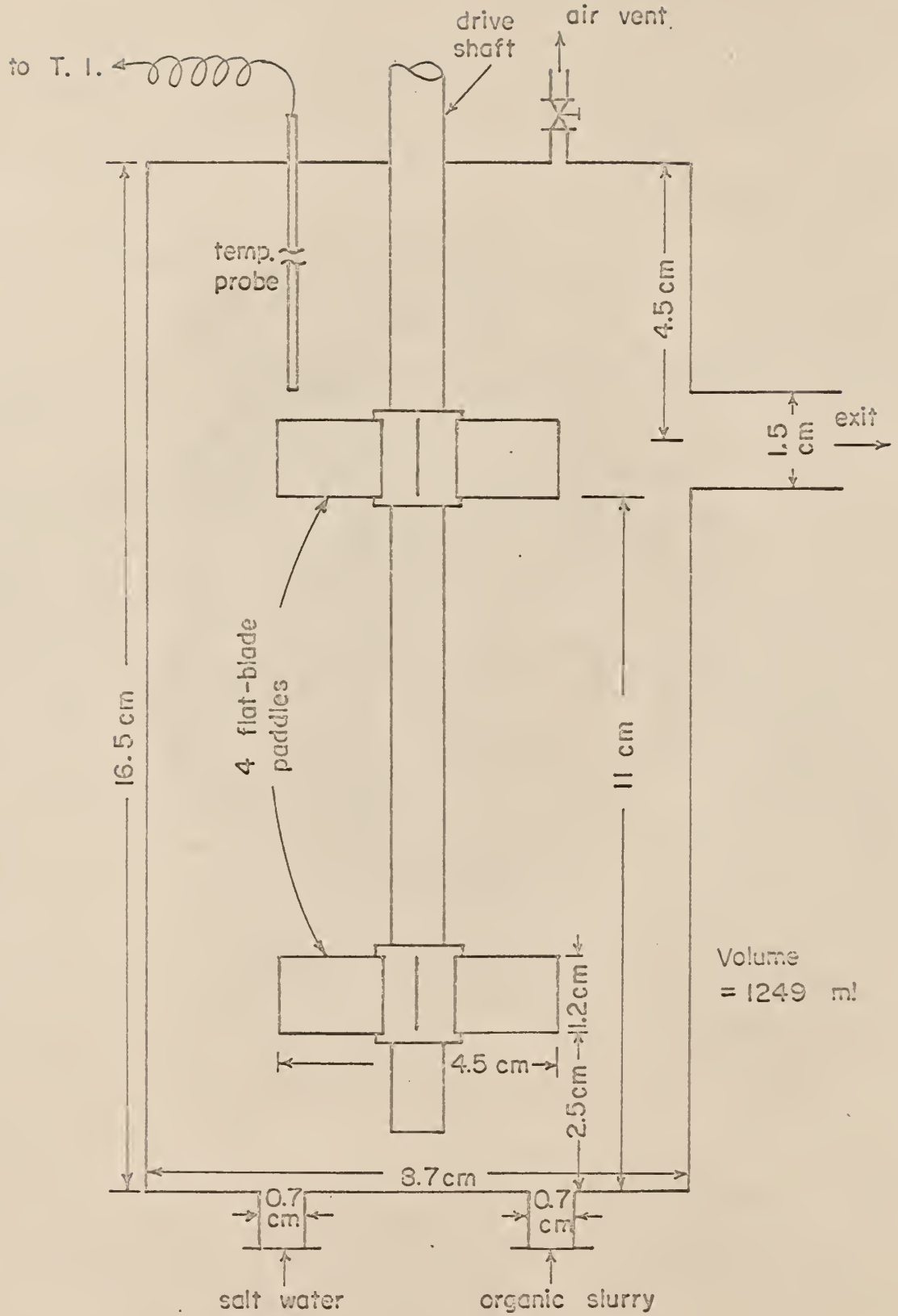


Fig. 8. The side view of the ice maker.

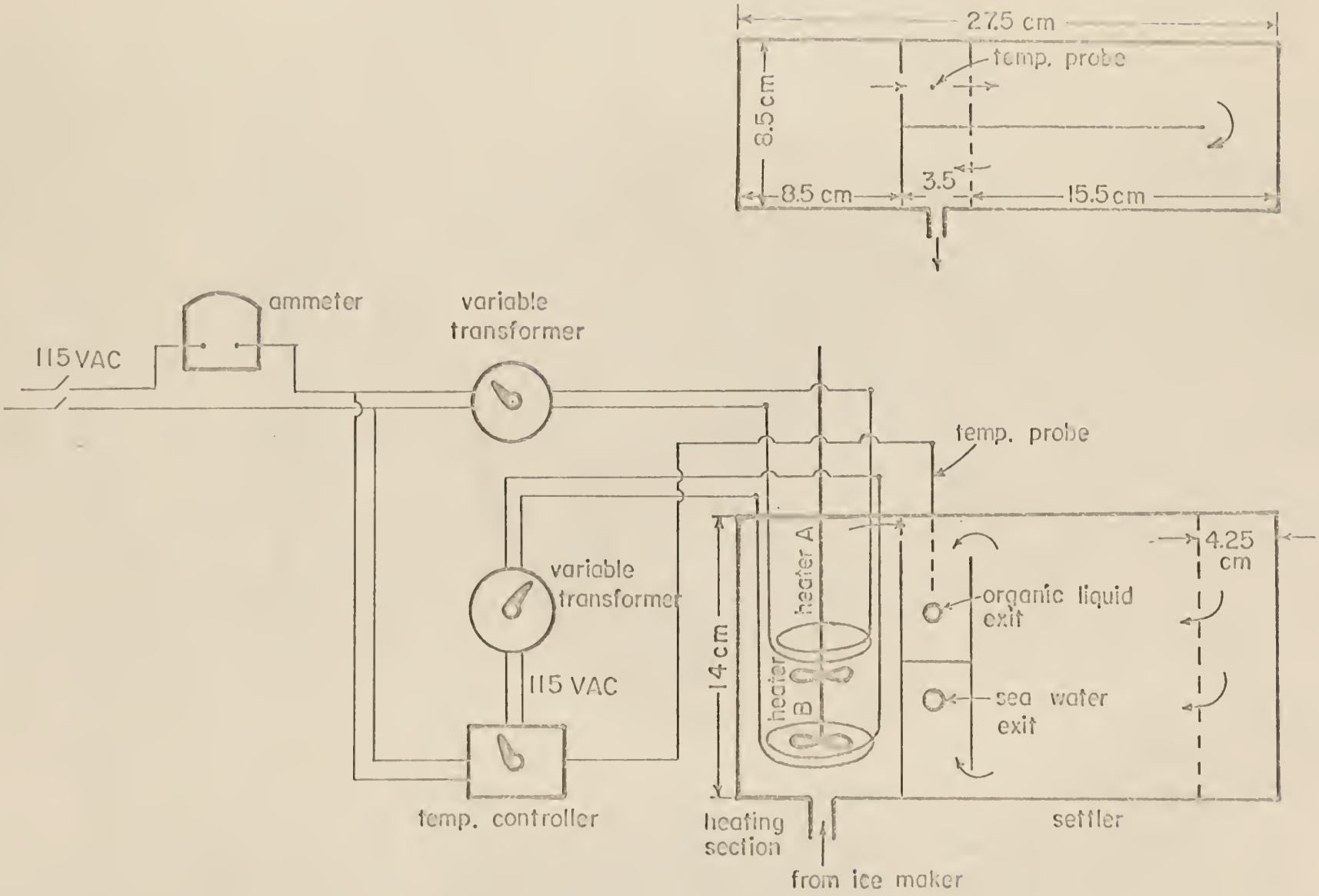


Fig. 9. Recycle vessel and its temperature control system.

phase was returned to the beginning of the process.

The heating section was agitated, and heat was supplied by two 750-walt stainless steel electric immersion heaters. A variable transformer (made by The Superior Electrical Co., Type 2PF1226, 0-240 VAC, 2.4 KVA) which was supplied with 105 VAC, was used to supply the desired voltage between the two ends of the heater A. The electric power to the heater B was controlled and regulated by an "on-off" type temperature controller (made by the Yellow Spring Instrument Co., Model 71. For detail, see the temperature controller of the Organic Slurry Maker, p. 19) in series with a variable transformer (made by The Superior Electric Co., Type 216, 0.270 VAC, 0.81 KVA). A temperature probe was installed at the exit of this section and connected to the controller. By adjusting the output voltage of the transformers, the exit stream temperature could be kept at a desired value. To assure complete melting of solids, the temperature was generally controlled at $\pm 1^{\circ}$ C. The mechanical agitation in this section was accomplished by two marine-type propellers. The drive motor was supplied by the Mixing Equipment Co., Model P.

The phase separation in the settler was caused by the difference in the density of the two phases (0.78 gr/cm$^3$ for organic and 1.027 gr/cm$^3$ for aqueous at $0^{\circ}$ C). The volume of this section was about 1.8 liters.

Organic liquid flow meter. The flow rate of the organic stream was measured with a rotameter after it left the settler. A Fischer-Porter Flow rater tube, No. 2F-$\frac{1}{4}$-25-5/70 was used. The rotameter was calibrated by measuring the time required to fill a

250 ml graduate cylinder with organic liquid at 0° C. The results of calibrations are given in Fig. B-2 in Appendix B.

Ice Crystal Sampling Column. This column was used to collect the ice crystals in the effluent of the Ice Maker. The salinity and the crystal size of the ice was then determined. This column was an extruded acrylic pipe, with a 2-in. ID, 2¼-in. OD, and 18-in. long. A piece of 60 mesh screen was installed at the bottom of the column, which let only the liquid part of the stream pass through. The liquid was accumulated in a closed 5 gallon tank to which an aspirator was connected to provide the driving force of liquid flow from the column.

A permeability measuring column was installed, but was not used in this research because of the very low ice production rate of the system. If a higher capacity system is studied, the permeability measuring column can then be used to measure the sizes of ice crystals (14).

Tubing and Insulation. Due to the strong corrosiveness of the salt water, Tygon tubing was used mostly in this system. Two-inch thick fiber glass was used to insulate the outside of the tubing to minimize the heat losses.

## EXPERIMENTAL PROCEDURE.

Preparation of the Salt Water. Throughout the experiment, 3.5% (wt.) NaCl Solution was used instead of sea water. It has been reported (2) that the prepared salt water gives results in desalination very similar to those using sea water. The salt water was prepared by disolving table salt in tap water and filter-

ing off undisolved material. The concentration was determined by electrical conductivity measurements.

Preparation of the Organic Mixtures. Mixtures of n-tridecane ($C_{13}H_{28}$) and n-tetradecane ($C_{14}H_{30}$) were used as the working medium in this work. Their physical properties are as follows:

| | $C_{13}H_{28}$ | $C_{14}H_{30}$ | ref. |
|---|---|---|---|
| Molecular wt. | 148.25 | 198 | (15) |
| Melting point (1 atm.), ($^{o}$C) | -6.2 | +5.5 | ( 9 ) |
| Heat of fusion, (cal/gram) | 37.0 | 54.4 | (15) |
| Solid heat capacity, (cal/$^{o}$C gr.) | 0.715(-10$^{o}$C) | 0.418(-3$^{o}$C) | (15) |
| Liquid heat capacity, (cal/$^{o}$C gr) | 0.641(-3$^{o}$C) | 0.515(+7$^{o}$C) | (15) |
| Sp. gr. (20$^{o}$C/4$^{o}$C) | 0.757 | 0.765 | ( 9 ) |

Technical grade n-tridecane and n-tetradecane were obtained from the South Hampton Company, Houston, Texas. Four different kinds of mixtures were prepared and used throughout this work. Their compositions and freezing points are presented below:

| Mixture | Composition (Vol.) | Freezing point, $^{o}$C | |
|---|---|---|---|
| A | 65% n-$C_{13}H_{28}$, 35% n-$C_{14}H_{30}$ | -4.40 | (measured) |
| B | 58% n-$C_{13}H_{28}$, 42% n-$C_{14}H_{30}$ | -3.60 | (measured) |
| C | 55% n-$C_{13}H_{28}$, 45% n-$C_{14}H_{30}$ | -3.26 | (measured) |
| D | 52% n-$C_{13}H_{28}$, 48% n-$C_{14}H_{30}$ | -3.07 | (measured) |

Description of the rocedure for an Experimental Run.

A. Determination of Heat Transfer Rate

(1) The Salt Water Constant Temperature Bath was set at $-1^{\circ}$ C.

(2) To decrease the time required for the system to achieve steady state temperature, the Salt Water Pump was started and the salt water (at $-1^{\circ}$ C) was circulated through the Ice Maker and the Recycle Column.

(3) The Organic Slurry Maker was started. The slurry temperature was controlled at a desired value.

(4) The Salt Water Pump was shut off temporarily and the Organic Slurry Pump was started. The torque convertor was adjusted for a desired organic flow rate as determined by the rotameter at the exit of the Settler. Meanwhere, the salt water exit valve of the settler was closed.

(5) The Salt Water Pump was started again. The flow rate was adjusted at a desired value as determined by the rotameter.

(6) The agitator of the Ice Maker was started. The rotary speed was adjusted as determined by the tachometer.

(7) The agitator of the Heating Section was started.

(8) The salt water valve at the exit of the settler was regulated to keep the interface level at the middle of the settler.

(9) The power to the immersion heaters was turned on after the temperature of the effluent from the Heat-

ing Section was as low as $\pm 1^{\circ}$ C. The outlet voltage of the transformers was adjusted to maintain the temperature at $\pm 1^{\circ}$ C. About 30 minutes were required for conditions to reach the steady state.

(10) The experimental conditions were recorded on a data sheet similar to the one given as Table 1.

(11) The samples of brine at the exit of the Ice Maker were taken through the sample plug by using a hypodermic syringe.

(12) The inlet flows to the Ice Maker and the agitator were shut off simultaneously. The water hold-up in the vessel was determined after the ice was melted.

B. Determination of Salinity and the Ice Crystal Size.

(1) —— (10) The same as those in Part A.

(11) The valves to the Ice Sampling Column and the Recycle Column were opened and closed respectively at the same time.

(12) Ice crystals were accumulated in the column. The liquid stream was directed into the storage tank.

Determination of the Brine Concentration. An electrical conductivity meter and probe were found to be a quick method for determining NaCl content of the sample solution. A Model RA4 Direct Reading Conductivity Meter, with conductivity range between 0 and 2500 micromhos/cm and with a probe with two platinized metal plates, supplied by Industrial Instruments, Inc., were used for this purpose. This concentration measuring system was calibrated by reading the conductivity of NaCl standard solutions. The re-

Table 1. Sample data sheet.

Data Sheet

Run No: 33 Date: Aug. 26, '67

Organic slurry:

composition: 55 % $n\text{-}C_{13}$ flow rate: 2.75 c.c./sec
Ice-Maker inlet temp.: -4.52 °C enthalpy of fusion: 139 cal/sec

Salt water:

composition: 3.5 % NaCl(wt.) flow rate: 3.5 c.c./sec
Ice-Maker inlet temp.: +3.6 °C

Agitation:

speed: 300 rpm or mech. HP: _____

Heater power input:

4.8 amp. X 105 volt or 121 cal/sec

Heating column exit stream temp.: +0.5 °C

Salt water hold-up in Ice-Maker: 500 c.c.

Residence time of salt water in Ice-Maker: 143 sec

Mother liquor analysis:

| sample: | 1 | 2 | 3 |
|---|---|---|---|
| amt. c.c. vol. of dist. water added: | 200 | 200 | |
| condutivity meter rdg: | 10.85 | 10.9 | |
| concentration (wt.% NaCl): | 4.29 | 4.34 | |

Heat transfer from salt water:

sensible heat: 19.0 cal/sec enthalpy for ice crystal formation: 55.6 cal/sec
total: 72.0, 74.6 cal/sec

Heat transfer efficiency: 51.8, 53.7 %

Comment: _____

sults of calibration are given is Fig. B-3 in appendix B.

To analyze a salt solution, a certain amount of dictilled water was added to dilute it so that its concentration was within the meter range (600 to 1400 ppm NaCl). The meter was checked frequently by reading the standard solutions to detect any change in the probe or meter.

Agitation Power Measurements. The power input to the impellers during the operation is essential for the scale-up of the system (16). In this work, the power measurements were done by measuring the electrical power input to the drive motor with an ammeter and a volt meter and changed to horse power with the conversion 1 hp = 745.5 watts. A correction for the electrical and mechanical power losses was made by referring to the motor efficiency

$$\eta = \frac{\text{Output power (agitation power)}}{\text{Input power (measured HP)}} .$$

Since the motor manufacturer was unable to supply the information about motor efficiency, data for various load conditions were obtained from reference books (17, 18).

In all experiments, air was removed from the Ice-Maker to prevent the aeration of the liquid.

# RESULTS AND DISCUSSION

There are several operating variables which affect the rate of production and the quality of ice crystals. Among them the following variables were studied: the thermal driving force, the degree of agitation, and the nominal residence time. Experiments were performed to investigate each of these while the other variables were held constant.

The thermal driving force is a quantity which is very difficult to evaluate in this complex process. Both organic and aqueous phases change their composition and temperatures simultaneously and therefore, the temperature difference between phases also changes continuously. In fact, the driving force for any single small portion of organic and aqueous phases can be quite different from any other meaning that the thermal driving force is really a statistical quantity. However, by using different organic mixtures with different incoming temperatures but the same solid content the effect of the thermal driving force on the heat transfer rate could be studied assuming that all the other variables were constant. By changing the salt water inlet flow rates while holding the inlet organic slurry and other variables constant, the effect of thermal driving force could also be detected. Likewise, keeping the temperature and composition of the incoming streams constant and varying the stirrer speed gave the effect of mixing on the heat transfer rate. Changing the total inlet flow rate but keeping the same flow rate ratio between two incoming streams enabled one to study the effect of residence time on heat transfer

efficiency.

The recorded experimental data are summarized and shown in Table C-1 in Appendix C. Calculations for a run were made as follows.

First, the ice crystal content of the product stream was calculated. This was done by using the feed and product assays of the salt water. Note that the reaction.

$$\text{Aqueous Solution } (C_1) + \text{Organic Solid} \rightarrow \text{Ice} + \text{Aqueous Solution } (C_2) + \text{Organic Liquid} \qquad (4)$$

removes fresh water from the salt solution, and, therefore, the salt concentration in the reactor brine increases. Using a certain amount of aqueous feed as a basis, the fraction of feed water solidified, and hence the weight percents of ice, salt, and water in the slurry could be calculated. Once the ice content was determined, the heat transferred for the ice formation could be calculated from the following equation

$$Q_f = W_a \cdot \frac{S}{100} \cdot \lambda_i \qquad (5)$$

where:

$Q_f$ = heat transferred for ice formation, cal/sec.

$W_a$ = mass flow rate of inlet salt water stream, gr/sec.

$S$ = weight percent ice in product stream, %.

$\lambda_i$ = latent heat of fusion of ice, 80 cal/gr.

Next, the heat transferred for the cooling of salt water from the inlet temperature to the freezing temperature was calculated in a straight forward manner from the following heat balance

equation

$$Q_s = W_a \cdot (t_{in,a} - t_{f,a}) \cdot \bar{C}_{pa} \qquad (6)$$

where:

$Q_s$ = heat transferred for cooling of salt water (or, sensible heat above the initial freezing point), cal/sec.

$t_{in,a}$ = salt water inlet temperature, °C.

$t_{f,a}$ = salt water initial freezing temperature, -2.05 °C.

$\bar{C}_{p,a}$ = mean specific heat of salt water, 0.952 cal/gr. °C for 3.5% (wt.) NaCl solution at about 0° C.

The total heat required to accomplish a known degree of ice formation may be written as

$$Q = Q_s + Q_f + Q_u + Q_i \qquad (7)$$

$Q_s$ and $Q_f$ were previously defined. $Q_u$ and $Q_i$ are the sensible heat of unfrozen brine and sensible heat of ice, respectively. Since the temperature of the product stream is generally not lower than -3.5 °C, a simple calculation may show that the sum of $Q_u$ and $Q_i$ account for only a small portion of total refrigeration requirement. Hence, $Q_u$ and $Q_i$ were neglected, and, consequently,

$$Q \cong Q_s + Q_f \qquad (8)$$

The total heat transfer efficiency in the Ice-Maker was calculated from the following expression

$$\theta = \frac{Q}{W_o \cdot h_{f,o}} \cdot 100 \qquad (9)$$

Where:

$\vartheta$ = total heat transfer efficiency, %.

$W_o$ = organic slurry mass flow rate, gr/sec.

$h_{f,o}$ = heat of fusion of organic solid in unit mass of organic slurry, cal/gr.

The calorimetric determination of $h_{f,o}$ and calculations of various results for a typical run are presented in the Appendix C.

Figure 10 is a plot of heat transfer rate in the Ice-Maker versus stirrer speed and power input for runs No.25 through 32. The stirrer speed was increased in increments from 300 to 900 rpm. The inlet conditions of salt water and organic slurry were held constant in each of these runs. On Figure 10, the topmost curve is the total amount of heat available for transfer from the heat of fusion of organic solid. The next curve down shows the total amount of heat transfer per unit time, which was used in the formation of ice crystals and the cooling of the salt water.

Lines representing the enthalpy - temperature relation of the aqueous system (consisting of brine and ice) and that of the organic system (consisting of solid and liquid phases) for this set of runs are shown in Fig. 11, where line a-b-c is for the aqueous system which released the heat, and line d-e-f is for the organic system which absorbed the heat. Line a-b-c was constructed as follows. Taking the salt water inlet temperature, $t_{in,a}$, as a reference temperature and the salt water mass flow rate as a basis, the enthalpy of the aqueous system ($H_t$) at any temperature (t) between $t_{in,a}$ and the initial freezing temperature of salt water

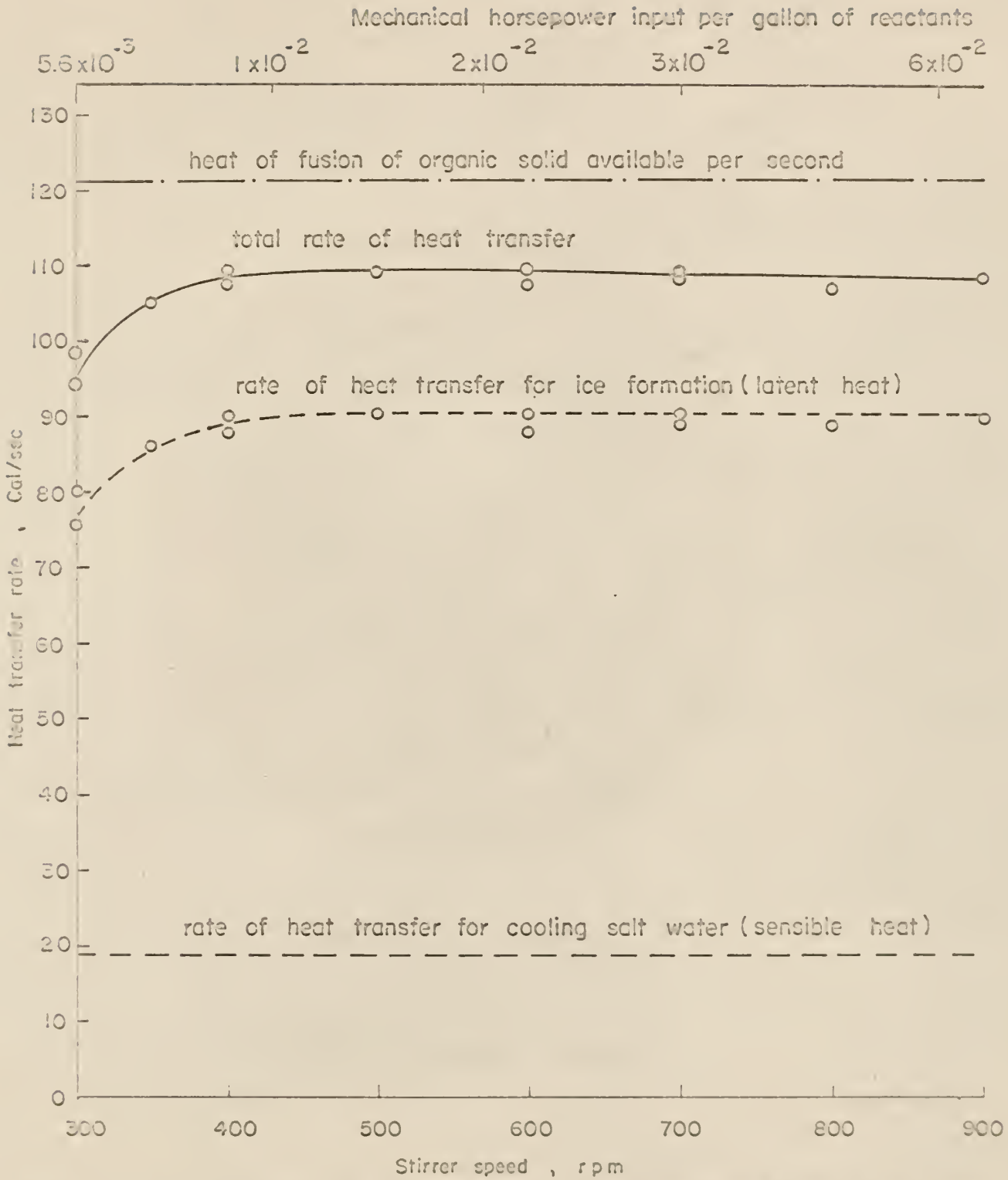


Fig. 10. Heat transfer rate vs. stirrer speed and power input. Org. mixture composition : 65% (vol.) n-$C_{13}$ , 35% n-$C_{14}$ ; org. slurry flow rate : 8.75 ml/sec; inlet temp. :-5.5°C . Salt water composition : 3.5% (wt.) NaCl ; flow rate: 3.5 ml/sec ; inlet temp. : 3.6 °C .

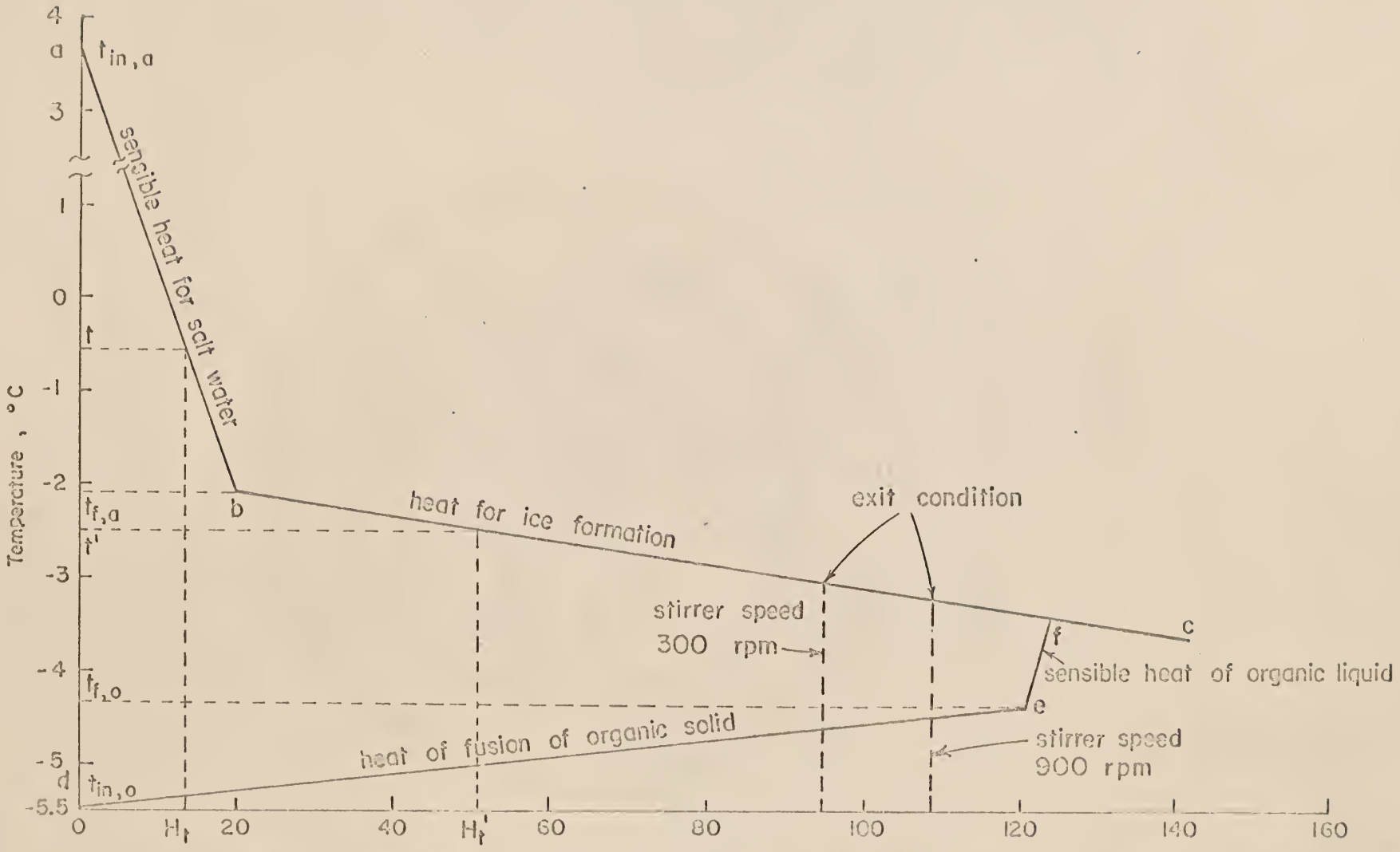


Fig. 11. Temperature-heat curves. Organic mixture composition : 65 % (vol.) n-$C_{13}$ , 35 % n-$C_{14}$ ; organic slurry flow rate : 8.75 ml/sec ; inlet temperature : -5.5 °C. Salt water composition : 3.5 % (wt.) NaCl ; flow rate : 3.5 ml/sec ; inlet temp. : 3,6 °C.

($t_{f,a}$) can be obtained by the equation

$$H_t = W_a \cdot \bar{C}_p \cdot (t - t_{in,a}) \tag{10}$$

where $W_a$ and $\bar{C}_p$ were as previously defined for Eq. (6). Line a-b corresponds to this equation which represents the relation between the temperature and the ethalpy change due to the sensible heat evolution of the aqueous system. At temperature $t_{f,a}$, ice was started forming, below $t_{f,a}$, (generally designated by t'), the H-t relation can be written as

$$H_{t'} = [x\, h_{i,t'} + (1 - x)\, h_{b,t'}] W_a \tag{11}$$

where:

$x$ = mass fraction of ice in the aqueous system

$h_{i,t'}$ = enthalpy of a unit mass of ice at t', cal/gr

$h_{b,t'}$ = enthalpy of a unit mass of unfrozen brine at t', cal/gr.

Assuming

$$h_{b,t'} = h_{i,t'} - \lambda_i \tag{12}$$

where $\lambda_i$ is the latent heat of fusion of ice, Equation (3) becomes

$$H_{t'} = (h_{b,t'} + x\lambda_i) \cdot W_a \tag{13}$$

$h_{b,t'}$ can be calculated by the relation

$$h_{b,t'} = \bar{C}_p \cdot (t' - t_{in,a}) \tag{14}.$$

The x-t relation was obtained by using the phase diagram of salt

(Fig. A-4 in Appendix A) and the mass balance relation. A reasonably linear x-t relation was obtained for the operating range used (as shown in Fig. A-5). Line b-c was constructed by using this figure together with Equations (13) and (14) to represent the relation between temperature and the enthalpy change after ice crystals started forming.

The enthalpy-temperature relations of the organic system, taking the slurry inlet temperature as a reference and the slurry mass flow rate as a basis, could have been determined in the same manner as that of the aqueous system. However, owing to the lack of a suitable phase diagram, some critical points on the H-t line were determined experimentally instead. On Fig. 11, point "d" represents the condition which corresponds to the inlet slurry temperature, $t_{in,a}$, and zero enthalpy ($t_{in,o}$ was taken as reference temperature). Point "e" was found by the experimental determination of the initial freezing temperature ($t_{f,o}$) of the specific mixture and the enthalpy of fusion of the organic solid in the slurry. Because of the lack of information about the x-t relation in this system, which was required for the construction of the H-t relation between points "d" and "e", a straight line was drawn for approximation. As the temperature went higher than $t_{f,o}$, the enthalpy change with temperature was completely caused by the sensible heat absorption and was determined by one equation similar to Eq. (10). One can clearly see on this figure that the salt water stream (at 3.5 ml/sec) entered the Ice-Maker at +3.6° C and was cooled to about -2 °C after 19 calories of heat had been transferred. At that point ice crystals started forming. One also

sees that the organic slurry entered at a temperature of -5.5 °C and was melted absorbing heat from the salt water. The formation of ice continued as the organic solid continued to melt. For a fixed flow rate and initial temperature, the amount of contact is dependent on the degree of mixing in the contactor. We would expect an increase in heat transfer rate with an increasing degree of mixing. This is indeed the case as shown by the ascending trend of the curves on Fig. 10. This can also be seen by comparing the two dashed lines parallel to the vertical axis on Fig. 11 showing the amount of heat transferred at stirrer speed of 300 and 900 rpm respectively. It should be noted that the total amount of heat transfer was always less than the amount of heat available for transfer from the heat of fusion of the organic solid. This reveals that not all of the organic solid was melted.

Figures 12, 13, and 14 were obtained in the same manner as Fig. 10 but using different organic mixtures with different incoming temperatures while the organic solid content in the incoming slurry in all cases was about the same. Data used in constructing these three figures were from runs No. 9-17, 18-24, and 33-39 respectively.

From the data used in Figs. 10-14, the curves of heat transfer efficiency vs. stirrer speed and the temperature vs. heat are shown on Fig. 15 and Fig. 16, respectively. Due to the difference in incoming organic slurry temperature and the changing stirrer speed, these two figures illustrate the expected tendencies of increasing total heat transfer efficiency and heat transfer rate with an increased in agitation and with an increased in the thermal

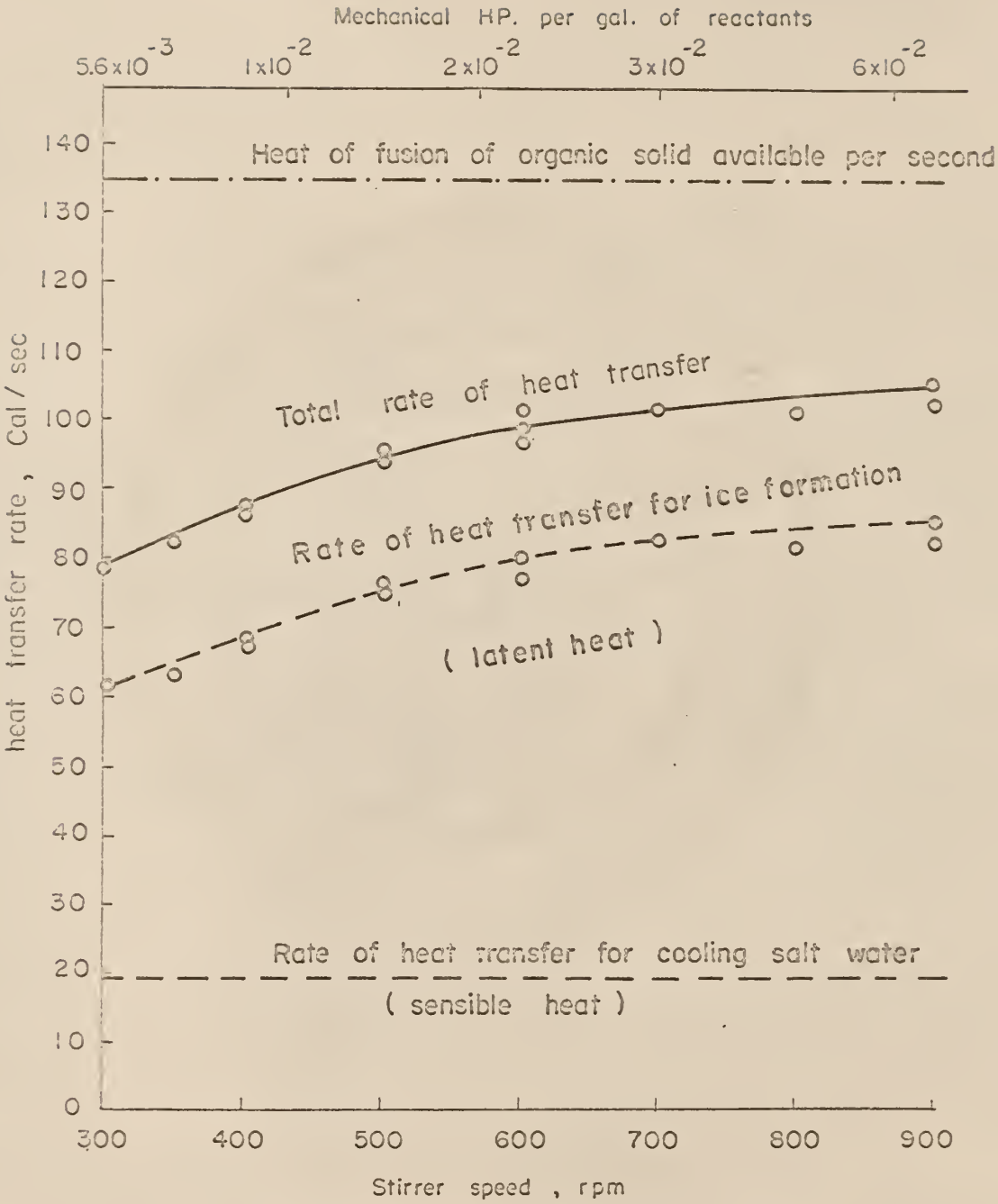


Fig. 12. Heat transfer rate vs. stirrer speed and power input. Org. mixture composition : 58 % (vol.) n - $C_{13}$ , 42 % n - $C_{14}$ ; org. slurry flow rate : 8.75 ml / sec ; inlet temp. : - 4.82 °C. Salt water inlet composition : 3.5% (wt.) NaCl ; flow rate : 3.5 ml / sec ; temp. : 3.6 °C.

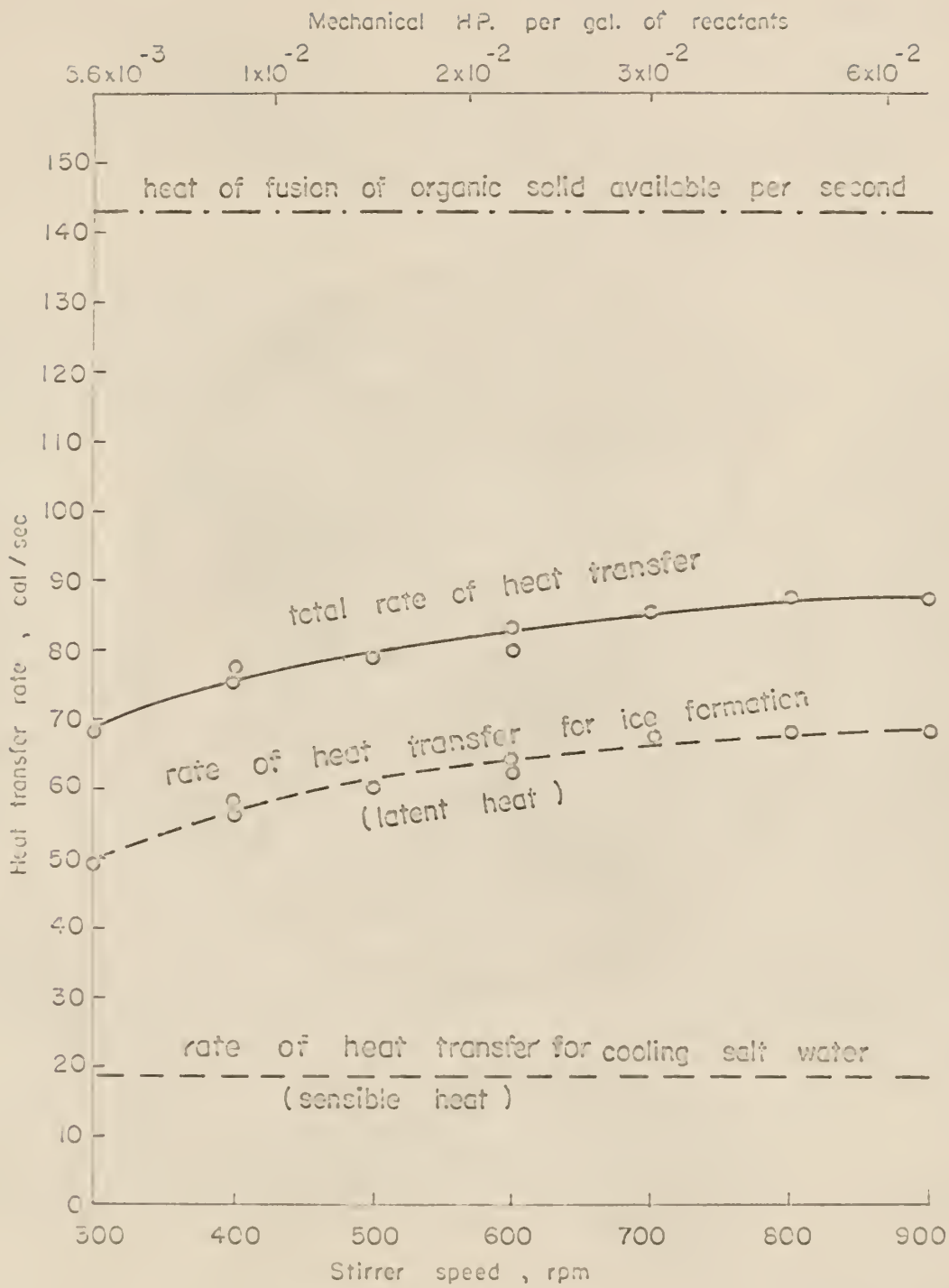


Fig. 13. Heat transfer rate vs. stirrer speed and power input. Org. mixture composition : 52 % (vol.) n-$C_{13}$ , 48 % n-$C_{14}$ ; org. slurry flow rate : 8.75 ml / sec ; inlet temp. : -4.35° C. Salt water inlet composition: 3.5 % (wt.) NaCl ; flow rate : 3.5 ml/sec ; temp. : 3.6°C.

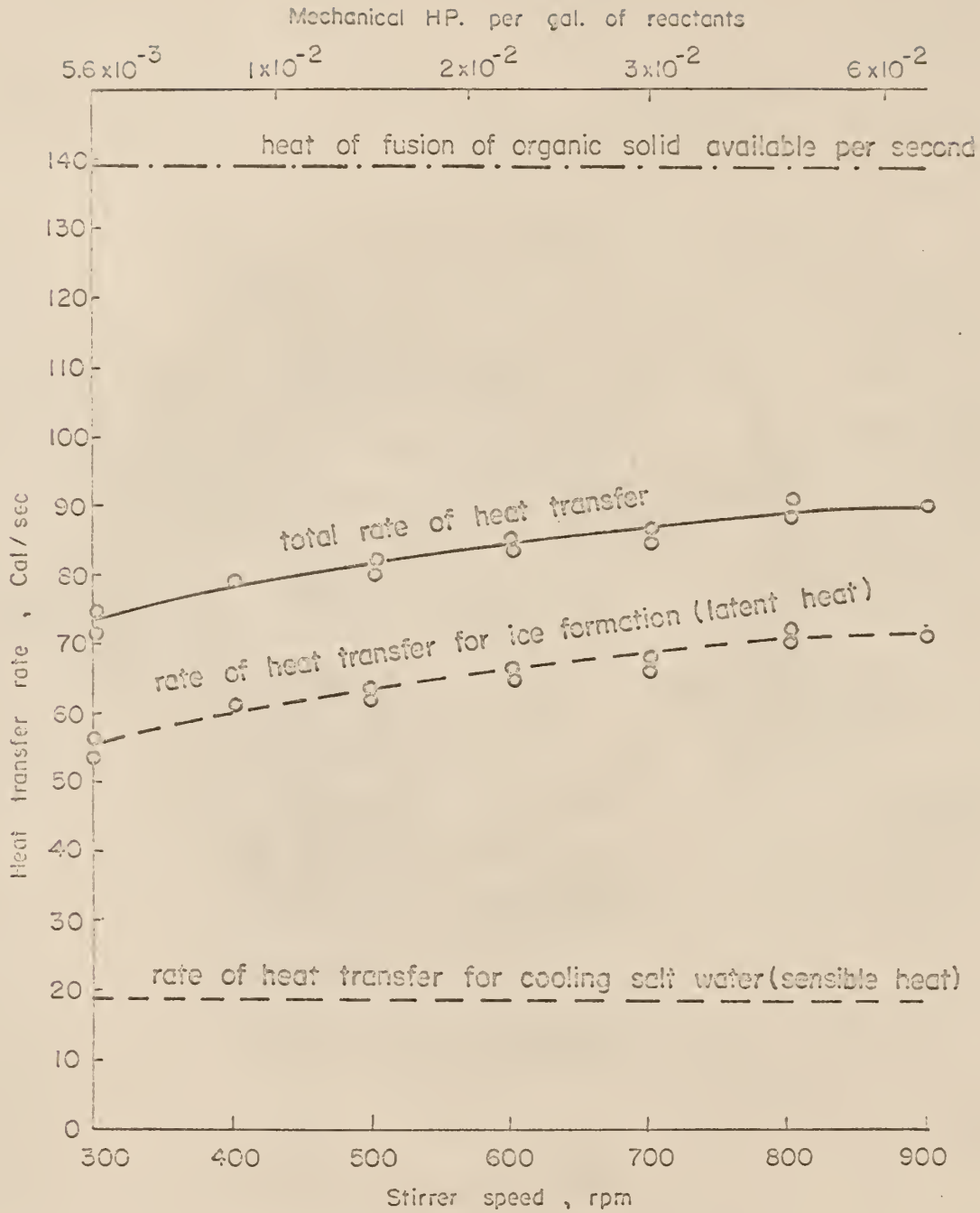


Fig. 14. Heat transfer rate vs. stirrer speed and power input. Org. mixture composition : 55 % (Vol.) $n\text{-}C_{13}$ , 45 % $n\text{-}C_{14}$ ; org. slurry flow rate : 8.75 ml/sec ; inlet temp.: -4.35°C. Salt water inlet composition : 3.5 % (wt.) NaCl ; flow rate : 3.5 ml/sec ; temp. : 3.6 °C .

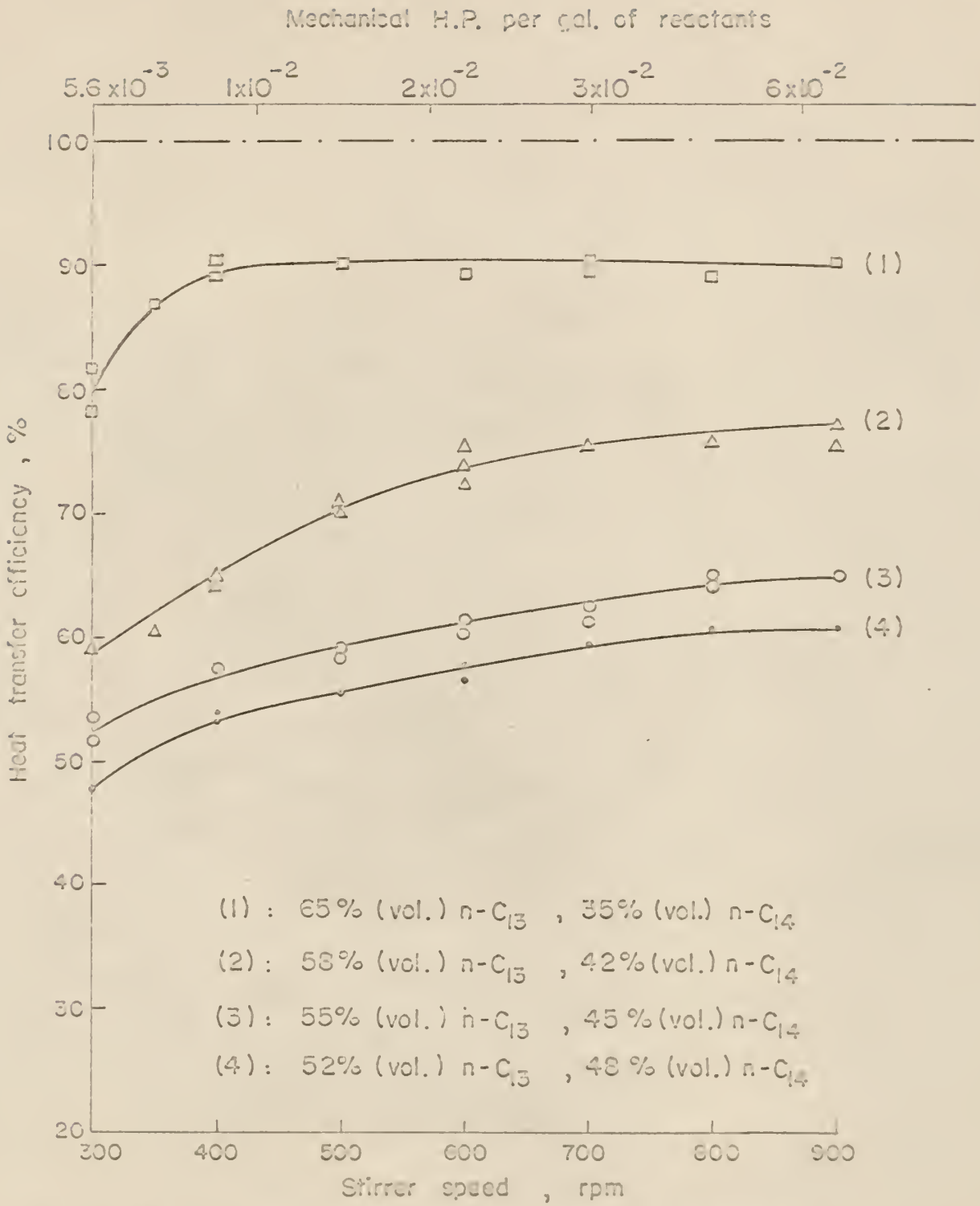


Fig. 15. Heat transfer efficiency vs. stirrer speed and power input.

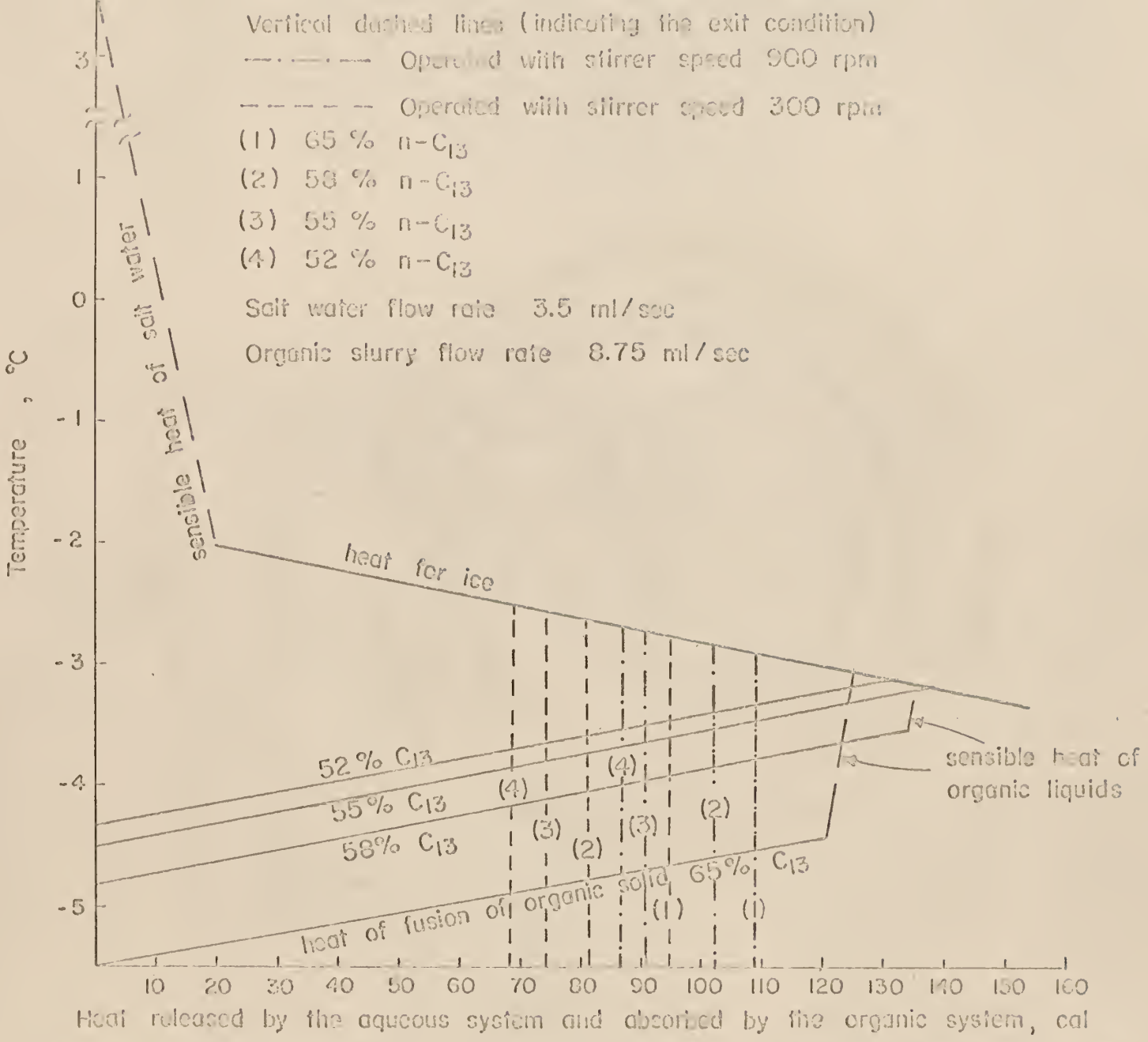


Fig. 16. Temperature-heat curve. With ranges of heat transfer in one second of operation and compositions of organic mixture indicated.

driving force. Here again one can note that the total amount of heat transfer was always less than the maximum amount of contact which could be accomplished by the complete melting of organic solid.

The effect of the thermal driving force on total heat transfer efficiency can also be evaluated from another set of experimental runs (see runs No. 1-8 in Appendix C). Here the salt water inlet flow rate was changed. However, the conditions of incoming organic slurry and other variables were kept constant. Figure 17 illustrates the results. Figure 18 shows the corresponding temperature-heat curves. The vertical dashed lines indicate the amount of contact in each of these runs. One can see that the amount of heat transfer increased even though the mean residence time decreased. The decrease of the mean residence time was caused by the increasing salt water flow rate. The increase in heat transfer rate with the increase in salt water flow rate can best be explained by the increasing salt water temperature in the product stream and consequent increase in the driving force for heat transfer as shown in Fig. 18.

The nominal residence time is defined as the ratio of the volume of aqueous slurry in the Ice-Maker to the volumetric feed rate of salt water. The effect of residence time on the total heat transfer efficiency is shown in Fig. 19. The data for this figure were obtained in runs No. 40 through 47. In these runs, the total flow rates were varied but the relative amounts of each inlet stream (aqueous and organic), solid content in the inflow organic slurry, and stirrer speed were kept constant. The effect

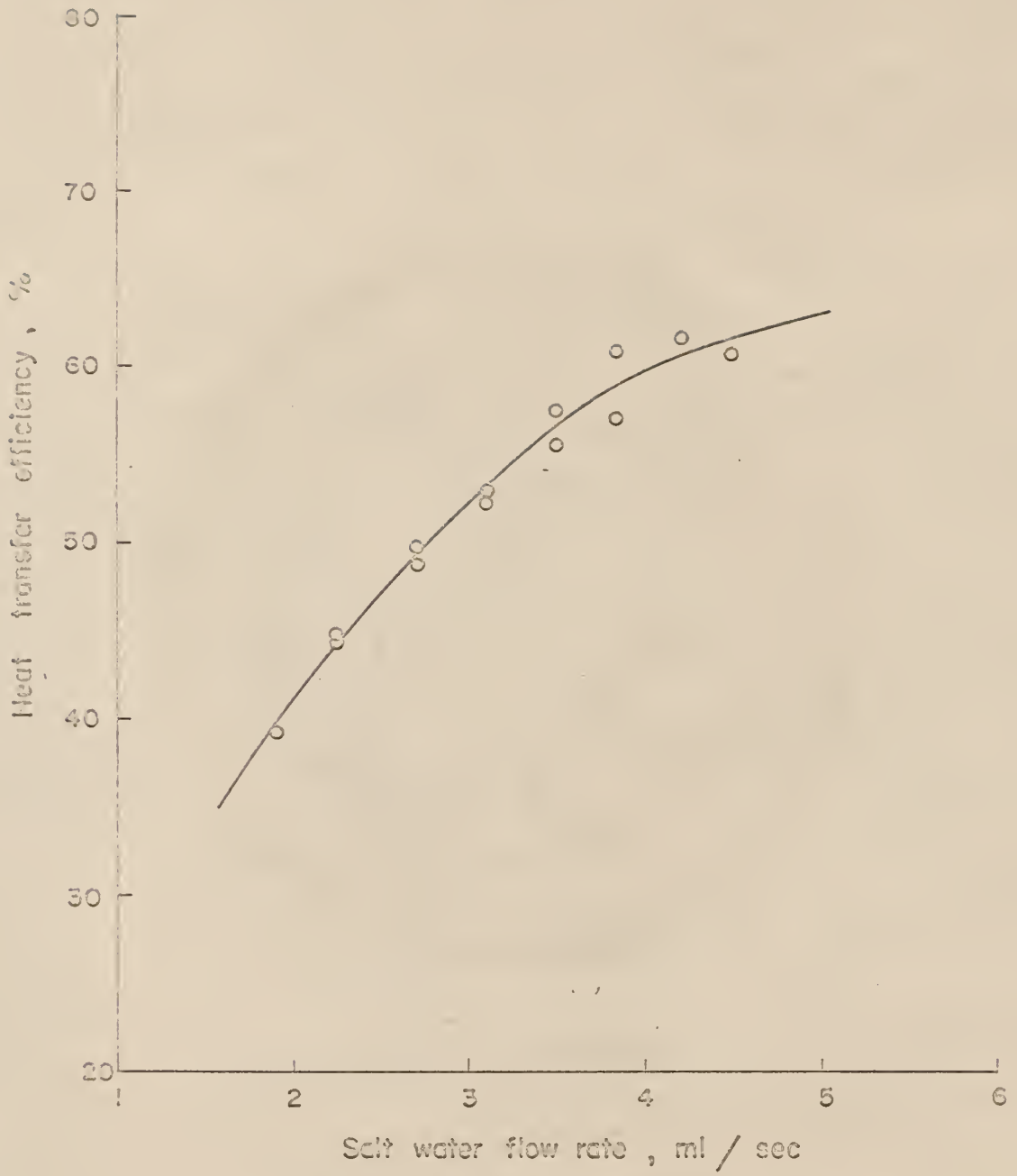


Fig. 17 . Heat transfer efficiency with changing salt water flow rate . organic mixture composition : 55 % (vol.) n-$C_{13}$ , 45 % n-$C_{14}$ ; slurry flow rate : 8.75 ml sec ; inlet temperature : 4.52°C . Salt wate composition : 3.5 % (wt.) NaCl. Stirrer speed : 400 rpm .

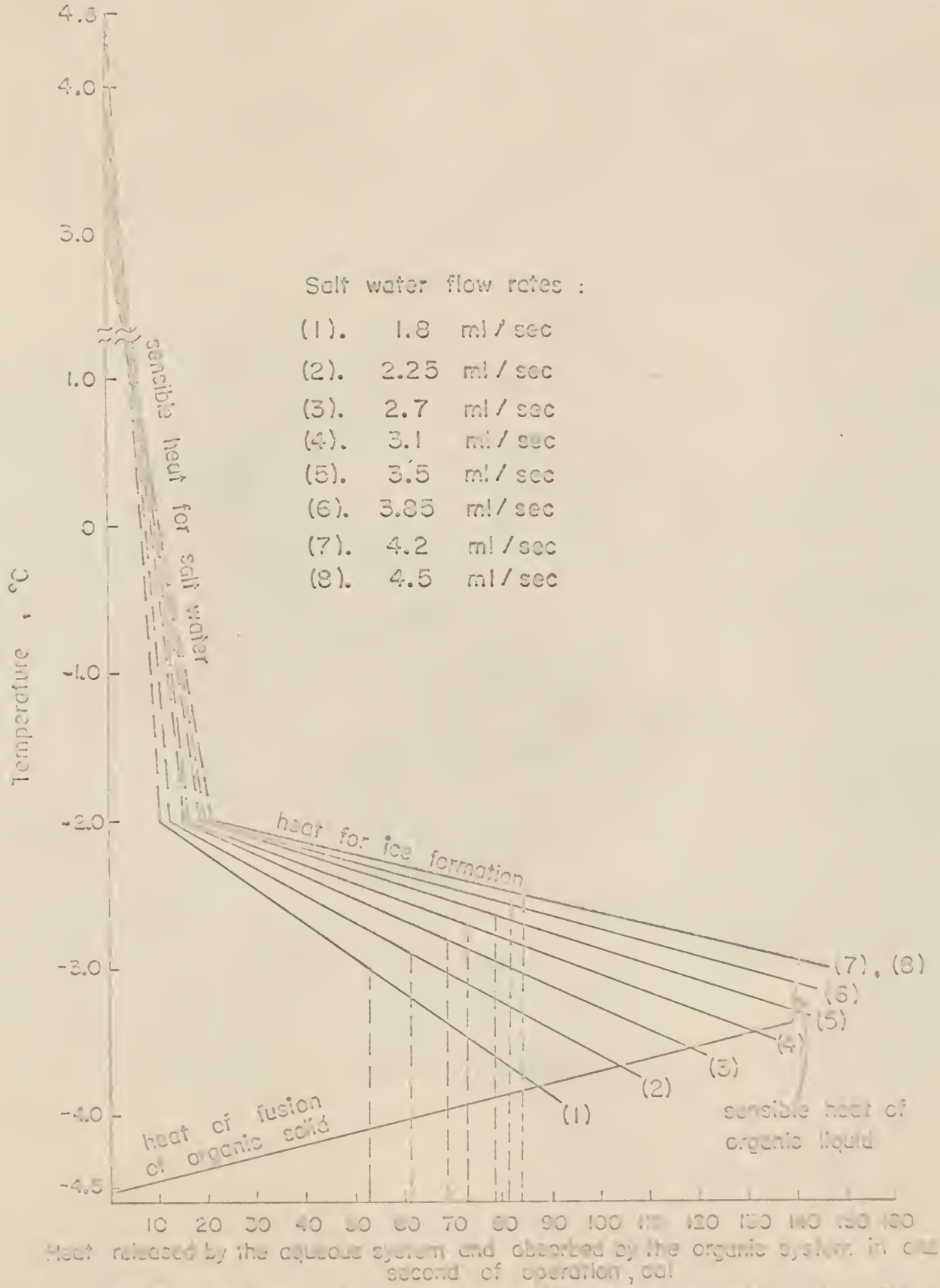


Fig. 18. Temperature – heat curves with changing salt water flow rates. Operating conditions are shown on Fig. 17.

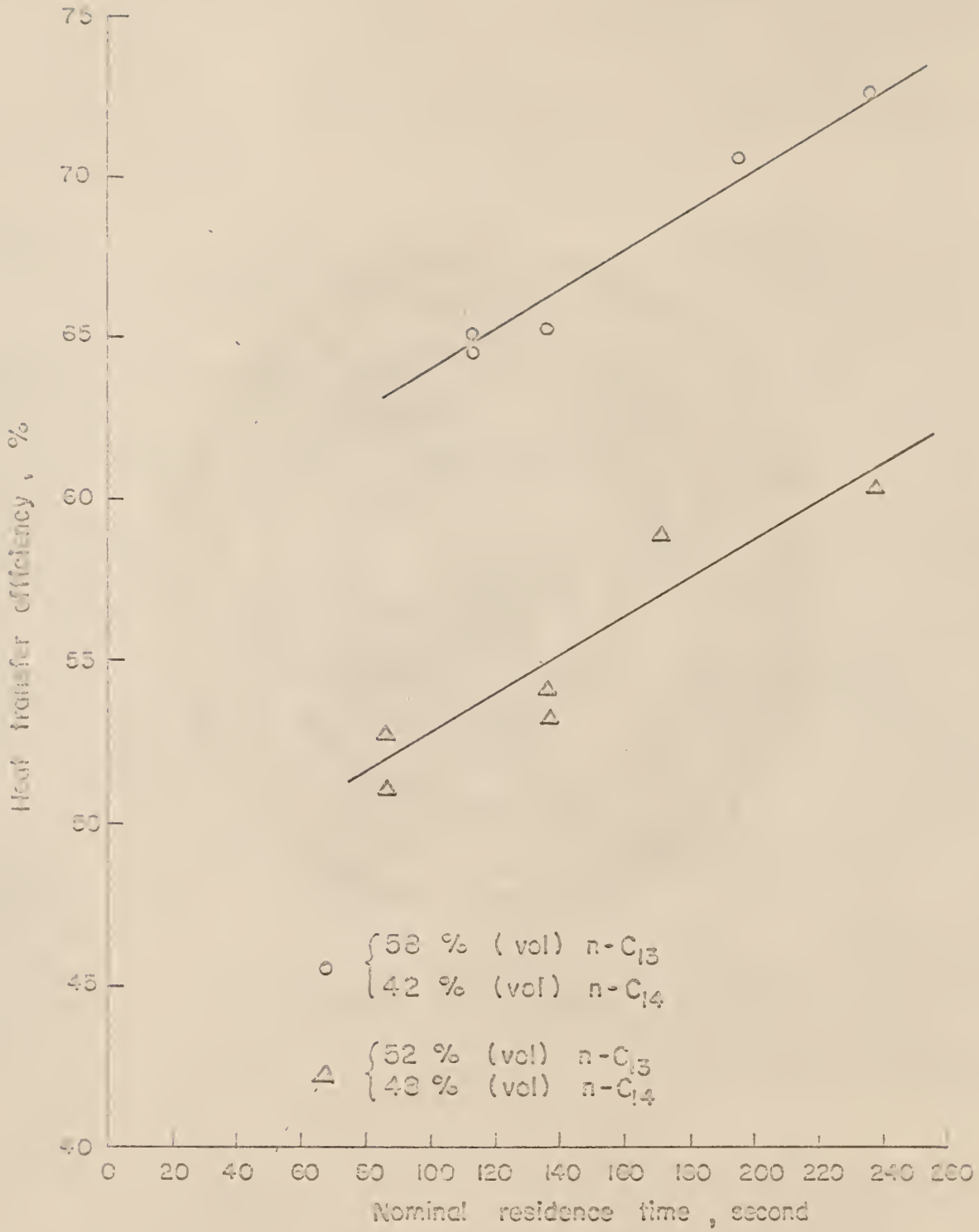


Fig. 19 . Heat transfer efficiency vs. nominal residence time.
Flow rate ratio : organic slurry / salt water = 10 / 4 .
Stirrer speed : 400 rpm .

of residence time on the amount of heat transfer could also be determined by changing contactor size. No attempt, however, was made to do so because it would require a change in the size of mixer also.

The ice crystals obtained from during the experimental runs were studied photographically. Figures 20 and 21 show the ice-crystal pictures which were taken through a microscope. As can be seen, the sizes of these crystals were in the range between 0.3 mm and 1.5 mm, and the crystals were generally rounded. It was found that thermal driving force and degree of agitation did affect the crystal sizes. A smaller thermal driving force and less agitation resulted in larger crystal sizes, and vise versa. But it was found that good size crystals (larger than 0.3 mm in average) could be obtained under almost any condition. The salinity of these crystals generally ranged between 200 and 300 ppm after washing in a packed bed formed in the Ice-Sampling Column with 15% (vol.) cold fresh water to the amount of ice obtained.

Recall that Figures 10 through 16 show that not all of the organic solid was melted in each run. This was expected because the ice-maker used was of the back-mixed type and therefore some organic solid had only a very brief contact time with the salt water and left the vessel unmelted.

To prove the back-mixedness, the residence time distribution of fluid in the Ice Maker were studied by using a tracer technique. The distribution of residence time with stirrer speed from 300 to 900 rpm was measured with a steady flow of fresh water and injection of saturated sodium chloride solution in the inlet stream as

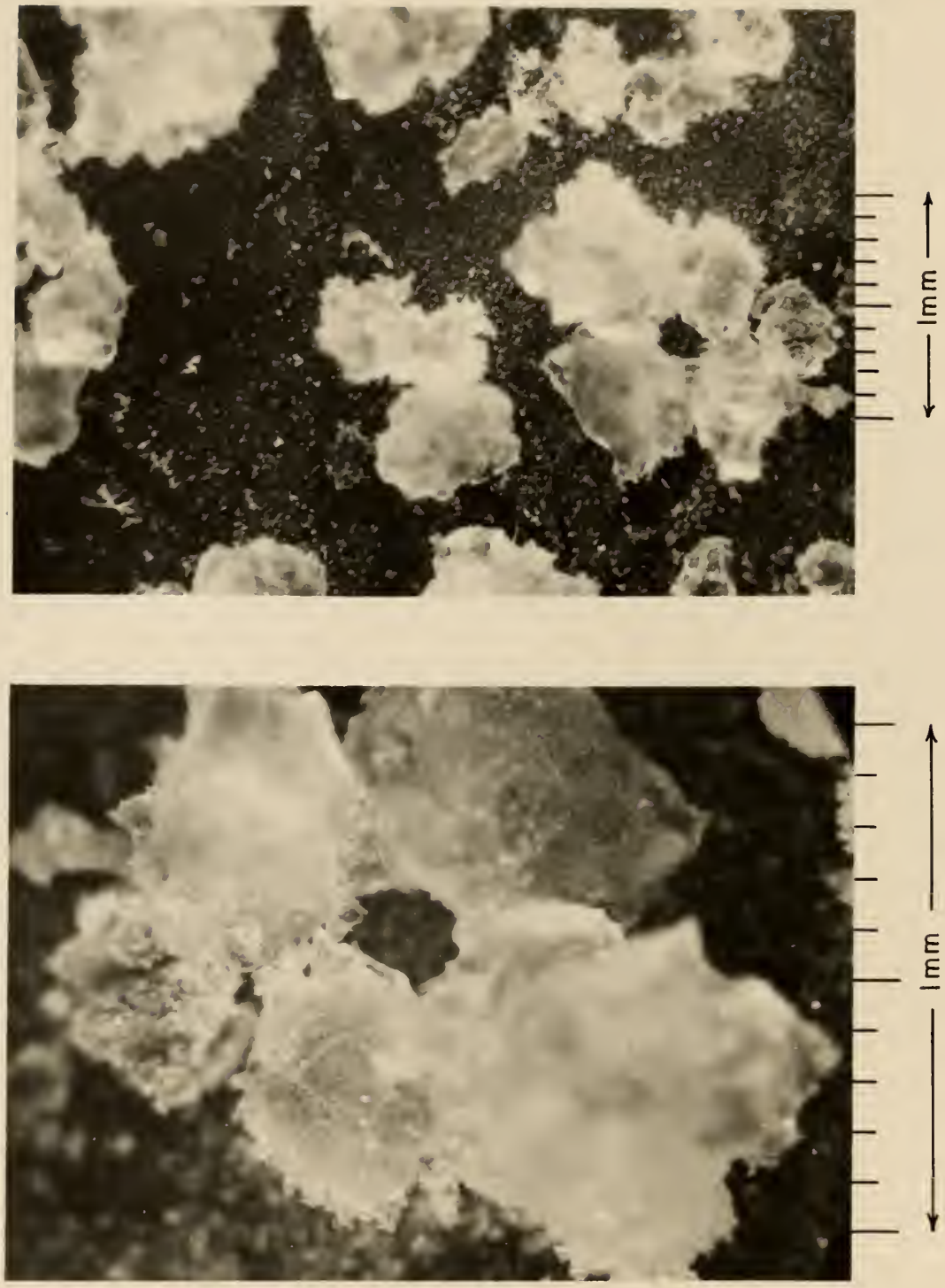


Fig. 20. Microscopic pictures of ice crystals. (1)
Operating conditions:
Agitation speed: 400 rpm
Organic mixture: 52% (vol.) $n\text{-}C_{13}$, 48% $n\text{-}C_{14}$
(freezing temp. -3.07 C)
flow rate = 8.75 ml/sec
Salt water: flow rate = 3.5 ml/sec


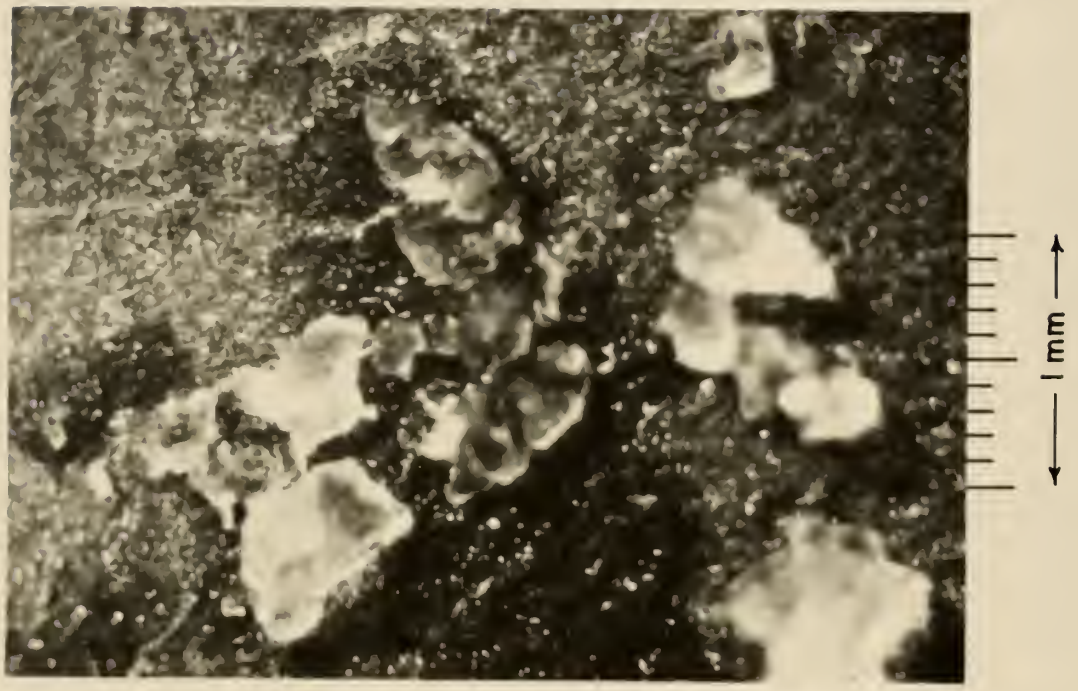


Fig. 21. Microscopic pictures of ice crystals. (2)
Operating condition:
Agitation speed: 400 rpm
Organic mixture: 65% $n\text{-}C_{13}$, 35% $n\text{-}C_{14}$
(freezing temp. -4.4 C)
flow rate = 8.75 ml/sec
Salt water: flow rate = 3.5 ml/sec

the tracer. The salt concentration in the outlet stream was measured and recorded by using a sensitive conductivity meter and a recorder. Both impulse and step inputs were introduced to obtain the C-curve (a response to an upstream impulse signal) and F-curve (a response to an upstream step signal).

The details of experimentation and data analysis of this part of work are presented in Appendix D.

The experimental F-curves and C-curves are summarized and shown in Figs. 22 and 23 which are the same as Figs. D-7 and D-8 respectively in Appendix D. The corresponding theoretical curves for various extents of backmixing as predicted by the dispersion model and tank-in-series model are included for comparison. From these two figures, one can see that the behavior of the Ice-Maker was close to perfect mixing in the experimental stirring range.

Using the experimental C-curves, the parameters which characterize the vessel behavior (i.e., extent of backmixing) were calculated. The results also indicate an approximately "completely mixed" condition in the Ice Maker.

As a matter of fact, the residence time distribution functions of fluid passing through the Ice Maker as found from tracer studies are only partial information on the details of the flow patterns. All that is known is the length of time certain fractions of the fluid stay in the vessel — i.e., information on "macromixing" (19), but not the molecule's duration of stay in the system nor its interaction with other molecules which it encounters during its stay in the system — i.e., information on "micromixing" (19,20).

In general, when one is to predict the performance of a reac-

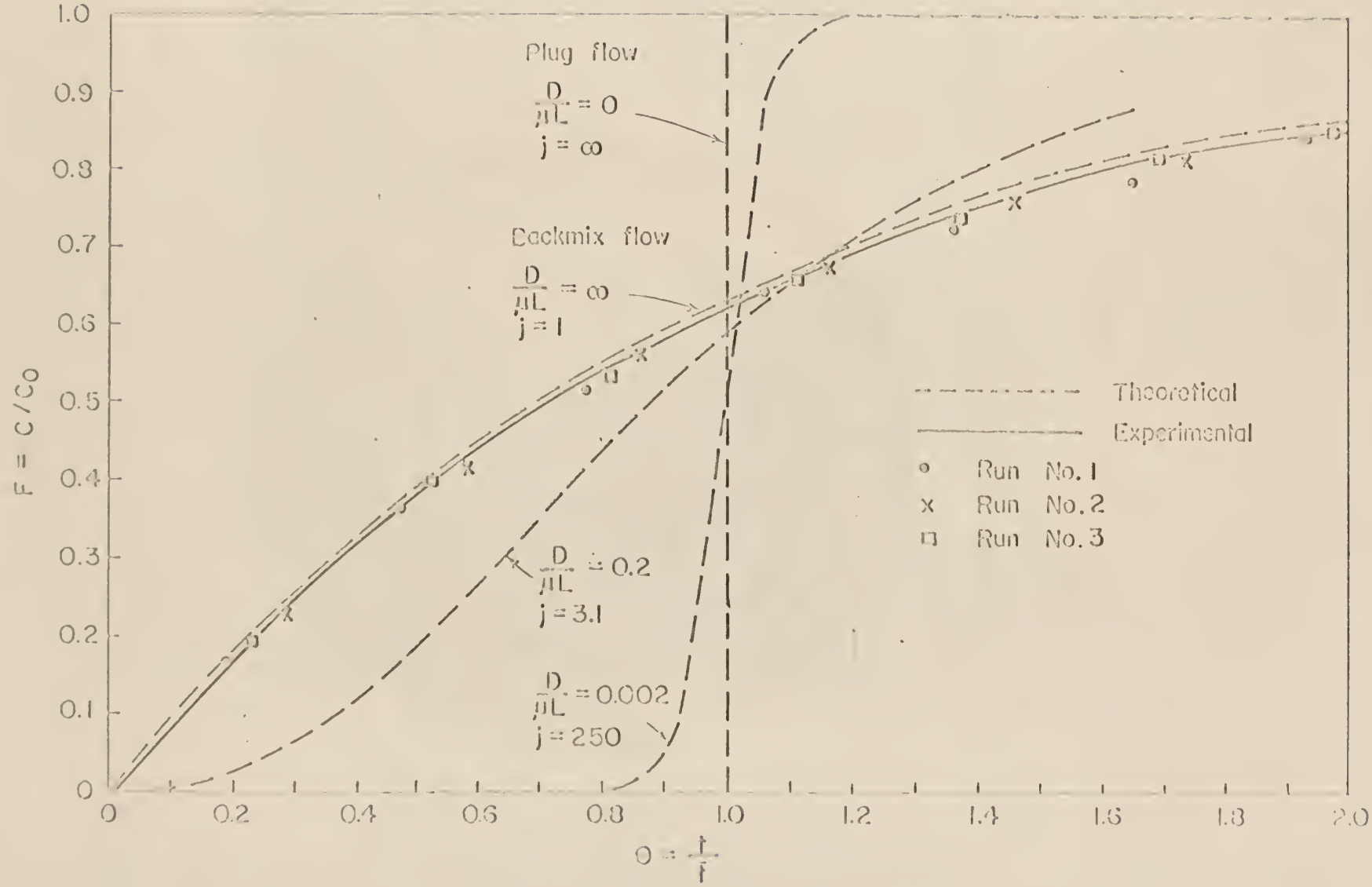


Fig. 22. Step-input response (or F-) curves.

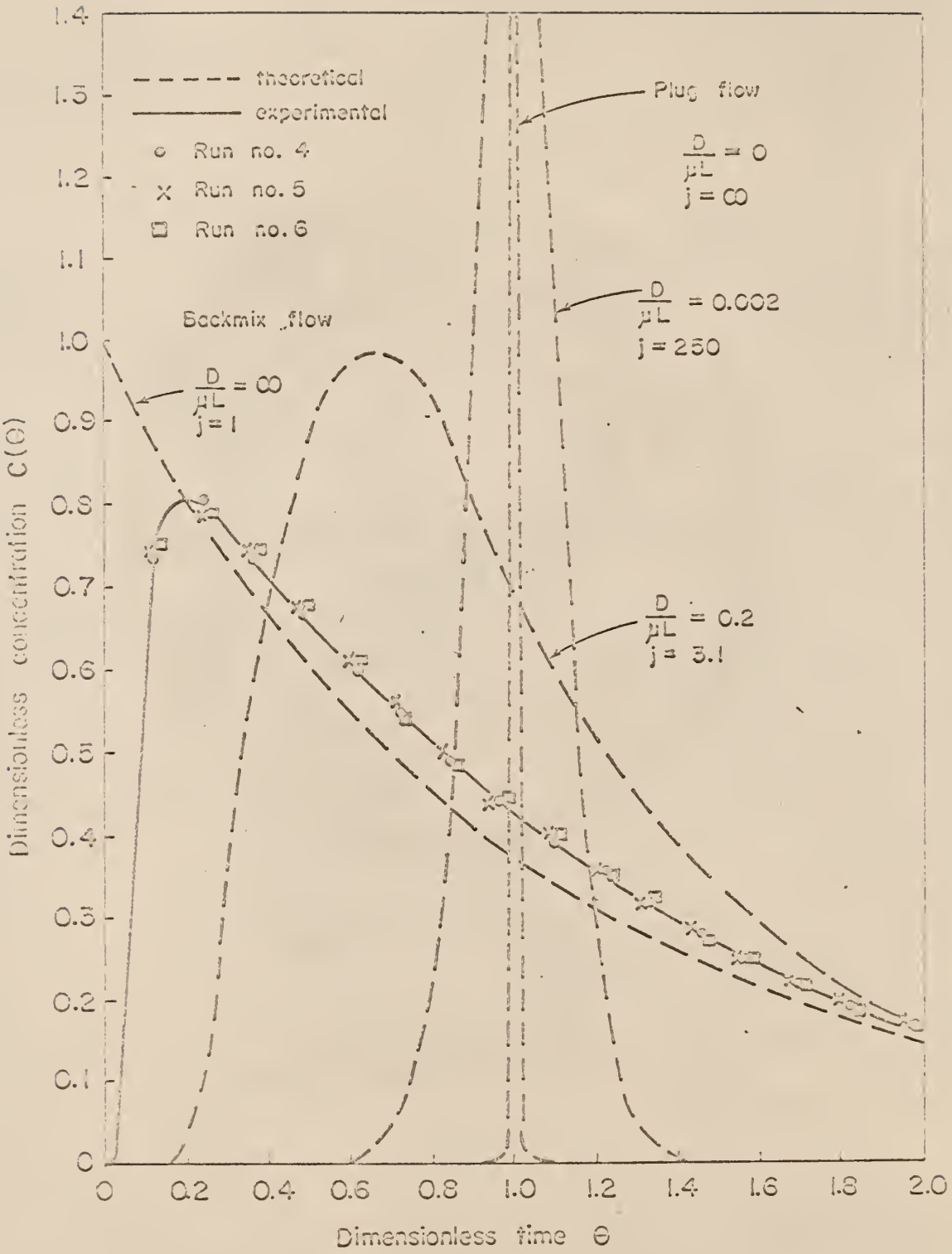


Fig. 23. Impulse input response (or C-) curves.

tor, two types of information are required: (a) the flow patterns (b) the rate phenomena (or kinetics). Since age distribution curves produce information about macromixing, but not micromixing, it is only for systems in which the interactions between different molecules do not affect the rates (i.e., first-order rate processes) that the equipment performance can be predicted solely from tracer curves plus kinectics (21). That is to say, the performance of a reactor is independent of conditions of micromixing (or degree of segregation) if the rate process is of the first order. For all other cases, in addition to age distribution, further details about the mixing are required in predicting the performance of equipment.

In this work, formation of ice crystals from salt water by contacting it with an organic slurry was accomplished through a series of heat and mass transfer including phase changes. With this rather complicated process, it is hard to conceive that the formation of ice is a first order process. Therefore, if one wishes to explain the relationship between heat transfer rate and stirrer speed, as shown of Figures 10 through 16, additional information about the mixing (i.e., micromixing or segregation) should be studied.

# CONCLUSION

From the results obtained in this work it may be concluded that the process is very promising because,

(1) The size of the ice-maker will be relatively small. From the rate data, it appears that 300 to 600 gallons of fresh water can be obtained from each cubic foot of the contactor per day.

(2) The ice crystals produced in this process were fairly large, well shaped, smooth and low in salt content. This indicates that the ice-washing operation can be easy to carry out.

## PROPOSED DESIGN OF A SEMI-PILOT PLANT

Data obtained in this work together with thermodynamic data of the working medium obtained by S. S. Maa can be useful for designing a continuously operating plant.

Figures 24 and 25 show the tentative design for a thousand gallon per day pilot plant. Table 2 gives the nomenclature and sizes of equipment shown in Figures 24 and 25.

One major piece of equipment that has not yet been investigated is the ice-washer. But the design and operation of this equipment have already been well developed in connection with the conventional freezing processes. Information could be obtained from literature.

Another major piece of equipment not yet studied is the high pressure ice-melter. But since ice-melting is simply the reverse operation of ice-making, it can be expected that the heat transfer rate will be similar to that in the ice-maker.

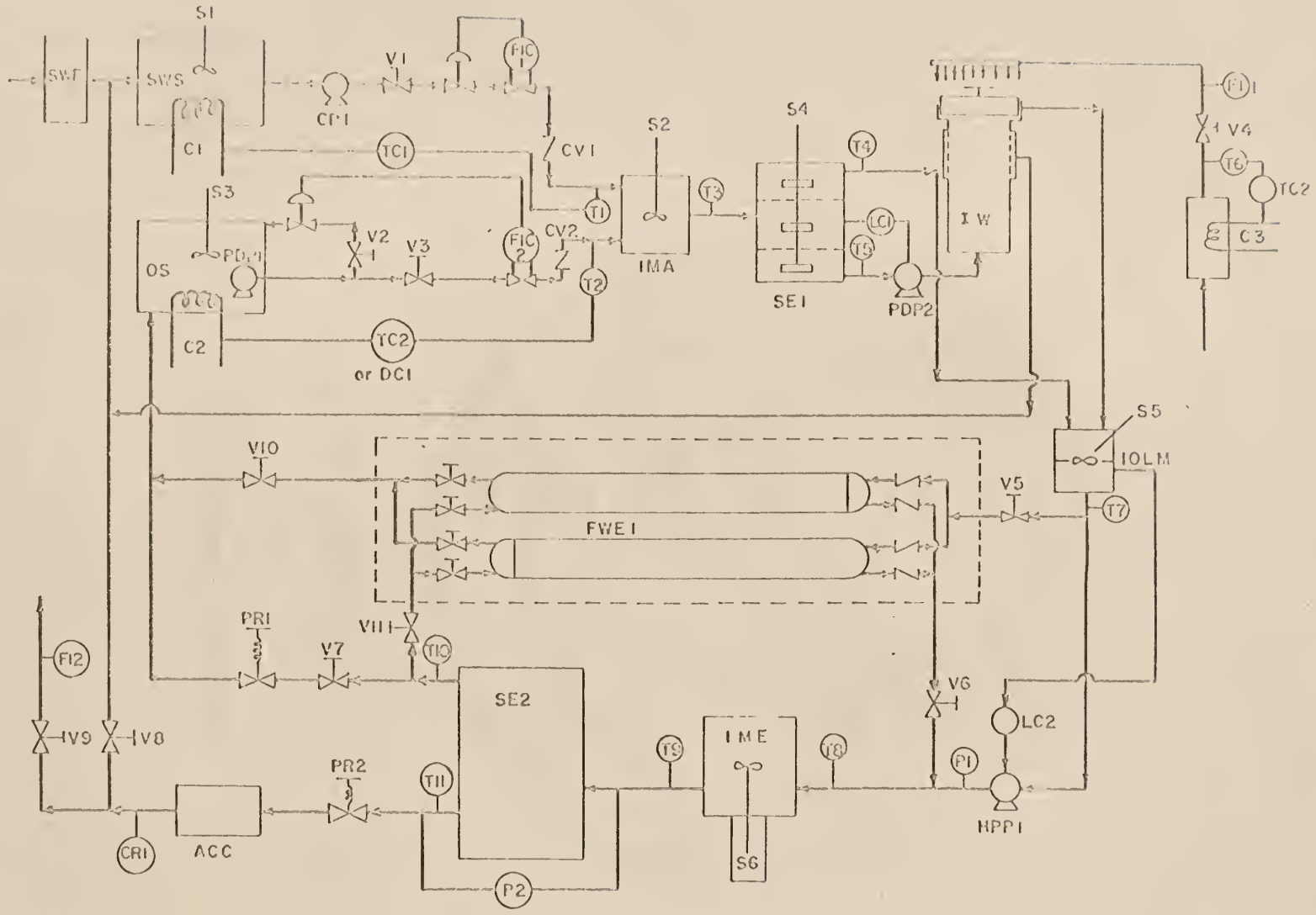


Fig. 24. Schematic diagram of the proposed semi-pilot plant with control equipment.

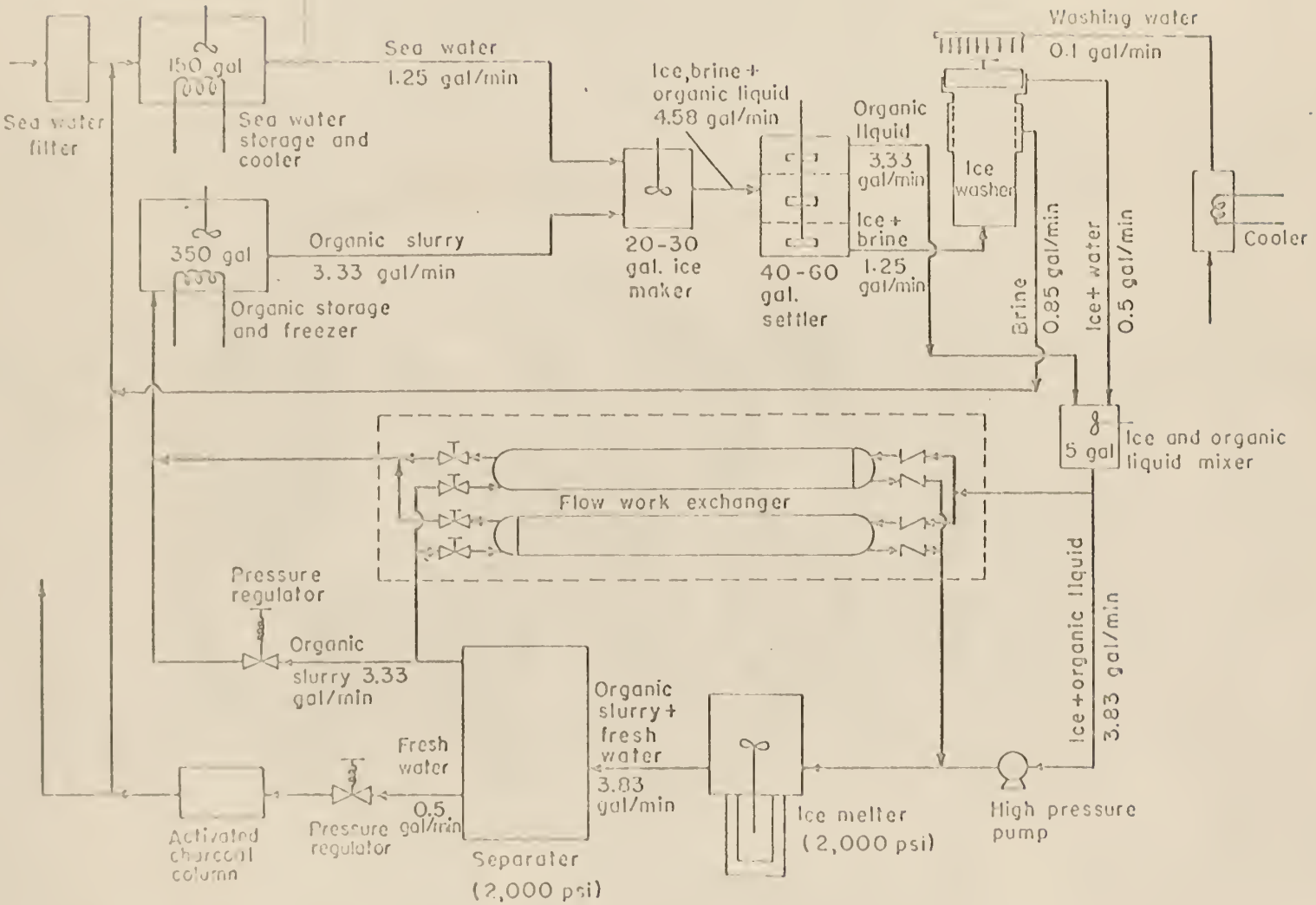


Fig. 25. Schematic diagram of the proposed semi pilot plant with flow rate at various point indicated.

Table 2. Summary of code letters for equipment

| Code | Name |
|---|---|
| SWF | Sea water filter |
| SWSC | Sea water storage and cooling |
| OS | Organic storage |
| IMA | Ice maker |
| SE1 | Settler 1 |
| IW | Ice washer |
| C | Cooler |
| IOLM | Ice organic liquid mixer |
| IME | Ice melter |
| SE2 | Setter 2 |
| ACC | Activated charcool column |
| S | Stirrer |
| PDP | Positive displacement pump |
| CP | Centrifugal pump |
| HPP | High pressure pump |
| PR | Pressure regulator |
| TC | Temperature controller, DC (Density control) |
| T | Temperature measurement |
| P | Pressure measurement |
| FL | Flow rate indicator |
| FIC | Flow rate indicator and controller |
| CR | Capacitiuity recorder |
| V | Valve |
| LC | Level controller |
| FWE | Flow work exchanger |
| CV | Check valve |

| Code | Quantities | Material | Capacity | Note |
|---|---|---|---|---|
| SWF | 1 | Sintered Metal | | |
| SWS | 1 | Stainless Steel | 150 Gal | with Cl ~ S1 Atm pressure |
| CS | 1 | Stainless Steel | 350 Gal | Atm pressure with vibrator C2~S3 |
| TMA | 1 | Stainless Steel | 20~30 Gal | Atm pressure with baffles S2 |
| SEI | 1 | Stainless Steel | 40~60 Gal | Atm pressure with baffles S4 |
| IW | 1 | | | ice scrapper speed adjustable |
| C | 3 | | | |
| IOLM | 1 | | 5 Gal | with vibrator? with S5 |
| IME | 1 | Stainless Steel | | 2000 psia with S6 tested 4000 psia |
| SE2 | 1 | | | cyclone type |
| ACC | 1 | | | |
| S | 6 | | | S2.S4 variable speed |
| PDP | 2 | | | |
| CP | 1 | | | |
| HPP | 1 | | | |
| PR | 2 | | | |
| TC | 3 | | | or DC1~TC2 |
| T | 11 | | | 16 channels temp-erature recorder |
| P | 2 | | | pressure gage 2 |
| FI | 2 | | | |
| FIC | 2 | | | |
| CR | 1 | | | |
| V | 11 | | | |
| LG | 2 | | | |
| FWE | 1 | | | with checkvalve V-4 |
| CV | 2 | | | |

# LITERATURE CITED


1. Office of Saline Water, U.S. Department of the Interior, "The A-B-Seas of Desalting".
2. Barduhn, A.J., "The Freezing Processes For Water Conversion In The United States". First International Symposium on Water Desalination (Oct. 3-9, 1965), Washington, D.C..
3. Cheng, C. Y., and S. W. Cheng, A. I. Ch. E. Journal 13, 41 (1967).
4. Ricci, J. E., "Phase Rule and Heterogeneous Equilibrium", P. 34, Von Nostrand, (1951).
5. Bridgman, P. W., "International Critical Tables", Vol. 4, pp. 4-22, McGraw-Hill Book Co. (1928).
6. Salzgeber, R., Compt. rend, 240, pp. 1642-44 (1955).
7. Maa, S. S., M.S. Thesis, Kansas State Univ., (1968).
8. Physical Properties of Chemical Compounds II, Advances in Chemistry Series No. 22.
9. Perry, J. H., "Chemical Engineer's Handbook" 3rd ed. pp. 147, McGraw-Hill Book Co., (1950).
10. South Hampton Company. Houston, Texas, Private communication.
11. Union Carbide Corp., New York City, Private communication.
12. International Critical Table, pp. 172-181.
13. Cheng, C. Y., S. W. Cheng and L. T. Fan, A. I. Ch. E. Journal, 13, 438, (1967).
14. Hahn, W. J., R. C. Burns, R. S. Fullerton, and D. J. Sandell Jr. O. S. W. Res. and Dev. Prog. Report No. 113 (June 1964).
15. Finke, H. L., M. R. Cines, F. E. Frey and J. G. Aston, J. Am.

Chem. Soc., 69, 1501 (1947).

16. McHland, F. A., and F. S. Chapman, "Liquid Mixing and Processing", pp. 42, Reinhold Publishing Corporation, (1966).

17. Croft, W. C., "American Electrician's Handbook", 7thed. pp. 859, McGraw-Hill Book Co. (1953).

18. Cook, A. L., "Elements of Electrical Engineering", pp. 176, John Wiley & Sons, Inc. (1924).

19. Danckwerts, P. V., Chem. Eng. Sci., 8, 93 (1958).

20. Zwietering, Th., Chem. Eng. Sci., 11, 1 (1959).

21. Lenvenspiel, O., "Chemical Reaction Engineering", pp. 253, John Wiley & Sons, Inc. New York (1962).

22. Lenvenspiel, O., "Chemical Reaction Engineering", pp. 242, John Wiley & Sons, Inc. New York (1962).

23. Danckwerts, D. V., Chem. Eng. Sci., 1, 1 (1953).

24. Lenvenspiel, O., and K.B. Bischoff, "Advances in Chemical Engineering", Vol. 4, Academic Press (1963).

# ACKNOWLEDGEMENTS

The author wishes to express his sincere gratitude to his major advisor, Dr. Liang-tseng Fan, for his excellent advice and constant encouragement.

The continuous and helpful suggestions from Dr. Richard G. Akins and Dr. Chen-yen Cheng are deeply appreciated.

A deep debt of gratitude is also due to the members of the supervisory committee, Dr. William H. Honstead, Head, Department of Chemical Engineering, and Dr. S. Thomas Parker, Professor, Department of Mathematics, Kansas State University.

The author is grateful for the financial support from the K.S.U. Engineering Experiment station under project 2434, supported by the office of Saline Water, U.S. Department of Interior, Grant No. 14-01-0001-670.

# APPENDIX A

## PHYSICAL PROPERTIES OF WORKING MEDIUMS AND SALT WATER

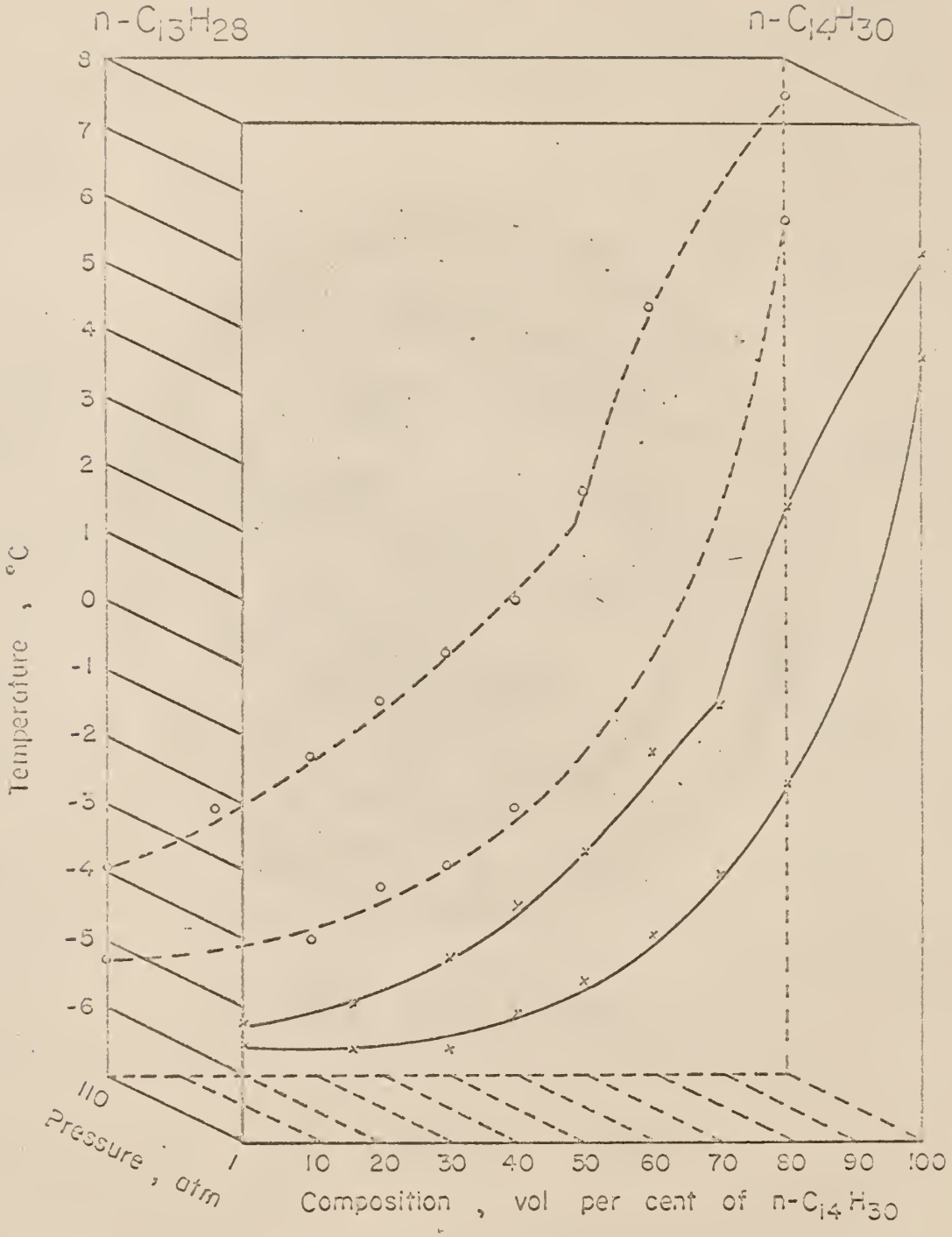


Fig. A-1. Phase diagrams of n-tridecane (pure grade) and n-tetradecane (pure grade) binary system.

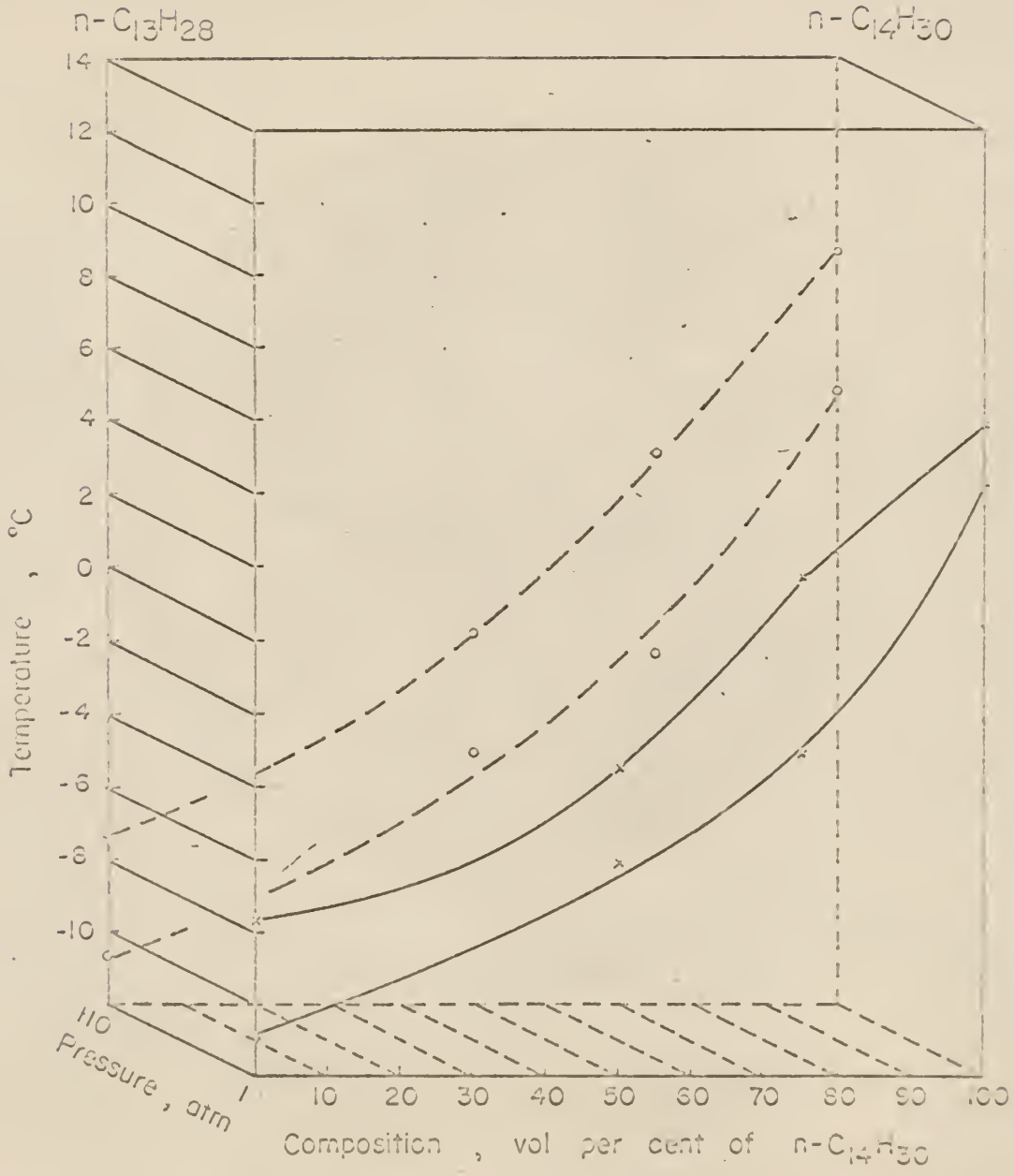


Fig. A-2. Phase diagrams of n-tridecane(technical grade) and n-tetradecane (technical grade) binary system.

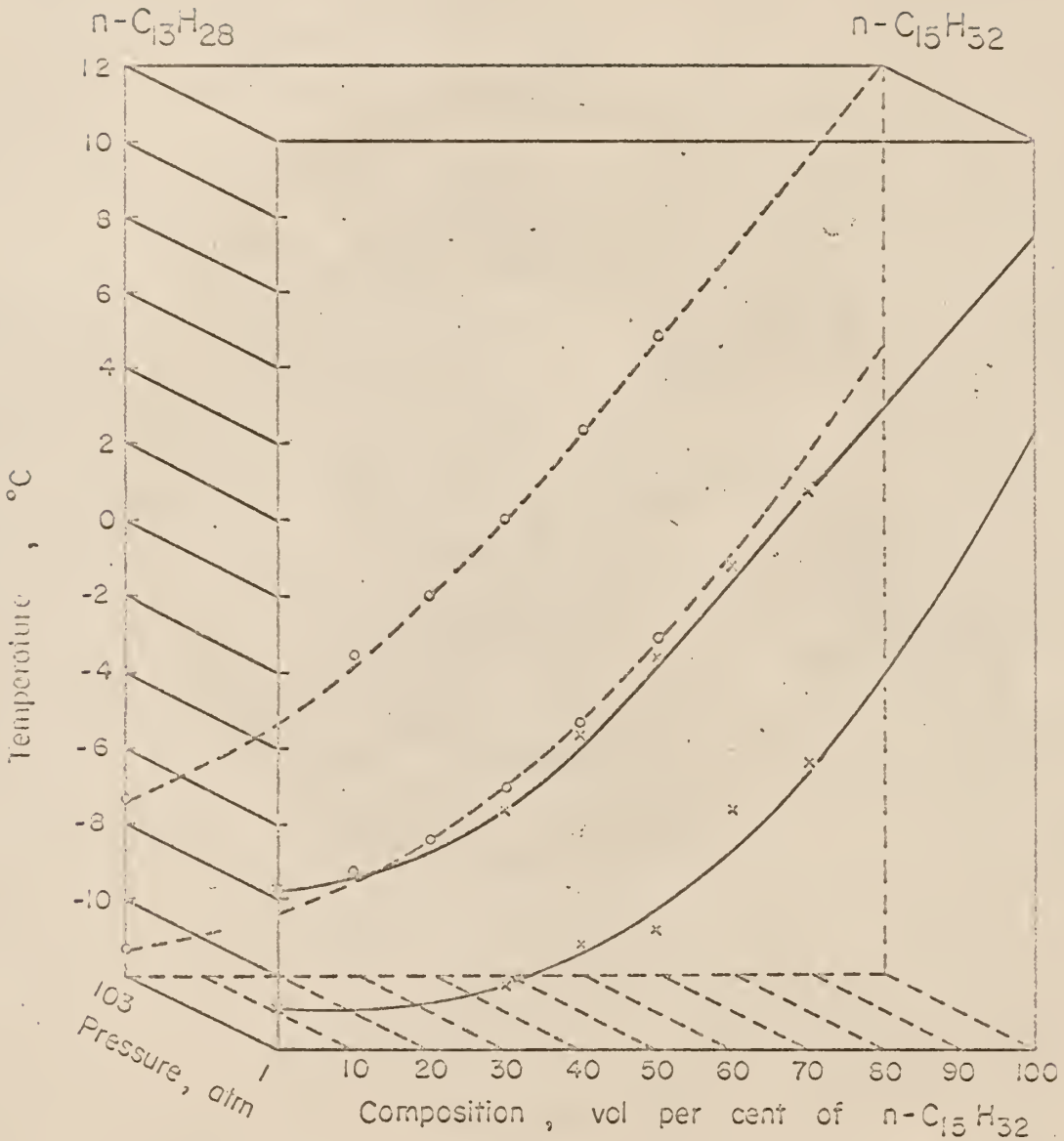


Fig. A-3. Phase diagrams of n-tridecane (technical grade) and n-pentadecane (technical grade) binary system.

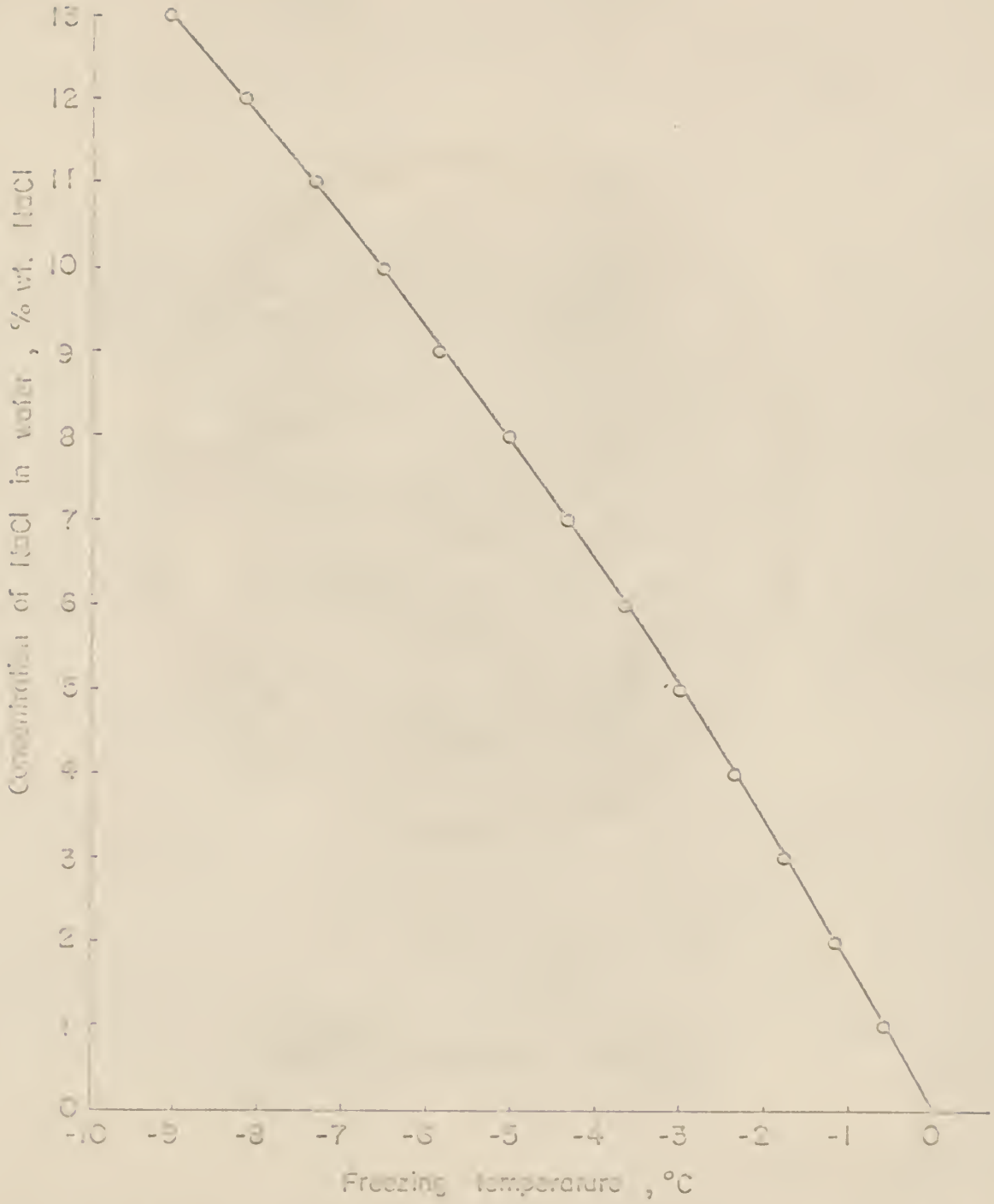


Fig. A-4. Freezing temperature vs. concentration of salt in water under atmospheric pressure.

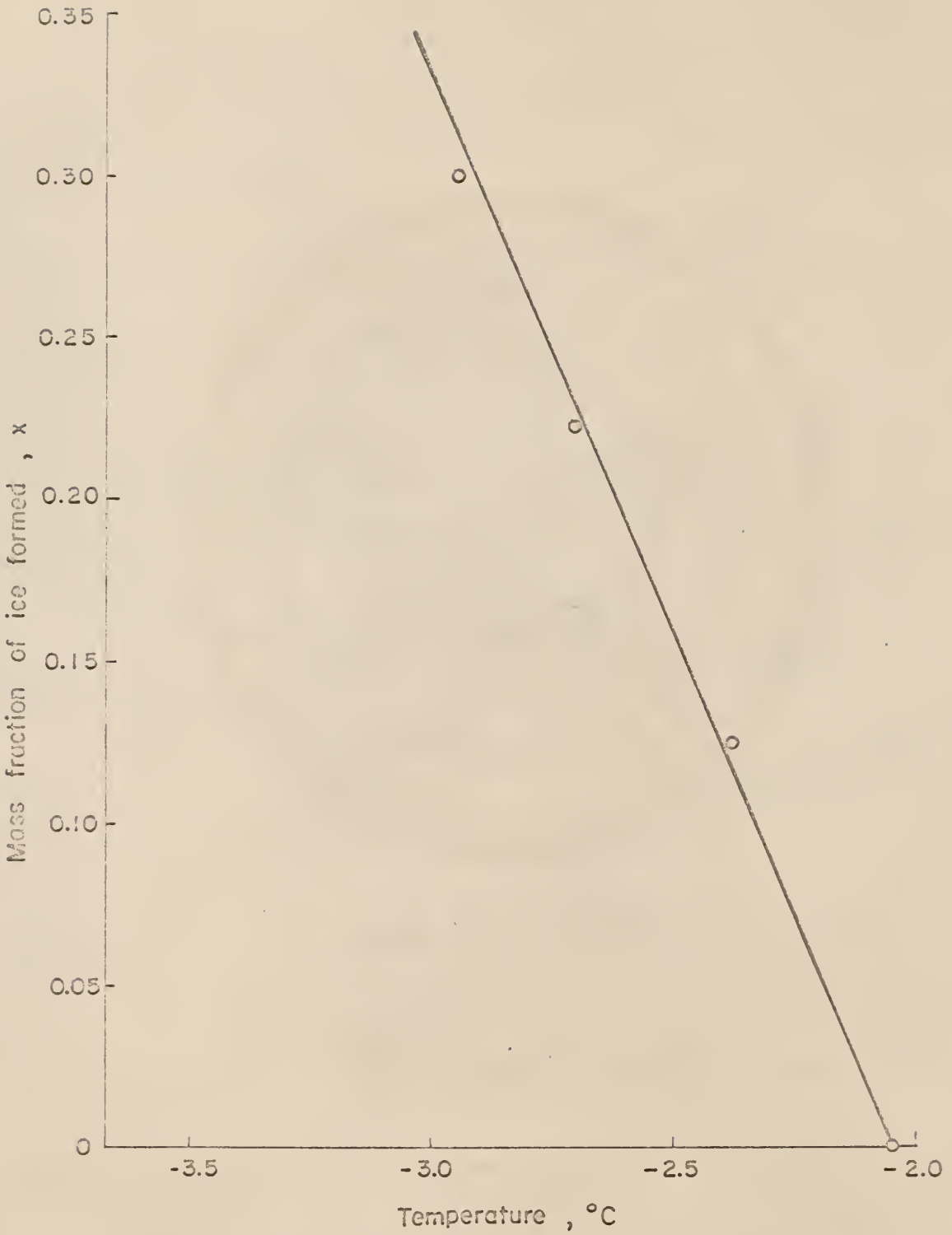


Fig. A-5. Temperature vs. mass fraction of ice formed for 3.5 % (wt.) NaCl solution.

# APPENDIX B

## CALIBRATIONS OF INSTRUMENTS

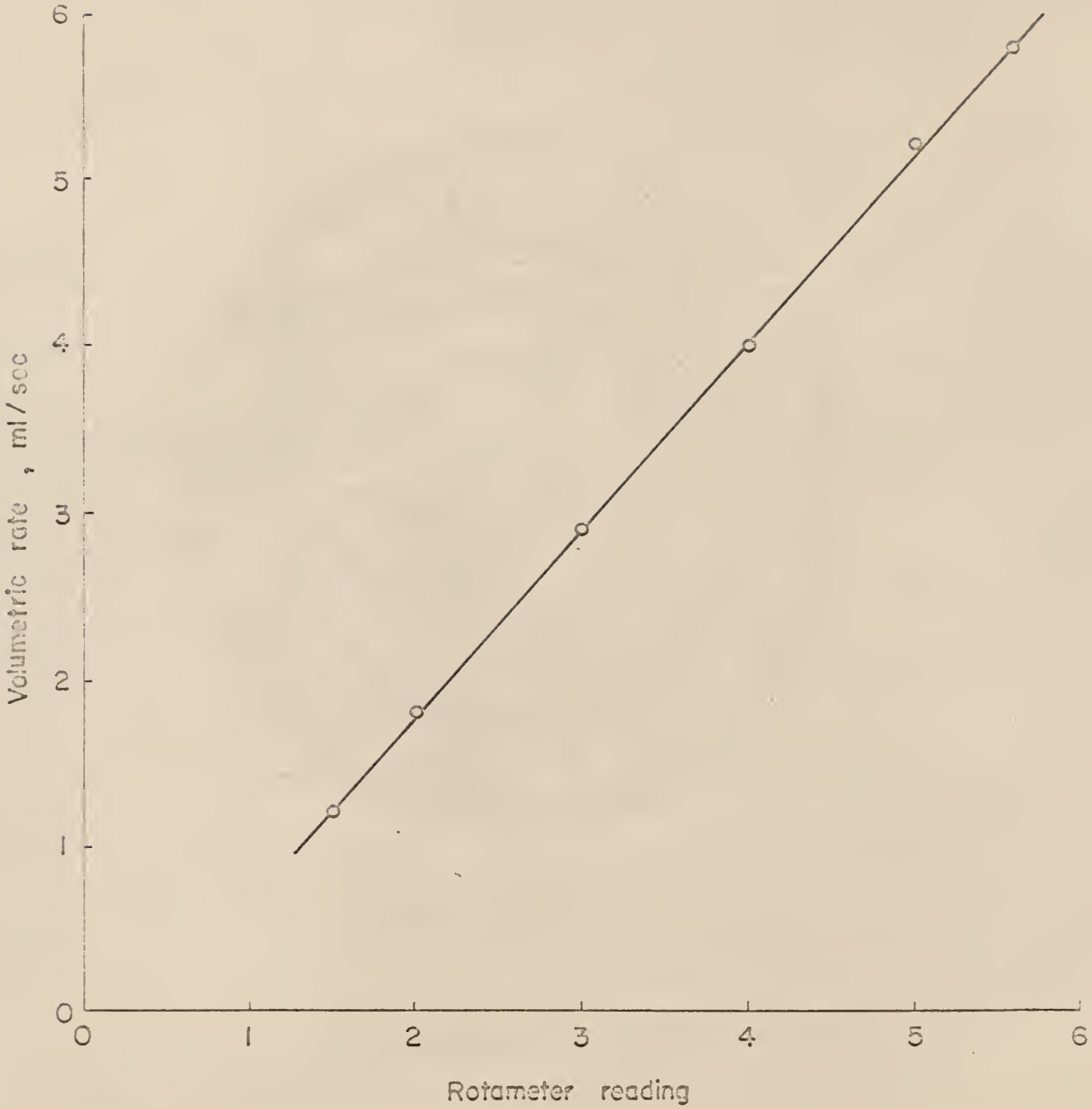


Fig. B-1. Salt water flow meter calibration , ±3 °C .

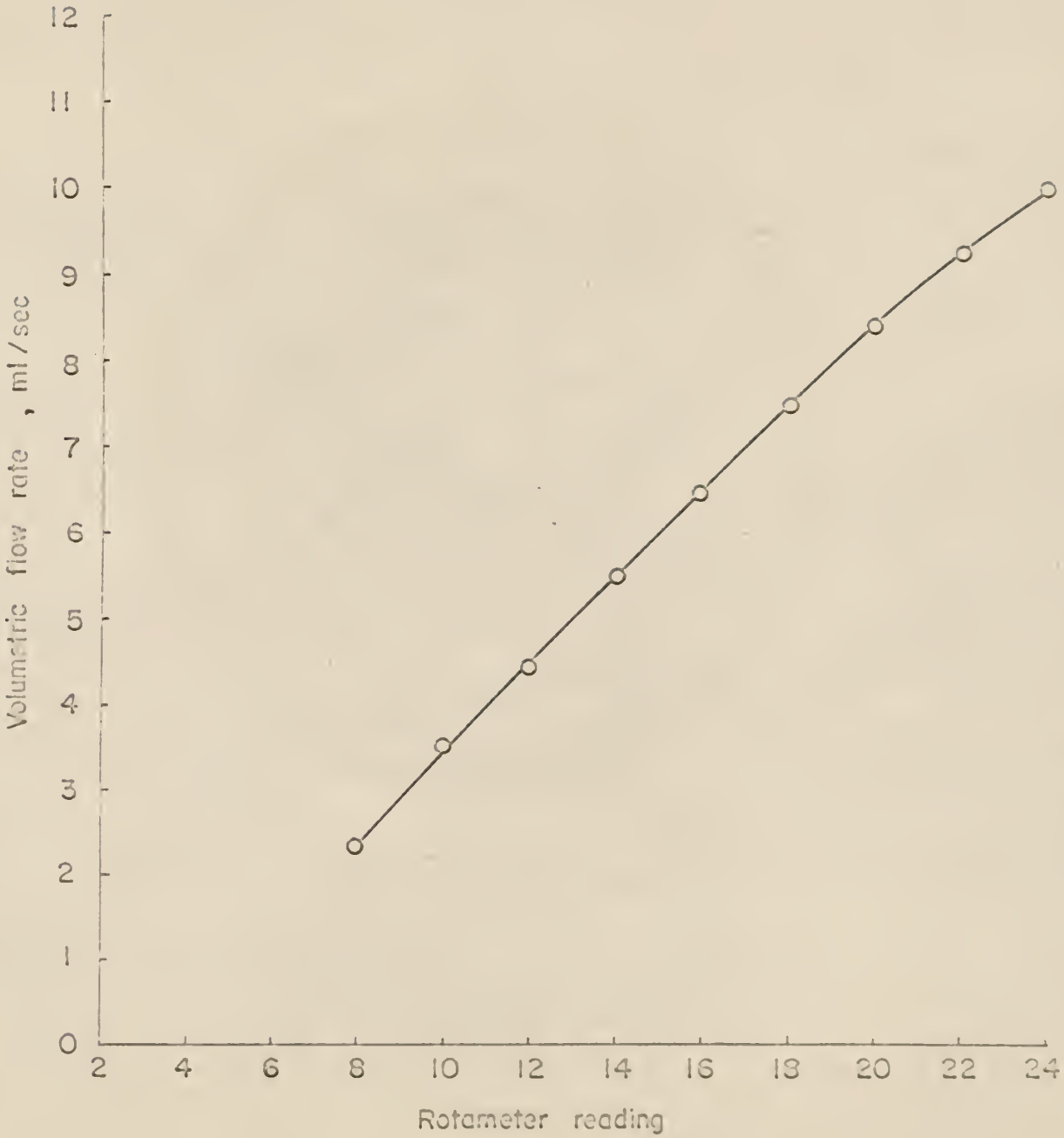


Fig. B-2. Organic liquid flow meter calibration, 0°C.

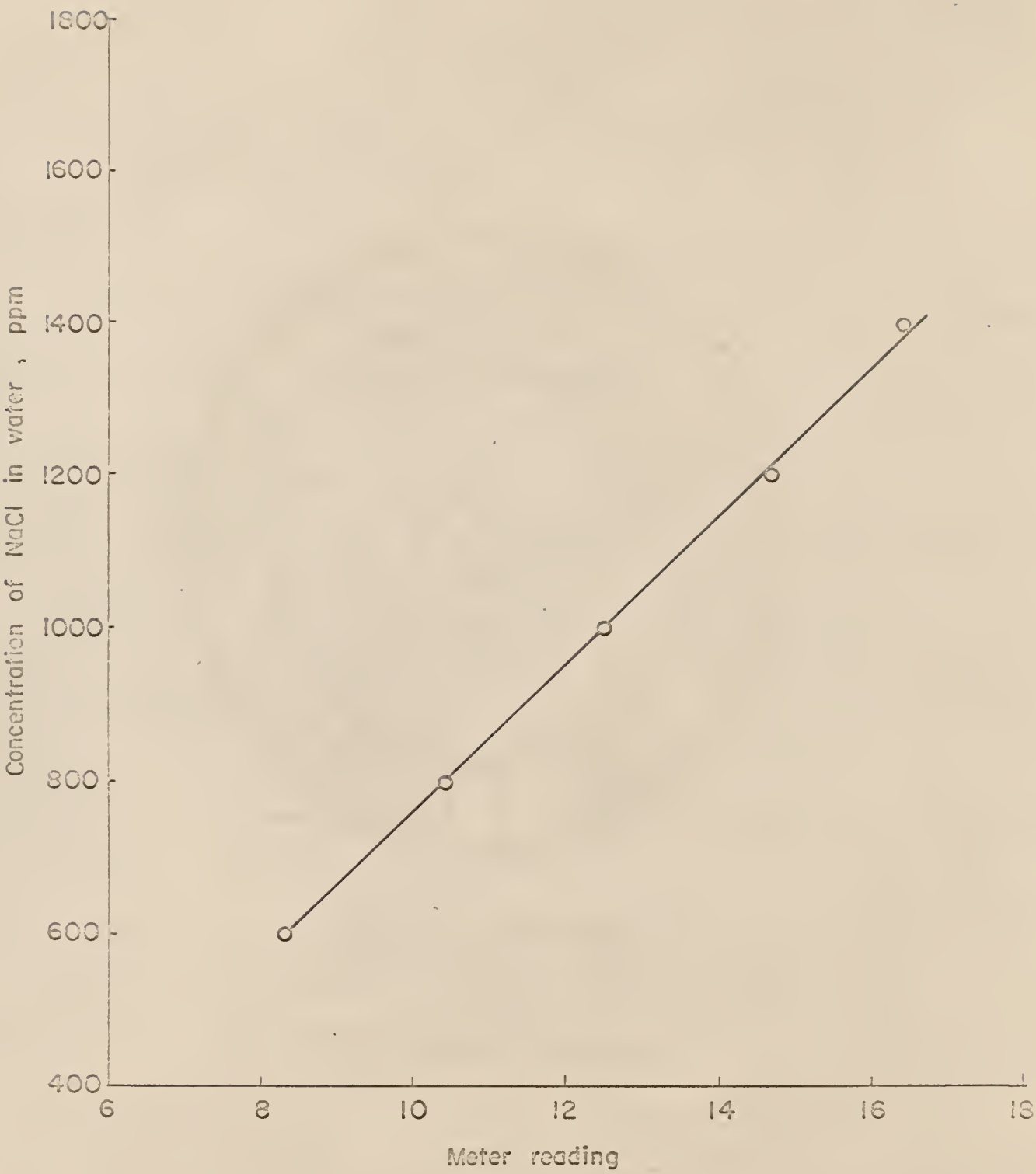


Fig. B-3. Conductivity meter calibration , 25 °C .

# APPENDIX C

SUMMARY OF EXPERIMENTAL RESULTS, AN EXAMPLE OF CALCULATION, AND DETERMINATION OF HEAT OF FUSION OF ORGANIC SOLID IN UNIT MASS OF ORGANIC SLURRY ($h_{f,o}$).

TABLE C-1

Summary of Data and Results of the Experiments for the Determination of Heat Transfer Rates

| Run No. | 1 | 2 | 3 | 4 | 5 | 6 | 7 | 8 |
|---|---|---|---|---|---|---|---|---|
| Org. mixture composition, vol. % n-$C_{13}$ | 55 | 55 | 55 | 55 | 55 | 55 | 55 | 55 |
| Org. slurry inlet Ice-Maker temp., °C | -4.52 | -4.52 | -4.52 | -4.52 | -4.52 | -4.52 | -4.52 | -4.52 |
| Org. slurry inlet Ice-Maker flow rate, ml/sec | 8.75 | 8.75 | 8.75 | 8.75 | 8.75 | 8.75 | 8.75 | 8.75 |
| Enthalpy of fusion of inlet org. solid, cal/sec | 139 | 139 | 139 | 139 | 139 | 139 | 139 | 139 |
| Stirring speed, rpm | 400 | 400 | 400 | 400 | 400 | 400 | 400 | 400 |
| Salt water hold-up in Ice-Maker, ml | | | | | | | | |
| Residence time, sec | | | | | | | | |
| Salt water inlet Ice-Maker flow rate, ml/sec | 1.8 | 2.25 | 2.7 | 3.1 | 3.5 | 3.85 | 4.2 | 4.5 |
| Salt water inlet Ice-Maker temp., °C | 4.5 | 4.0 | 3.9 | 3.8 | 3.7 | 3.3 | 3.2 | 3.0 |
| Wt. % NaCl feed stream | 3.5 | 3.5 | 3.5 | 3.5 | 3.5 | 3.5 | 3.5 | 3.5 |
| Wt. % NaCl product stream, sample 1 | 4.92 | 4.8 | 4.66 | 4.52 | 4.42 | 4.25 | 4.23 | 4.24 |
| sample 2 | | 4.75 | 4.62 | 4.55 | 4.47 | 4.33 | 4.33 | 4.25 |
| Cal'd heat transfer rate, cal/sec, | | | | | | | | |
| 1) for sensible heat | 11.5 | 13.5 | 15.5 | 17.5 | 19.5 | 20.0 | 21.4 | 21.9 |
| 2) for ice crystal form'n: | | | | | | | | |
| sample 1 | 41.6 | 48.7 | 53.7 | 56.0 | 58.4 | 54.4 | 58.1 | 62.8 |
| sample 2 | | 48.3 | 52.4 | 57.1 | 60.8 | 59.0 | 64.4 | 62.8 |
| Total: | | | | | | | | |
| sample 1 | 53.1 | 62.2 | 69.2 | 73.5 | 77.9 | 74.4 | 79.5 | 84.7 |
| sample 2 | | 61.8 | 67.9 | 74.6 | 80.3 | 79.4 | 85.3 | 84.7 |
| Heat transfer efficiency, % | | | | | | | | |
| sample 1 | 38.2 | 44.7 | 49.8 | 52.9 | 56.0 | 53.5 | 57.2 | 61.0 |
| sample 2 | | 44.4 | 48.8 | 53.7 | 57.8 | 57.1 | 61.2 | 61.0 |

TABLE C-1 (Cont'd)

Summary of Data and Results of the Experiments for the Determination of Heat Transfer Rates

| Run No. | 9 | 10 | 11 | 12 | 13 | 14 | 15 | 16 | 17 |
|---|---|---|---|---|---|---|---|---|---|
| Org. mixture composition, vol. % n-$C_{13}$ | 58 | 58 | 58 | 58 | 58 | 58 | 58 | 58 | 58 |
| Org. slurry inlet Ice-Maker temp., °C | -4.82 | -4.82 | -4.82 | -4.82 | -4.82 | -4.82 | -4.82 | -4.82 | -4.82 |
| Org. slurry inlet Ice-Maker flow rate, ml/sec | 8.75 | 8.75 | 8.75 | 8.75 | 8.75 | 8.75 | 8.75 | 8.75 | 8.75 |
| Enthalpy of fusion of inlet org. solid, cal/sec | 135 | 135 | 135 | 135 | 135 | 135 | 135 | 135 | 135 |
| Stirring speed, rpm | 300 | 350 | 400 | 500 | 600 | 600 | 700 | 800 | 900 |
| Salt water hold-up in Ice-Maker, ml | 500 | 435 | 467 | 430 | 377 | 385 | 358 | 355 | 355 |
| Residence time, sec | 143 | 138 | 133 | 123 | 108 | 110 | 102 | 101 | 101 |
| Salt water inlet Ice-Maker flow rate, ml/sec | 3.5 | 3.5 | 3.5 | 3.5 | 3.5 | 3.5 | 3.5 | 3.5 | 3.5 |
| Salt water inlet Ice-Maker temp., °C | 3.6 | 3.6 | 3.6 | 3.6 | 3.6 | 3.6 | 3.6 | 3.6 | 3.6 |
| Wt. % NaCl feed stream | 3.5 | 3.5 | 3.5 | 3.5 | 3.5 | 3.5 | 3.5 | 3.5 | 3.5 |
| Wt. % NaCl product stream, sample 1 | 4.43 | 4.48 | 4.58 | 4.74 | 4.86 | 4.81 | 4.91 | 4.91 | 4.91 |
| sample 2 | 4.46 | 4.43 | 4.60 | 4.76 | 4.91 | | 4.91 | 4.91 | 5.01 |
| Cal'd heat transfer rate, cal/sec, 1) for sensible heat | 19.0 | 19.0 | 19.0 | 19.0 | 19.0 | 19.0 | 19.0 | 19.0 | 19.0 |
| 2) for ice crystal form'n: sample 1 | 60.4 | 62.9 | 67.7 | 75.2 | 80.5 | 78.4 | 80.5 | 80.5 | 80.5 |
| sample 2 | 61.8 | 62.9 | 68.8 | 76.2 | 82.6 | | 80.5 | 80.5 | 83.7 |
| Total: sample 1 | 79.4 | 81.9 | 86.7 | 94.2 | 99.5 | 97.4 | 99.5 | 99.5 | 99.5 |
| sample 2 | 80.8 | 81.9 | 87.8 | 95.2 | 101.6 | | 99.5 | 99.5 | 105.7 |
| Heat transfer efficiency, % sample 1 | 58.8 | 60.4 | 64.2 | 69.2 | 73.6 | 72.1 | 73.6 | 73.6 | 73.6 |
| sample 2 | 59.8 | 60.4 | 65.0 | 70.5 | 75.2 | | 73.6 | 73.6 | 78.1 |

TABLE C-1 (Cont'd)

Summary of Data and Results of the Experiments for the Determination of Heat Transfer Rates

| Run No. | 18 | 19 | 20 | 21 | 22 | 23 | 24 | 25 |
|---|---|---|---|---|---|---|---|---|
| Org. mixture composition, vol. % n-C13 | 52 | 52 | 52 | 52 | 52 | 52 | 52 | 65 |
| Org. slurry inlet Ice-Maker temp., °C | -4.35 | -4.35 | -4.35 | -4.35 | -4.35 | -4.35 | -4.35 | -5.5 |
| Org. slurry inlet Ice-Maker flow rate, ml/sec | 8.75 | 8.75 | 8.75 | 8.75 | 8.75 | 8.75 | 8.75 | 8.75 |
| Enthalpy of fusion of inlet org. solid, cal/sec | 143 | 143 | 143 | 143 | 143 | 143 | 143 | 121 |
| Stirring speed, rpm | 300 | 400 | 500 | 600 | 700 | 800 | 900 | 300 |
| Salt water hold-up in Ice-Maker, ml | 500 | 470 | 430 | 380 | 360 | 355 | 356 | 500 |
| Residence time, sec | 143 | 134 | 123 | 108.5 | 103 | 101 | 101 | 143 |
| Salt water inlet Ice-Maker flow rate, ml/sec | 3.5 | 3.5 | 3.5 | 3.5 | 3.5 | 3.5 | 3.5 | 3.5 |
| Salt water inlet Ice-Maker temp., °C | 3.6 | 3.6 | 3.6 | 3.6 | 3.6 | 3.6 | 3.6 | 3.6 |
| Wt. % NaCl feed stream | 3.5 | 3.5 | 3.5 | 3.5 | 3.5 | 3.5 | 3.5 | 3.5 |
| Wt. % NaCl product stream, | | | | | | | | |
| sample 1 | 4.23 | 4.37 | 4.41 | 4.50 | 4.55 | 4.59 | 4.59 | 4.76 |
| sample 2 | 4.23 | 4.40 | 4.41 | 4.46 | | | | 4.86 |
| Cal'd heat transfer rate, cal/sec, | | | | | | | | |
| 1) for sensible heat | 19.0 | 19.0 | 19.0 | 19.0 | 19.0 | 19.0 | 19.0 | 19.0 |
| 2) for ice crystal form'n: | | | | | | | | |
| sample 1 | 49.6 | 57.2 | 59.3 | 64.0 | 65.8 | 68.2 | 68.2 | 76.2 |
| sample 2 | 49.6 | 58.8 | 59.3 | 61.9 | | | | 80.5 |
| Total: | | | | | | | | |
| sample 1 | 68.6 | 76.2 | 78.3 | 83.0 | 84.8 | 87.2 | 87.2 | 95.2 |
| sample 2 | 68.6 | 77.8 | 78.3 | 80.9 | | | | 99.5 |
| Heat transfer efficiency, % | | | | | | | | |
| sample 1 | 48.0 | 53.3 | 54.7 | 58.0 | 59.4 | 60.9 | 60.9 | 78.7 |
| sample 2 | 48.0 | 54.3 | 54.7 | 56.5 | | | | 82.0 |

TABLE C-1 (Cont'd)

Summary of Data and Results of the Experiments for the Determination of Heat Transfer Rates

| Run No. | 26 | 27 | 28 | 29 | 30 | 31 | 32 | 33 |
|---|---|---|---|---|---|---|---|---|
| Org. mixture composition, vol. % n-$C_{13}$ | 65 | 65 | 65 | 65 | 65 | 65 | 65 | 55 |
| Org. slurry inlet Ice-Maker temp., °C | -5.50 | -5.50 | -5.50 | -5.50 | -5.50 | -5.50 | -5.50 | -4.52 |
| Org. slurry inlet Ice-Maker flow rate, ml/sec | 8.75 | 8.75 | 8.75 | 8.75 | 8.75 | 8.75 | 8.75 | 8.75 |
| Enthalpy of fusion of inlet org. solid, cal/sec | 121 | 121 | 121 | 121 | 121 | 121 | 121 | 139 |
| Stirring speed, rpm | 350 | 400 | 500 | 600 | 700 | 800 | 900 | 300 |
| Salt water hold-up in Ice-Maker, ml | | | | | | | | |
| Residence time, sec | | | | | | | | |
| Salt water inlet Ice-Maker flow rate, ml/sec | 3.5 | 3.5 | 3.5 | 3.5 | 3.5 | 3.5 | 3.5 | 3.5 |
| Salt water inlet Ice-Maker temp., °C | 3.6 | 3.6 | 3.6 | 3.6 | 3.6 | 3.6 | 3.6 | 3.5 |
| Wt. % NaCl feed stream | 3.5 | 3.5 | 3.5 | 3.5 | 3.5 | 3.5 | 3.5 | 3.5 |
| Wt. % NaCl product stream, sample 1 | 5.01 | 5.03 | 5.10 | 5.06 | 5.10 | 5.06 | 5.10 | 4.29 |
| sample 2 | | 5.10 | | | 5.08 | | | 4.34 |
| Cal'd heat transfer rate, cal/sec, 1) for sensible heat | 19.0 | 19.0 | 19.0 | 19.0 | 19.0 | 19.0 | 19.0 | 19.0 |
| 2) for ice crystal form'n: sample 1 | 86.7 | 87.5 | 90.2 | 88.6 | 90.2 | 88.6 | 90.2 | 53.0 |
| sample 2 | | 90.2 | | | 89.2 | | | 55.6 |
| Total: sample 1 | 105.7 | 106.5 | 109.2 | 107.6 | 109.2 | 107.6 | 109.2 | 72.0 |
| sample 2 | | 109.2 | | | 108.2 | | | 74.6 |
| Heat transfer efficiency, % sample 1 | 87.1 | 88.0 | 90.2 | 89.0 | 90.2 | 89.0 | 90.2 | 51.8 |
| sample 2 | | 90.2 | | | 89.5 | | | 53.7 |

TABLE C-1 (Cont'd)

Summary of Data and Results of the Experiments for the Determination of Heat Transfer Rates

| Run No. | 34 | 35 | 36 | 37 | 38 | 39 | 40 | 41 |
|---|---|---|---|---|---|---|---|---|
| Org. mixture composition, vol. % n-$C_{13}$ | 55 | 55 | 55 | 55 | 55 | 55 | 58 | 58 (from #11) |
| Org. slurry inlet Ice-Maker temp., °C | -4.52 | -4.52 | -4.52 | -4.52 | -4.52 | -4.52 | -4.82 | -4.82 |
| Org. slurry inlet Ice-Maker flow rate, ml/sec | 8.75 | 8.75 | 8.75 | 8.75 | 8.75 | 8.75 | 10.0 | 8.75 |
| Enthalpy of fusion of inlet org. solid, cal/sec | 139 | 139 | 139 | 139 | 139 | 139 | 154 | 135 |
| Stirring speed, rpm | 400 | 500 | 600 | 700 | 800 | 900 | 400 | 400 |
| Salt water hold-up in Ice-Maker, ml | | | | | | | 458 | 467 |
| Residence time, sec | | | | | | | 114 | 133 |
| Salt water inlet Ice-Maker flow rate, ml/sec | 3.5 | 3.5 | 3.5 | 3.5 | 3.5 | 3.5 | 4.0 | 3.5 |
| Salt water inlet Ice-Maker temp., °C | 3.6 | 3.6 | 3.6 | 3.6 | 3.6 | 3.6 | 3.3 | 3.6 |
| Wt. % NaCl feed stream | 3.5 | 3.5 | 3.5 | 3.5 | 3.5 | 3.5 | 3.5 | 3.5 |
| Wt. % NaCl product stream, sample 1 | 4.44 | 4.47 | 4.52 | 4.55 | 4.64 | 4.66 | 4.60 | 4.58 |
| sample 2 | 4.44 | | 4.55 | 4.58 | 4.66 | | 4.62 | 4.60 |
| Cal'd heat transfer rate, cal/sec, 1) for sensible heat | 19.0 | 19.0 | 19.0 | 19.0 | 19.0 | 19.0 | 20.6 | 19.0 |
| 2) for ice crystal form'n: sample 1 | 60.8 | 62.5 | 65.0 | 66.4 | 70.6 | 71.5 | 78.6 | 67.7 |
| sample 2 | 60.8 | 63.3 | 66.4 | 67.9 | 71.5 | | 79.6 | 68.8 |
| Total: sample 1 | 79.8 | 81.5 | 84.0 | 85.4 | 89.6 | 90.5 | 99.2 | 86.7 |
| sample 2 | 79.8 | 82.3 | 85.4 | 86.9 | 90.5 | | 100.2 | 87.8 |
| Heat transfer efficiency, % sample 1 | 57.4 | 58.6 | 60.5 | 61.4 | 64.5 | 65.0 | 64.4 | 64.2 |
| sample 2 | 57.4 | 59.2 | 61.4 | 62.5 | 65.0 | | 65.9 | 65.0 |

TABLE C-1 (Cont'd)

Summary of Data and Results of the Experiments for the Determination of Heat Transfer Rates

| Run No. | 42 | 43 | 44 | 45 | 46 | 47 |
|---|---|---|---|---|---|---|
| Org. mixture composition, vol. % n-$C_{13}$ | | | (from #19) | | | |
| | 58 | 58 | 52 | 52 | 52 | 52 |
| Org. slurry inlet Ice-Maker temp., °C | -4.92 | -4.92 | -4.35 | -4.35 | -4.35 | -4.35 |
| Org. slurry inlet Ice-Maker flow rate, ml/sec | 6.0 | 5.0 | 13.0 | 8.75 | 7.0 | 5.0 |
| Enthalpy of fusion of inlet org. solid, cal/sec | 92.5 | 77 | 212 | 143 | 114 | 81.7 |
| Stirring speed, rpm | 400 | 400 | 400 | 400 | 400 | 400 |
| Salt water hold-up in Ice-Maker, ml | 420 | 477 | 445 | 470 | 475 | 478 |
| Residence time, sec | 136 | 238 | 86 | 134 | 170 | 238 |
| Salt water inlet Ice-Maker flow rate, ml/sec | 2.4 | 2.0 | 5.2 | 3.5 | 2.8 | 2.0 |
| Salt water inlet Ice-Maker temp., °C | 4.0 | 4.5 | 2.6 | 3.6 | 3.9 | 4.5 |
| Wt. % NaCl feed stream | 3.5 | | | | | |
| Wt. % NaCl product stream, sample 1 | 4.73 | 4.76 | 4.36 | 4.37 | 4.51 | 4.50 |
| sample 2 | | 4.76 | 4.42 | 4.40 | | |
| Cal'd heat transfer rate, cal/sec, | | | | | | |
| 1) for sensible heat | 14.0 | 12.6 | 23.3 | 19.0 | 16.0 | 12.6 |
| 2) for ice crystal form'n: | | | | | | |
| sample 1 | 51.2 | 43.4 | 84.7 | 57.2 | 51.5 | 36.6 |
| sample 2 | | 43.4 | 88.7 | 58.8 | | |
| Total: | | | | | | |
| sample 1 | 65.2 | 56.0 | 108.0 | 76.2 | 67.5 | 49.2 |
| sample 2 | | 56.0 | 112.0 | 77.8 | | |
| Heat transfer efficiency, % | | | | | | |
| sample 1 | 70.5 | 72.7 | 51.0 | 53.3 | 59.2 | 60.2 |
| sample 2 | | 72.7 | 52.7 | 54.3 | | |

An example of calculations for an experimental run. Run No. 33. The experimental data are listed in Table C-3. The necessary calculations are presented below.

1. Calculation of heat transfer rate for ice formation.

From sample 1:

4 ml of mother liquor was diluted with 200 ml of distilled water. Conductivity measurement showed the diluted solution has a reading of 10.85 on the meter, which corresponds to a NaCl conc. of 842 ppm.

Hence, using mass balance, wt. % of NaCl in the mother liquour was

$$X = \frac{204}{4} \times \frac{842}{1,000,000} \times 100 = 4.29$$

In the feed stream, the wt. % of NaCl was 3.5.

Taking 100 gr. of feed as basis, and, again, using mass balance, the mass of ice formed in the product stream, S, was estimated from the equation

$$100 \times 0.035 = (100 - S) \times 0.0429$$

This gave

$$S = 18.4 \text{ gr/100 gr of feed.}$$

That is, in 100 gr of salt water feed, 18.4 gr of ice was produced.

The salt water volumetric inlet flow rate was 3.5 ml/sec corresponding to the mass flow rate of

$W_a = 3.5 \times 1.027 = 3.595$ gr/sec.

Therefore, ice production rate was

$$3.595 \times \frac{18.4}{100} = 0.661 \text{ gr/sec.}$$

Finally, the heat transfer rate for ice formation was computed as

$$Q_f = 0.661 \times 80 = 53.0 \text{ cal/sec.}$$

From sample 2:

Again, 4 ml of mother liquor was diluted with 200 ml of distilled water. The conductivity measurement showed the diluted solution had a concentration of 850 ppm and thus

$$X = \frac{204}{4} \times \frac{850}{1,000,000} \times 100 = 4.34.$$

Further more, the material balance,

$$100 \times 0.035 = (100 - S) \times 0.0434,$$

gave

$$S = 19.35 \text{ gr/100 gr of feed.}$$

Therefore, the ice production rate in this run was

$$3.595 \times \frac{19.35}{100} = 0.695 \text{ gr/sec,}$$

and heat transfer rate for ice formation was

$$Q_f = 0.695 \times 80 = 55.6 \text{ cal/sec.}$$

2. Calculation of the heat transfer rate for the cooling of salt water.

$$t_{in,a} = 3.6^\circ \text{ C}$$

$$t_{f,a} = -2.05^\circ \text{ C}$$

$$C_{p,a} = 0.952 \text{ cal/gr } ^\circ\text{C}$$

$$W_a = 3.595 \text{ gr/sec}$$

From equation (6), $Q_s$ was calculated as

$$Q_s = 3.595 \left[3.6 - (-2.05)\right] 0.952$$

$$= 19 \text{ cal/sec.}$$

3. Calculation of total heat transfer rate.

From sample 1:

Using equation (8),

$$Q = Q_f + Q_s = 53.0 + 19.0 = 72.0 \text{ cal/sec.}$$

From sample 2:

$$Q = Q_f + Q_s = 55.6 + 19.0 = 74.6 \text{ cal/sec.}$$

4. Calculation of total heat transfer efficiency.

The heat of fusion of organic solid entering the Ice-Maker was 139 cal/sec.

According to Equation (9)

$$\theta = \frac{72}{139} = 0.518 \text{ or } 51.8\% \text{ for sample 1}$$

$$\theta = \frac{74.6}{139} = 0.537 \text{ or } 53.7\% \text{ for sample 2.}$$

5. Calculation of the mean residence time.

The aqueous slurry hold-up in the Ice-Maker was 500 ml, and the volumetric inlet flow rate of salt water was 3.5 ml/sec.

Thus, the nominal residence time was $\frac{500}{3.5} = 143$ seconds.

Determination of $h_{f,o}$. The heat of fusion of organic solid was determined calorimetrically. A 200 ml vacuum bottle provided with a cork, a ring stirrer made of copper wire, and an electric immersion heater with 44.5 ohms resistance was used as a calorimeter. An ammeter with an accuracy of 0.1 ampere and a variable transformer were used to measure and adjust the current to the heater. The temperature recorder described on page 23 was used to indicate and record the temperature in the bottle.

The total energy required to heat the whole system from its initial temperature to a temperature a few degrees Centigrade higher than the freezing point of the organic mixture could be written as

$$H = H_s + H_{f,o} + H_u + H_i + H_c \qquad (c\text{-}1)$$

where:

$H$ = total energy required for heating, cal.

$H_s$ = sensible heat of organic liquid above the initial freezing temperature, cal.

$H_{f,o}$ = heat of fusion of organic solid, cal.

$H_u$ = sensible heat of organic liquid below the initial freezing point, cal.

$H_i$ = sensible heat of organic solid, cal.

$H_c$ = heat absorbed by the calorimeter, cal.

$H_s$ and $H_c$ could be calculated from the following equations

$$H_s = M_o \cdot (t_e - t_{f,o}) \cdot C_{p,ol} \qquad (c\text{-}2)$$

$$H_c = (t_e - t_{ini}) \cdot C_{p,c} \qquad (c\text{-}3)$$

where:

$M_o$ = mass of organic mixture in the calorimeter, gr.

$t_{ini}$ = initial slurry temperature, $^oC$.

$t_e$ = final temperature of heating, $^oC$.

$t_{f,o}$ = organic mixture initial freezing temperature, $^oC$.

$C_{p,ol}$ = specific heat of organic liquid, cal $deg^{-1}$ $gr^{-1}$.

$C_{p,c}$ = heat capacity of calorimeter, cal $deg^{-1}$.

$C_{p,ol}$ was determined by the composition of the mixture and specific heat of n-tridecane and n-tetradecane. $C_{p,c}$ was determined experimentally.

$H_u$ and $H_i$ in Eq. (c-1) were neglected because they account for only a very small portion of H.

Hence, Equation (c-1) becomes

$$H = M_o \cdot (t_e - t_{f,o}) \cdot C_{p,ol} + H_{f,o} + (t_e - t_{ini}) \cdot C_{p,c} \qquad (c\text{-}4).$$

The heat absorbed by the system equals to the total heat input because of the conservation of energy.

Neglecting the energy input from the stirrer and surroundings, the total energy input was from the electric heater, that is,

$$E = i^2 Rt \text{ joules} = \frac{i^2 Rt}{4.184} \text{ cal} \qquad (c\text{-}5)$$

where:

E = total electrical energy input, cal.

i = electric current to the heater, amp.

R = heater resistance, ohms.

t = total heating time, seconds.

Equating Eqs. (c-4) and (c-5) yielded

$$H_{f,o} = \frac{i^2 Rt}{4.184} - M_o(t_e - t_{f,o}) \cdot C_{p,ol} - (t_e - t_{ini}) \cdot C_{p,c} \quad \text{.....} \quad \text{(c-6).}$$

The heat of fusion of organic solid in a unit mass of organic slurry could be obtained by dividing both sides of Eq. (c-6) with $M_o$.

$$h_{f,o} = \frac{H_{f,o}}{M_o}$$

$$= \frac{i^2 Rt}{4.184\ M_o} - (t_e - t_{f,o}) \cdot C_{p,ol} - \frac{1}{M_o}(t_e - t_{ini}) \cdot C_{p,c}$$

The results of this part of work are given below.

| Mixture | Composition (vol.) | Initial Slurry Temperature, $t_{ini}$, $^oC$ | $h_{f,o}$, cal/gr |
|---|---|---|---|
| A | 65% n-$C_{13}H_{28}$<br>35% n-$C_{14}H_{30}$ | -5.50 | 17.73 |
| B | 58% n-$C_{13}H_{28}$<br>42% n-$C_{14}H_{30}$ | -4.82 | 19.78 |
| C | 55% n-$C_{13}H_{28}$<br>45% n-$C_{14}H_{30}$ | -4.52 | 20.37 |

| | | | |
|---|---|---|---|
| D | 52% $n\text{-}C_{13}H_{28}$<br>48% $n\text{-}C_{14}H_{30}$ | -4.35 | 20.95 |

# APPENDIX D

## ANALYSIS OF RESIDENCE TIME DISTRIBUTION OF FLUID IN ICE MAKER

Two ideal flow patterns which are often used to approximate real systems are plug flow and complete mixing. Patterns of flow other than plug flow or complete mixing are called non-ideal flow patterns (22).

Knowledge of the complete flow pattern of the fliid in the system is required if one is to account for non-ideal flow. Due to the difficulties associated with obtaining and interpreting such information, an alternate approach is used which requires knowledge only of how long different elements of fluid reside in the system. This partial information is relatively simple to obtain experimentally, can be easily interpreted, and yields information which in many cases allows a satisfactory accounting of the non-ideal flow.

The experimental technique used for finding this desired distribution of residence times of fluid elements in the system is a stimulus -response technique using some sort of tracer material in the inlet fluid stream. The injection is the stimulus and the response is the tracer concentration measured in the outlet stream. The tracer can be radio-active, or a colored dye, or a salt solution, or any material depending on the particular situation. Tracer is injected into the inlet stream in some known fashion, such as a step, a pulse, a semi-wave or other cyclic signal, or even a random signal with known properties.

Quantitative definitions and discussions of the age distribution functions developed by Danckwerts and others could be found in the literatures (22,23). Some particular terms used in this work are discussed below:

The F-Curve. With no tracer initially present, let a step tracer signal of concentration $C_o$ be introduced into the fluid entering the system in such a manner that the volumetric flow rate to the vessel remains constant. Then the concentration-time curve for tracer in the exit fluid stream, measured in terms of inlet tracer concentration and reduced time is called the F-Curve. The range of F is 0 to 1.

Reduced time, $\theta$, is defined as

$$\theta = \frac{t}{\bar{t}} \qquad \text{(D-1)}$$

where $\bar{t}$, the mean residence time of fluid in a vessel is defined as

$$\bar{t} = \frac{\text{Volume of the vessel available for flow}}{\text{Volumetric flow rate of fluid through the vessel}} \qquad \text{(D-2)}$$

The C-Curve. The curve which describes the concentration-time function of tracer in the exit stream of a system in response to a delta function or unit impulse input is called the C-Curve. As with the F-Curve, the range and domain are dimensionless. Concentrations are mearsured in terms of the initial concentration, $C^o$, as if it were evenly distributed through out the system.

## MODELS FOR NONIDEAL FLOW

There are many types of models which can be used to characterize nonideal flow patterns within vessels (24). Two models which will be employed are briefly discussed below:

Dispersion Model (Dispersed Plug Flow Model). This model was

drawn on the basis of analogy between mixing in actual flow and a diffusional process, with a constant dispersion coefficient and a flat velocity profile in the vessel considered. The parameter which characterizes the degree of back mixing during flow is a dimensionless group $D/\mu L$, called the vessel or reactor dispersion number. It changes from zero for plug flow to infinity for back-mix flow and is the reciprocal of the axial Peclet number for mass transfer.

To characterize flow in a real vessel, one needs to select from the family of theoretical F or C curves the curve that most closely fits the experimental F or C curve. From the $D/\mu L$ of this fitted curve the behavior of the vessel as a reactor can then be predicted.

Another convenient way to predict the reactor behavior is to equate the variance of an experimental C curve to that of a selected theoretical C curve. For the C curve in a closed vessel,

$$\sigma_\theta^2 = \frac{\sigma_t^2}{\bar{t}^2} = 2\frac{D}{\mu L} - 2\left(\frac{D}{\mu L}\right)^2 (1-e^{-\mu L/D}) \qquad (d-3)$$

where

$\bar{t}$ = mean age of the exit stream

$\sigma_\theta^2$, and $\sigma_t^2$ = variance of the C curve, which measures the spread of the distribution about the mean.

From Eq. D-3, $\frac{D}{\mu L}$ for a actual reactor could be solved for with a $\sigma_\theta^2$ obtained from the experimental C-curve.

Completely Stirred Tank In series Model. This model is based on the assumption that the actual reactor can be represented

by a series of j equal sized backmix flow vessels. The output C curve for this model is

$$C = \frac{j^j \theta^{j-1}}{(j-1)!} e^{-j\theta} \qquad \text{(D-4)}$$

with mean $\overline{\theta}_c = 1$

and variance $\sigma_\theta^2 = \frac{1}{j}$.

From experimental variance measurements j can be found.

EXPERIMENTAL.

In this work, the residence time distribution of fluid in the Ice Maker was measured with a steady flow of fresh water and an injection of saturated sodium chloride solution as a tracer. A 10 ml. syringe was used to create an impulse input, and a "Compact Infusion Pump", made by Harvard Apparatus Company, Model 975, with a 50 ml. syringe to create a step input. A conductivity cell was installed at the outlet of the vessel along with a Model RA4 Direct Reading Conductivity Meter (see p.31) and a Honeywell Electronic 19* Lab Recorder (see p.23) which gave a record that was both continuous and linear with concentration.

The experimental runs were made with stirrer speeds of 300, 600, and 900 rpm.

RESULTS AND ANALYSES.

The experimental conditions for each run are summarized and shown in Table D-1.

Table D-1

Summary of experimental conditions for each run of residence time distribution study.

| Run No. | Type of input | Water flow rate ml/sec | Mean residence time, sec.+ | Stirrer speed |
|---|---|---|---|---|
| 1 | step* | 12.1 | 103 | 300 |
| 2 | step* | 12.1 | 103 | 600 |
| 3 | step* | 12.1 | 103 | 900 |
| 4 | impulse* | 12.1 | 103 | 300 |
| 5 | impulse* | 12.1 | 103 | 600 |
| 6 | impulse* | 12.1 | 103 | 900 |

\+ vessel volume 1249 ml.

* the tracer injection rate was 0.103 ml/sec.

* the amount of tracer used was 10 ml., time width about 3 seconds.

The experimental traces of individual runs are reproduced in Figs. D-1 through D-6. The recorded curves are quite smooth.

The tracer concentration readings obtained from the experimental traces are presented in Tables D-2 and D-4. Tables D-3, D-5, and D-6 show the calculated values of $F(\theta)$, $D/\mu L$ and j, and $C(\theta)$ respectively. Figures D-1 and D-2 are the plots of F-curves and C-curves. The theoretical curves for various extents of back-mixing as predicted by the dispersion model and tank-in-series model are included for comparison.

In comparing the experimental F-curve with theoretical ones, one can see that the behavior of the Ice-Maker in the operating stirrer speed range was very close to the " completely mixed" condition. But, the C-curves and the calculated values of mixing parameters indicate that there was a small degree of deviation from the conditions as F-curves implied. This was due to the assumption of "impulse input" in the analysis. Actually, the true impulse should be done by injecting an finite amount of tracer over an infinitesimal period of time, and this is really a physical impossibility. The assumption of tracer injection in this work (injection time width about 3 seconds, mean residence time of fluid in the vessel about 100 seconds) is, in fact, an approximation. Therefore, it may be concluded that the F-curve gives a better interpretation of reality, and the behavior of the vessel was close to perfect mixing (or well-stirred).

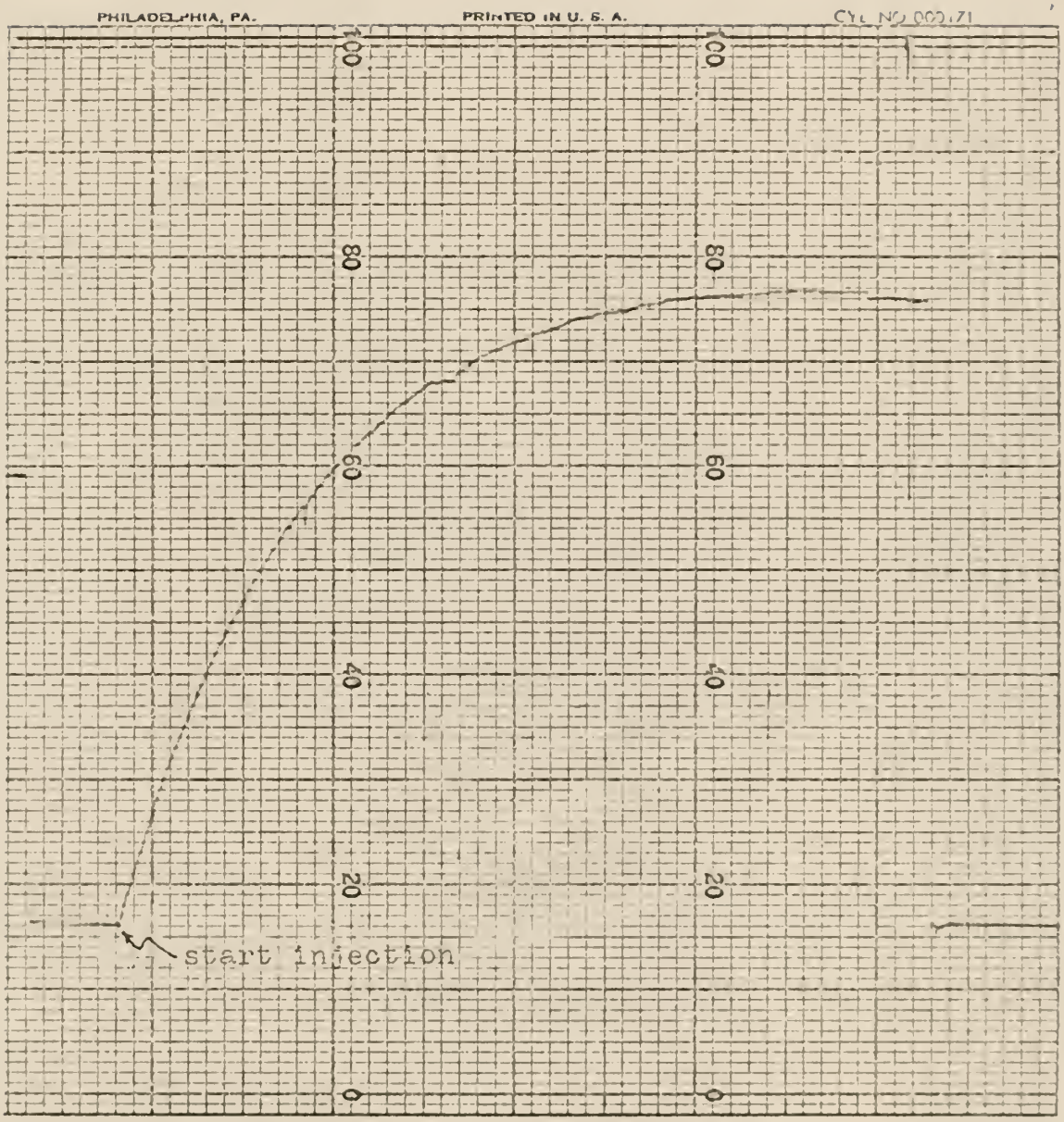


Fig. D-1. Response curve of run No.1 (step-input, 300rpm)
Recorder chart speed: 0.5 in/min.

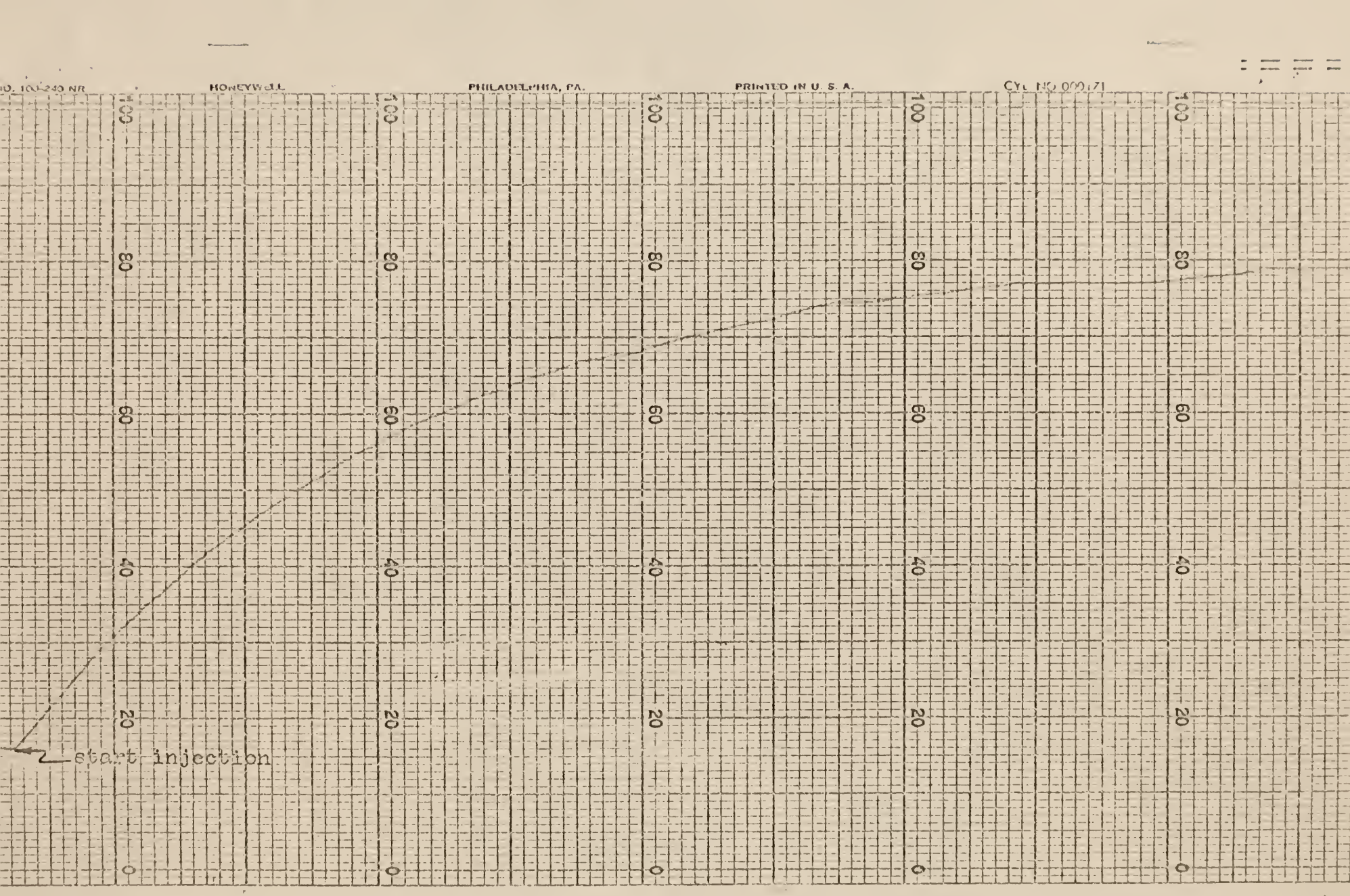


Fig. D-2. Response curve of run No.2 (step-input, 600rpm)
Recorder chart speed: 1.5 in/min.

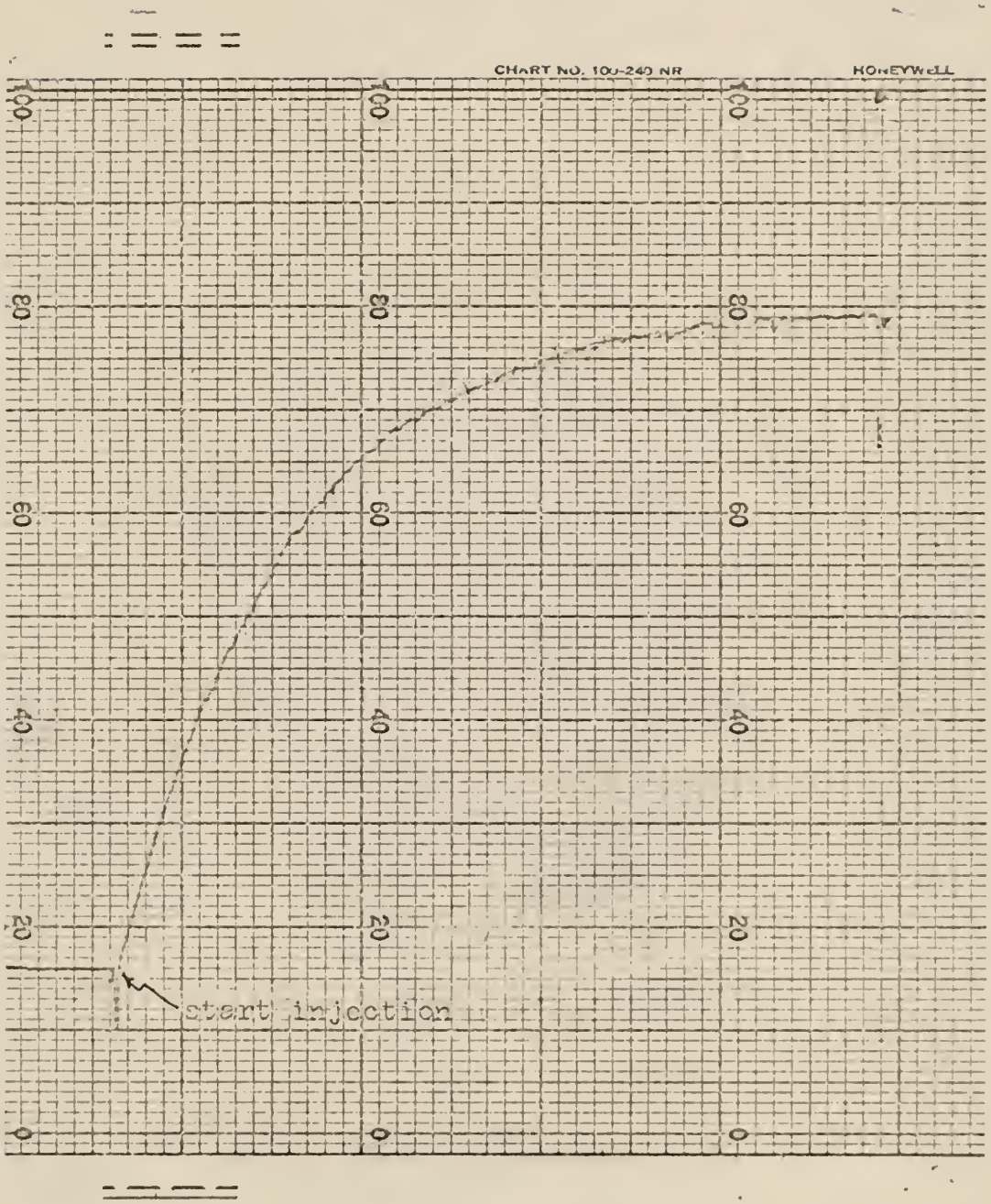


Fig. D-3. Response curve of run No.3 (step-input, 900 rpm)
Recorder chart speed: 0.5 in/min.

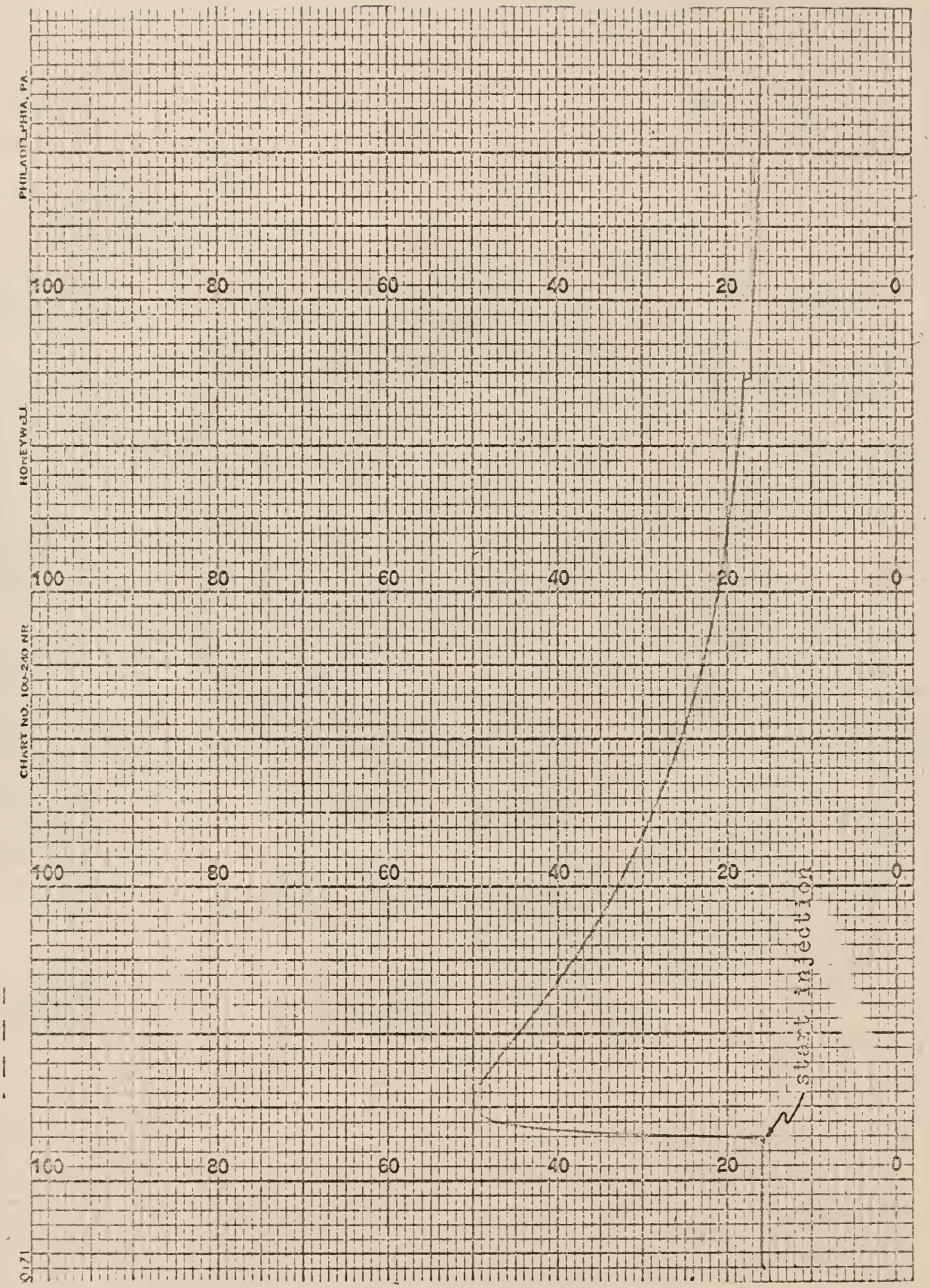


Fig. D-4. Response curve of run No.4 (impulse-input, 300rpm)
Recorder chart speed: 1 in/min.

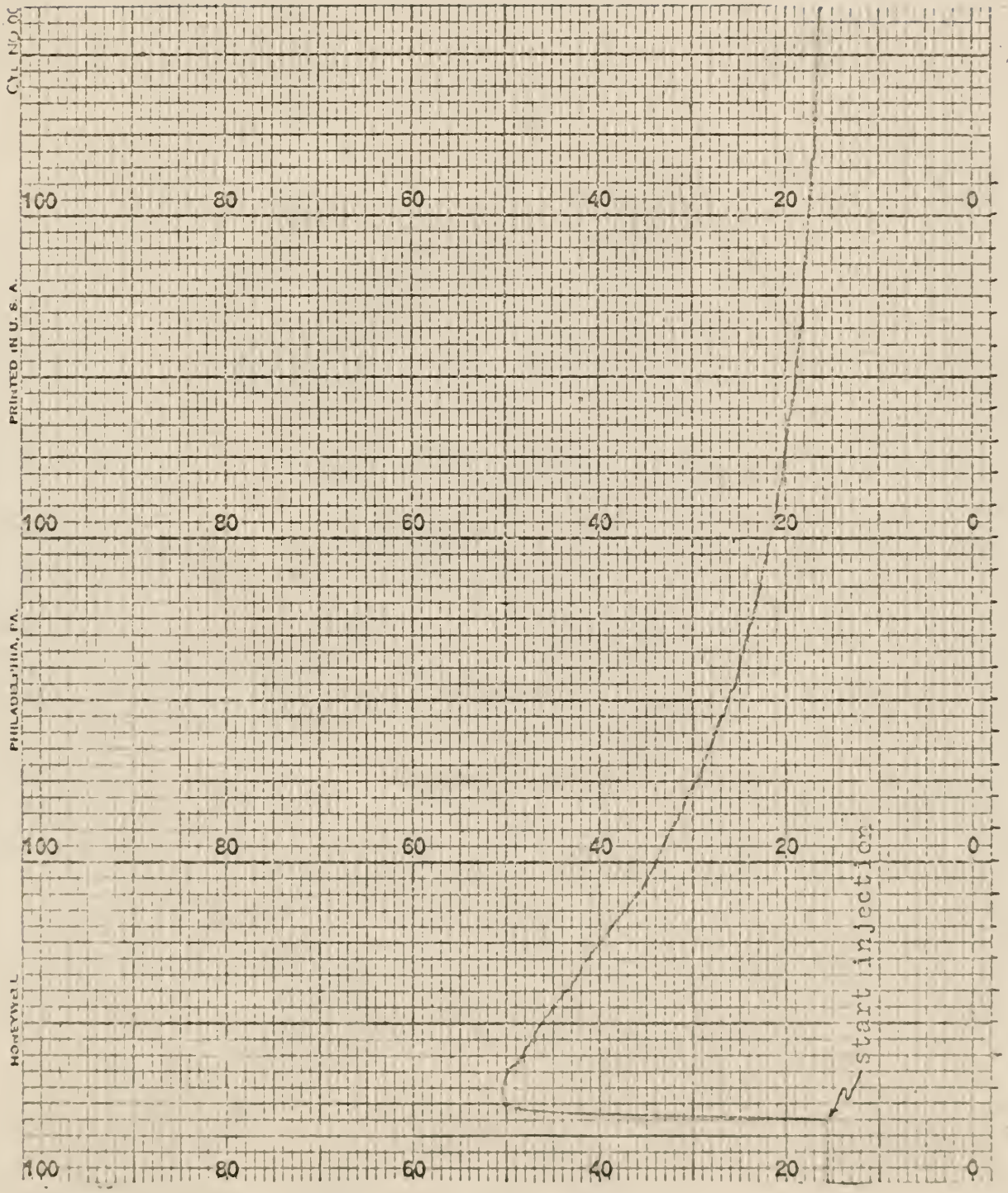


Fig. D-5. Response curve of run No.5 (impulse-input, 600rpm)
Recorder chart speed: 1 in/min.

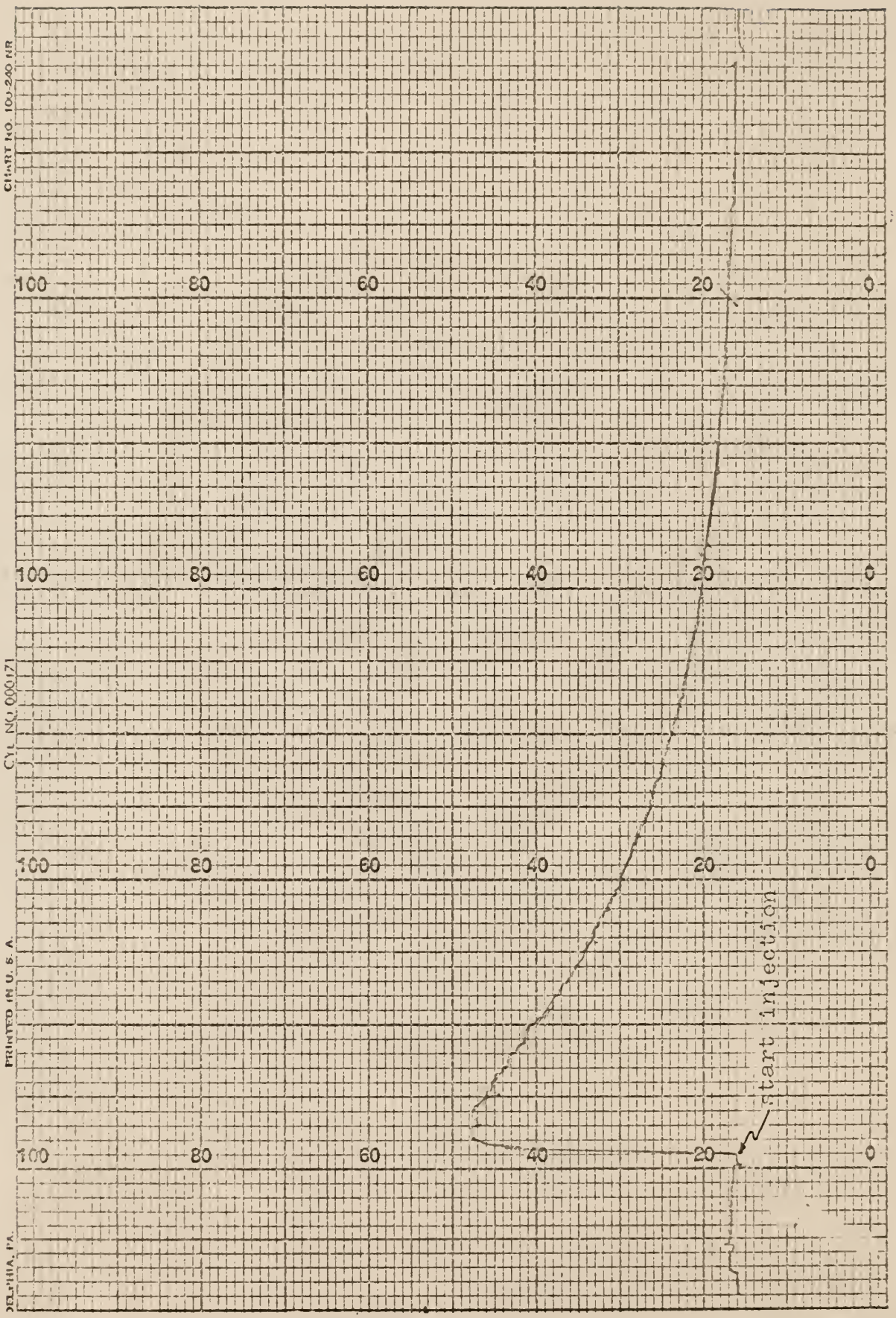


Fig. D-6. Response curve of run No.6 (impulse-input, 900rpm)
Recorder chart speed: 1 in/min.

Table D-2

Experimental data (step-input response)

| Run No. 1 | | Run No. 2 | | Run No. 3 | |
|---|---|---|---|---|---|
| Time (sec) | Tracer Conc. (ppm) | Time (sec) | Tracer Conc. (ppm) | Time (sec) | Tracer Conc. (ppm) |
| 0 | 0 | 0 | 0 | 0 | 0 |
| 20 | 260 | 30 | 370 | 24 | 310 |
| 50 | 550 | 60 | 650 | 54 | 620 |
| 80 | 765 | 90 | 865 | 84 | 830 |
| 110 | 940 | 120 | 1050 | 114 | 1010 |
| 140 | 1080 | 150 | 1175 | 144 | 1145 |
| 170 | 1180 | 180 | 1270 | 174 | 1280 |
| 200 | 1265 | 210 | 1340 | 204 | 1320 |
| 230 | 1320 | 240 | 1420 | 234 | 1380 |
| 260 | 1380 | 270 | 1455 | 264 | 1430 |
| 290 | 1450 | 300 | 1490 | 294 | 1455 |
| 320 | 1465 | 330 | 1520 | 324 | 1490 |
| 350 | 1480 | 360 | 1530 | 354 | 1510 |
| 380 | 1485 | 390 | 1545 | 384 | 1530 |
| 410 | 1500 | 420 | 1550 | 414 | 1540 |
| 440 | 1500 | 450 | 1550 | 444 | 1550 |
| | | | | 474 | 1550 |
| $\bar{t}$ = 103 sec | | $\bar{t}$ = 103 sec | | $\bar{t}$ = 103 sec | |
| Co = 1500 ppm | | Co = 1550 ppm | | Co = 1550 ppm | |

Table D-3

Dimensionless data (step-input response)

$$\theta = \frac{t}{\bar{t}} \qquad F(\theta) = \frac{C_i}{C_o}$$

| Run No. 1 | | Run No. 2 | | Run No. 3 | |
|---|---|---|---|---|---|
| $\theta$ | $F(\theta)$ | $\theta$ | $F(\theta)$ | $\theta$ | $F(\theta)$ |
| 0 | 0 | 0 | 0 | 0 | 0 |
| 0.194 | 0.173 | 0.291 | 0.239 | 0.233 | 0.20 |
| 0.485 | 0.367 | 0.583 | 0.419 | 0.524 | 0.40 |
| 0.777 | 0.510 | 0.874 | 0.558 | 0.815 | 0.535 |
| 1.067 | 0.626 | 1.165 | 0.677 | 1.107 | 0.652 |
| 1.359 | 0.720 | 1.456 | 0.758 | 1.398 | 0.738 |
| 1.650 | 0.787 | 1.748 | 0.819 | 1.689 | 0.825 |
| 1.942 | 0.843 | 2.039 | 0.865 | 1.981 | 0.852 |
| 2.233 | 0.880 | 2.330 | 0.916 | 2.272 | 0.890 |

Table D-4

Experimental data (impulse-input response)
(smoothed to equidistant points)

| Time (sec) | Run No.4 (300 rpm) Concentration (ppm NaCl) | Run No.5 (600 rpm) Concentration (ppm NaCl) | Run No.6 (900 rpm) Concentration (ppm NaCl) |
|---|---|---|---|
| 0 | 0 | 0 | 0 |
| 12 | 740 | 750 | 700 |
| 24 | 810 | 800 | 743 |
| 36 | 740 | 750 | 693 |
| 48 | 675 | 685 | 630 |
| 60 | 615 | 625 | 560 |
| 72 | 555 | 565 | 510 |
| 84 | 500 | 505 | 460 |
| 96 | 450 | 450 | 420 |
| 108 | 400 | 410 | 370 |
| 120 | 360 | 370 | 330 |
| 132 | 323 | 323 | 300 |
| 144 | 285 | 290 | 260 |
| 156 | 250 | 255 | 235 |
| 168 | 222 | 225 | 205 |
| 180 | 200 | 205 | 180 |
| 192 | 173 | 180 | 160 |
| 204 | 152 | 160 | 140 |
| 216 | 135 | 140 | 122 |
| 228 | 120 | 125 | 105 |

Table D-4(Cont'd)

Experimental data (impulse-input response)
(smoothed to equidistant points)

| | Run No.4 (300 rpm) | Run No.5 (600 rpm) | Run No.6 (900 rpm) |
|---|---|---|---|
| Time (sec) | Concentration (ppm NaCl) | Concentration (ppm NaCl) | Concentration (ppm NaCl) |
| 240 | 105 | 110 | 95 |
| 252 | 90 | 100 | 85 |
| 264 | 80 | 88 | 75 |
| 276 | 70 | 75 | 65 |
| 288 | 60 | 65 | 55 |
| 300 | 50 | 55 | 48 |
| 312 | 43 | 50 | 40 |
| 324 | 36 | 45 | 35 |
| 336 | 30 | 35 | 30 |
| 348 | 25 | 25 | 25 |
| 360 | 20 | 20 | 20 |

Table D-5

Calculation Results (impulse-input response)

| | Run No. 4 | Run No. 5 | Run No. 6 |
|---|---|---|---|
| $\Sigma C_i$ | 8314 | 8481 | 7696 |
| $\Sigma C_i \Delta t = 12 \times \Sigma C_i$ | 99,768 | 101,722 | 92,352 |
| $\Sigma C_i t_i$ | 824,196 | 853,968 | 762,372 |
| $\bar{t} = \frac{\Sigma C_i t_i}{\Sigma C_i}$ (sec) | 99.13 | 100.69 | 99.06 |
| $\Sigma C_i t_i^2$ | 130,429,872 | 137,318,400 | 121,147,488 |
| $\sigma_t^2 = \frac{\Sigma C_i t_i^2}{\Sigma C_i} - (\bar{t})^2$ | 5861.22 | 6052.82 | 6,413.68 |
| $\sigma_\theta^2 = \frac{\sigma_t^2}{(\bar{t})^2}$ | 0.5965 | 0.5970 | 0.6536 |
| Dispersion Model Parameter($D/\mu L$) | 0.557 | 0.558 | 0.698 |
| Tank in Series Model Parameter (j) | 1.6766 | 1.675 | 1.5299 |

Table D-6

Dimensionless data (impulse-input response)

$$\theta = t/\bar{t}$$

$$C_i(\theta) = \frac{C_i}{\Sigma C_i\, t}\,\bar{t}$$

| Run No. 4 | | Run No. 5 | | Run No. 6 | |
|---|---|---|---|---|---|
| $\theta$ | $C_i(\theta)$ | $\theta$ | $C_i(\theta)$ | $\theta$ | $C_i(\theta)$ |
| 0 | 0 | 0 | 0 | 0 | 0 |
| 0.121 | 0.735 | 0.119 | 0.742 | 0.121 | 0.751 |
| 0.242 | 0.805 | 0.238 | 0.791 | 0.242 | 0.797 |
| 0.363 | 0.735 | 0.358 | 0.742 | 0.363 | 0.743 |
| 0.484 | 0.671 | 0.477 | 0.678 | 0.484 | 0.676 |
| 0.605 | 0.611 | 0.596 | 0.618 | 0.605 | 0.601 |
| 0.726 | 0.551 | 0.715 | 0.559 | 0.726 | 0.547 |
| 0.847 | 0.497 | 0.834 | 0.500 | 0.848 | 0.493 |
| 0.968 | 0.447 | 0.954 | 0.445 | 0.969 | 0.450 |
| 1.089 | 0.397 | 1.073 | 0.406 | 1.090 | 0.397 |
| 1.210 | 0.358 | 1.192 | 0.366 | 1.211 | 0.354 |
| 1.331 | 0.321 | 1.311 | 0.320 | 1.333 | 0.322 |
| 1.453 | 0.283 | 1.430 | 0.287 | 1.454 | 0.279 |
| 1.574 | 0.248 | 1.549 | 0.252 | 1.575 | 0.252 |
| 1.695 | 0.221 | 1.668 | 0.223 | 1.696 | 0.220 |
| 1.816 | 0.199 | 1.788 | 0.203 | 1.817 | 0.193 |
| 1.937 | 0.172 | 1.907 | 0.178 | 1.938 | 0.172 |
| 2.058 | 0.151 | 2.026 | 0.158 | 2.059 | 0.150 |

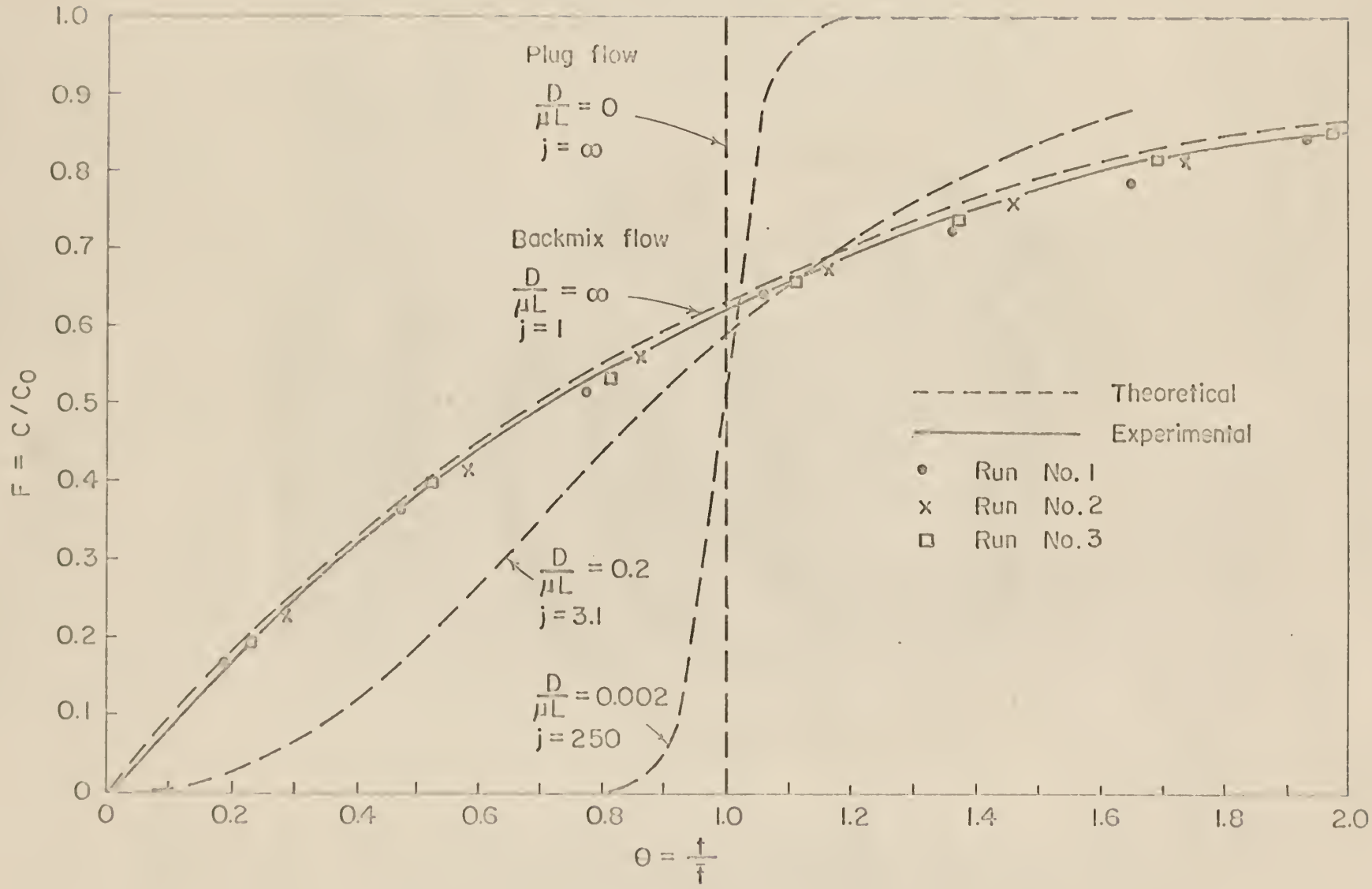


Fig. D-7. Step-input response (or F-) curves.

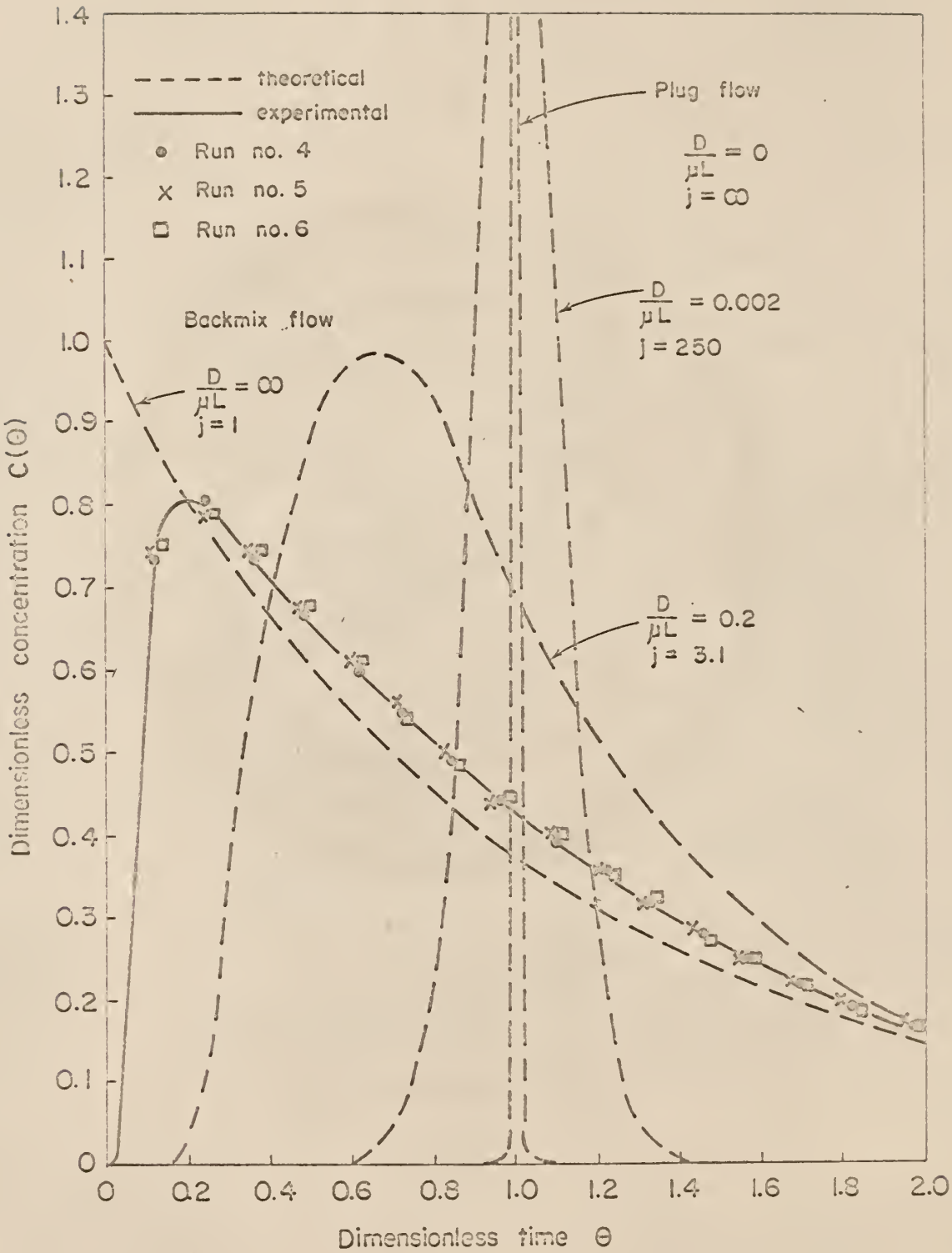


Fig. D-8. Impulse input response (or C-) curves.

# A STUDY OF THE ICE MAKING OPERATION IN THE DESALINATION FREEZING PROCESS BASED ON THE INVERSION OF MELTING POINTS DUE TO APPLIED PRESSURE

by

SHEN-YANN CHIU

B.S., National Taiwan University, 1962

---

AN ABSTRACT OF A MASTER'S THESIS

submitted in partial fulfillment of the

requirements for the degree

MASTER OF SCIENCE

Department of Chemical Engineering

KANSAS STATE UNIVERSITY
Manhattan, Kansas

1968

ABSTRACT

Experimental equipment was designed and built to test the ice-making of the Inversion Desalination Freezing Process at atmospheric pressure. A back-mixed type contactor was used to produce ice from salt water by direct contact freezing with a mixture of n-tridecane and n-tetradecane as a working medium.

The thermal driving force, degree of mixing, and nominal residence time were considered as controlling variables for the ice production rate and have been studied. Forty seven experimental runs were carried out using four different working media. The agitation speed ranged from 300 to 900 rpm, and the nominal residence time from 86 to 238 seconds. In addition to the ice production rate, the sizes of ice-crystals obtained under different operating conditions were investigated photographically. The pictures showed the crystals were fairly large, well shaped, and smooth.

The results of the production rate study can be used to design a larger scale plant. The experimental data reveal that very reasonably sized equipment may be used with this process. The quality of ice indicates that the ice-washing should present no problems.